Distant Tsunami Threats to the Ports of Los Angeles and Long Beach, California

Burak Uslu

Marie Eblé

Vasily Titov

Eddie Bernard

NOAA Center for Tsunami Research
Pacific Marine and Environmental Laboratory
Seattle, WA
March 2010

DISTANT TSUNAMI THREATS TO THE PORTS OF LOS ANGELES AND LONG BEACH, CALIFORNIA

Burak Uslu[1,2], Marie Eblé[2], Vasily Titov[2] and Eddie Bernard[2]

[1]Joint Institute for the Study of the Atmosphere and Ocean (JISAO), University of Washington, Seattle, WA

[2]NOAA/Pacific Marine Environmental Laboratory (PMEL), Seattle, WA

March 2010

Contents

List of Figures

List of Tables

Acknowledgements

The authors wish to thank Chris Chamberlin, Joint Institute for the Study of Atmosphere and Ocean, for his help in developing the Ports of Los Angeles and Long Beach numerical grids. We also thank A. E. Cannon, Technical Writer with Telcordia Technologies, Inc. for editorial review. Collaborative contributions of the National Geophysical Data Center, and the National Data Buoy Center were invaluable.

Funding for this work was provided by the Alfred E. Alquist Seismic Safety Commission under contract number 50ABNR200053. This publication was partially funded by the Joint Institute for the Study of the Atmosphere and Ocean (JISAO) under NOAA Cooperative Agreement No. NA17RJ1232.

Executive Summary

Tsunamis have been recognized as a potential hazard to United States coastal communities, harbors, and ports, including those in the State of California since multiple destructive events impacted California's coast in the mid–twentieth century. In response, the United States National Oceanographic and Atmospheric Administration began a tsunami research program at the Pacific Marine Environmental Laboratory to develop tools for measuring, modeling, and assessing the hazard posed by tsunamis. The destruction and unprecedented loss of life following the December 2004 Sumatra tsunami served as the catalyst to refocus these activities, and on 20 December 2006, the United States Congress passed the "Tsunami Warning and Education Act." The act mandated specific education and warning activities and dedicated resources to accelerate the pace of tsunami product development, including those applicable to comprehensive hazard assessment of coastal communities.

The State of California shares longer than 1,300 km of coastline with the tectonically active Pacific Ocean. Along the southern portion of this coastline, in Los Angeles County, reside two of the busiest container ports in the United States: the Port of Los Angeles and the Port of Long Beach. Adjacent to one another, the ports combine to be the fifth busiest in the world, handling more than 10 million containers annually and providing 30,000 jobs which, in turn, support the local economy. Greater than 300,000 jobs in a five county area in Southern California are tied to the ports, as are an estimated 1.1 million jobs throughout the state. In addition, the contribution of the ports to the economy of California and to the United States as a whole is significant. Annual state and local tax revenue exceeds five billion dollars (Port of Los Angeles, 2009; Port of Long Beach, 2009; Coastal Conservancy, 2009).

A tsunami impact to the ports of Los Angeles and Long Beach would potentially cause significant damage and disrupt port operations for an extended period of time. The tsunami generated by the 1964 Great Alaska Earthquake caused strong surges that tore 75 small vessels from their moorings and sank three boats in the ports of Los Angeles and Long Beach. Potential damage to the ports, and the disruption that would likely occur today, would have severe repercussions for the economy of the State of California. which relies heavily on port activities for revenue, trade, and employment. Past events and comprehensive studies of the region have documented the seismic history of the Southern California coastal region and point to the potential hazard from tsunamis. A detailed sensitivity study has been performed with synthetic tsunamis generated by M_w 9.3 earthquakes along Pacific Ocean subduction zones to identify probable maximum tsunamis. A total of 56 scenarios generated from sources along

the Alaska–Aleutian subduction zone, 106 from Central and South America, 13 from the Nankai Trough and Ryuku, 28 from the Solomons and Vanuatu, 30 from New Zealand, 6 from New Guinea, 8 from Manus, 66 from the Kurils and Mariana, and 9 from the Eastern Philippines, for a total of 322 synthetic scenarios, were investigated. Of these 322 scenarios, tsunamis from 11 source regions in Alaska, Chile, Philippines, Manus, New Zealand, and Vanuatu are identified as having the potential to generate a tsunami significant to the ports of Los Angeles and Long Beach, so these are investigated in detail. Study results suggest that M_w 9.3 earthquakes can trigger a tsunami with wave amplitude reaching up to 2 m (≈ 6.5 ft) and currents exceeding 8 knots (≈ 4 m/s) in the ports of Los Angeles and Long Beach. Currents are particularly noteworthy since those exceeding 8 knots (≈ 4 m/s) are known to break mooring lines and damage harbor piers and other structures.

Chapter 1

Introduction

Los Angeles County hosts two container ports adjacent to one another in San Pedro Bay that are operated separately by the cities of Los Angeles and Long Beach. The satellite image shown in Figure 1.1 provides a view of San Pedro Bay in which each port and harbor system is distinguished from the other. Although the ports compete for business, they are the two busiest container ports in the United States and together combine as the world's fifth busiest (15.7 million total TEU–Twenty–Foot Equivalent Unit), following the ports of Singapore (27.9 million TEU), Shanghai (26.2 million TEU), Hong Kong (23.9 million TEU), and Shenzhen, China (21.1 million TEU). The ports contribute significantly to the economy of California and to the United States as a whole. Annual state and local tax revenue exceeds 5 billion dollars. The contribution of trade to the economy of California is approximately $58 billion and approximately $20 billion throughout the entire United States (Port of Los Angeles, 2009; Port of Long Beach, 2009; Coastal Conservancy, 2009).

A deterministic tsunami hazard assessment is provided for the ports of Los Angeles and Long Beach. The goal of this assessment study is to identify probable maximum tsunamis (tsunamis with potential high impact) by investigating many possible source scenarios under which a magnitude M_w 9.3 earthquake would generate a tsunami with impact on the Ports. This work leverages previous investigations (Borrero et al., 2004; Borrero, 2002; Borrero et al., 2001) of the near–field fault line sources of Santa Catalina Island, Santa Monica, Newport–Inglewood, and San Mateo, as well as landslide sources from the Channel Islands and off of Palos Verdes (Figure 1.2). Later investigations conducted by Moffatt and Nichol expanded these studies to include Cascadia sources. Prior to the November 2006 Kuril Island event, most studies focused on wave heights as the dominant measure of hazard. However, the impact of the Kuril Island tsunami on Crescent City demonstrated that distant sources have the potential of inducing strong currents with small amplitude waves in harbors that can cause substantial damage. The Tsunami Forecast Database of tsunami source

Figure 1.1: Satellite image of the Ports of Los Angeles and Long Beach (TerraServer–USA and USGS). The red dotted line demarks the border that separates the two ports. Model validation is based on the Los Angeles tide gauge located at Berth 60, as shown and marked in blue. The low elevations surrounding the Ports of Los Angeles and Long Beach makes the region vulnerable during a tsunami event. Residents of the densely populated cities of San Pedro, Harbor City, Long Beach, and Rancho Palos Verdes along with the many tourists that visit attractions including Cabrillo Beach Park, the Queen Mary, and the Aquarium of the Pacific are at risk from tsunami impact.

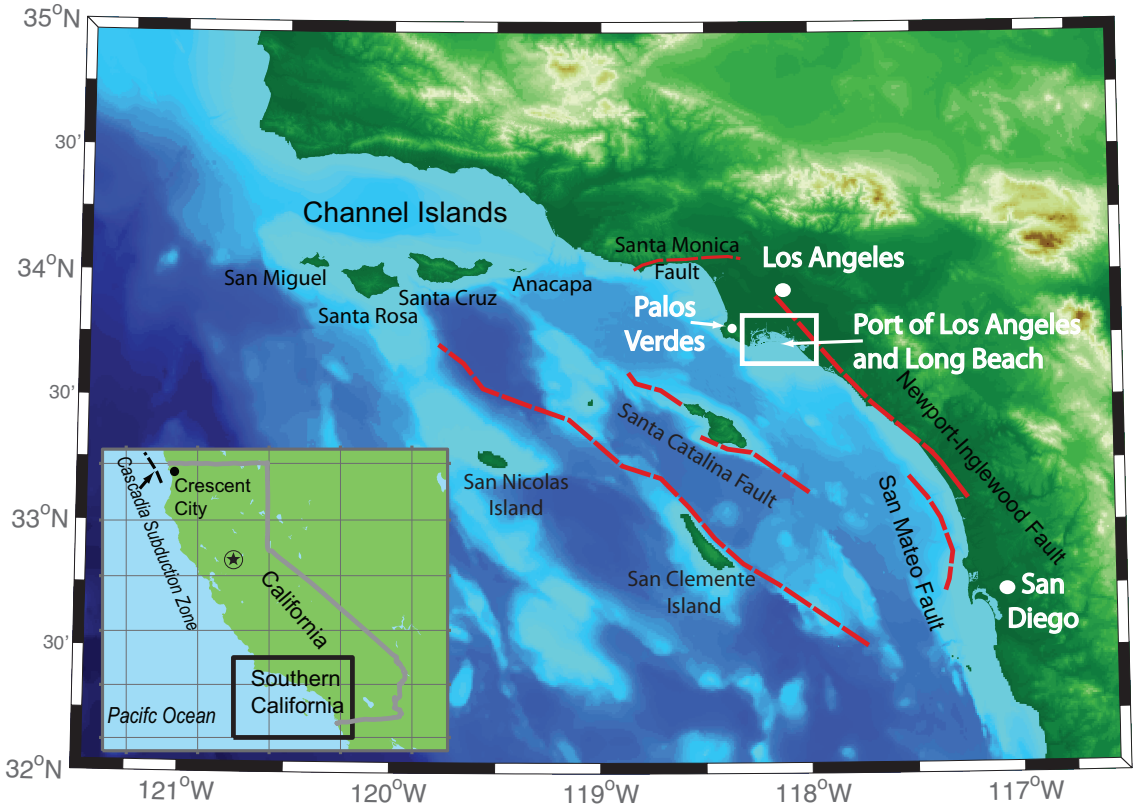

Figure 1.2: Regional setting showing geographic features of Southern California and surrounding major offshore fault lines with respect to Ports of Los Angeles and Long Beach.

functions was used in the study to develop all tsunami propagation scenarios. Tsunami Source Functions are a collection of tsunami propagation model runs that have been pre-computed for selected locations along known and potential earthquake zones. The forecast database for the Pacific consists of over 850 source functions, equivalent to a tsunami generated by a M_w 7.5 earthquake. These were used to develop combination sources for larger events of this study. Only the sources that can potentially produce significant impact at the studied location have been used in the high-resolution computations. To investigate the hazard posed by currents, a sensitivity study was performed for 322 synthetic tsunami sources for M_w 9.3 earthquakes along Pacific Rim subduction zones using the Method of Splitting Tsunamis model (Titov and Synolakis, 1998). Of the scenarios investigated, 11 sources in Alaska, Chile, Philippines, Manus, New Zealand, and Vanuatu have been identified as posing the greatest risk to the ports of Los Angeles and Long Beach. There are no potential Hawaiian tsunami sources, with the exception of a catastrophic yet improbable slope failure. Consideration of such an event is not addressed as part of this study. Tsunami amplitudes are computed at the Los Angeles tide gauge for each synthetic M_w 9.3 earthquake generated as a result of a 30–m rupture on a 1000–km × 100–km area along each subduction zone. In total, 322 scenarios are considered: 56 from Alaska/Aleutians, 106 from Central and South America, 13 from Nankai Trough and Ryuku, 28 from Solomons and Vanuatu, 30 from New Zealand, 6 from New Guinea, 8 from Manus, 66 from Kurils and Mariana, and 9 from the Eastern Philippines. Results of this study suggest that a great M_w 9.3 earthquake could potentially trigger a tsunami with wave amplitudes reaching up to 2 m (≈ 6.5 ft) and current velocities exceeding 4 m/s (≈ 8 knots) inside the harbors in which the Ports of Los Angeles and Long Beach are located. Study results also suggest that Pacific Basin subduction zones in addition to those in Alaska and along the Aleutians and Cascadia are capable of generating tsunamis that pose a threat to Ports of Los Angeles and Long Beach.

1.1 Review of Earlier Work

The first detailed study of the hazard posed to California by tsunamis generated in the far field was conducted by Houston and Garcia (1974). In this study, the 100–year and 500–year tsunami runup heights for selected locations along the California coastline were computed using a combination of numerical and analytical methods. Tsunamis generated in both the Alaska–Aleutians subduction zones and the South America Subduction Zones, based on the 1964 Great Alaska and 1960 Chilean earthquakes, were considered in the study. Houston and Garcia's approach involved breaking up the Alaska–Aleutian subduction zone into twelve discrete segments to identify "worst–case scenarios." A

maximum vertical uplift of 8–10 m was assumed based on initial ground deformations due to the hypothetical uplifting of an ellipsoidal mass approximately 1000 km long having an aspect ratio of 1:5. Using a one–dimensional linear shallow–water equation in spherical coordinates, Houston and Garcia propagated their initial waves from the Alaskan and Chilean sources to California. At the continental shelf, an analytical expression was derived to match the inner– and outer–harbor wave amplitudes and obtained a simple amplification factor to produce wave amplitudes at offshore locations. Three limitations to their solution were noted. First, a one–dimensional model was applied for the solution of near–field events. This solution, however, is not *a priori* appropriate for complex nearshore bathymetry, such as in narrow bays. Second, they used a sinusoidal wave in the analytical solution close to shore, but this can lead to substantial errors in the solutions of the runup. Third, small–scale nearshore features affect local inundation and runup to first order, but were neglected in the coarse gridded computation of Houston and Garcia (1974).

McCulloch (1985) built on the results of Houston and Garcia (1974) and Houston (1980) from far–field tsunamis. McCulloch assessed the tsunami threat using an empirical formulation that related earthquake magnitude to tsunami wave height without the use of a hydrodynamic model. Synolakis et al. (1997) explained that such empirical formulas were developed for use in specific locales within Japan, and, as a result, generally under–predicted the runup in other earthquake regions.

Following the 1992 Cape Mendocino earthquake and tsunami that struck the coastline within minutes of the earthquake, McCarthy et al. (1993) performed a systematic analysis of all available historical records to assess future tsunami hazards to California. Investigators divided California into four coastal sections and qualitatively evaluated each section according to tsunami risk. They determined the risk of tsunami as *high* along the coastline from Crescent City to Cape Mendocino, *moderate* from south of Cape Mendocino to north of Monterey, *high* from Monterey to Palos Verdes, and then *moderate* from south of Palos Verdes to San Diego. These results provided the baseline for future investigations such as that of Borrero (2002), who applied developments in numerical modeling to show the limitations of McCarthy et al.'s (1993) results. Synolakis et al. (2002) used the 1998 M_w 7.0 Papua New Guinea event, in which greater than 1000 people lost their lives, to prove that even a moderate earthquake could have a highly localized catastrophic impact as the result of a submarine landslide. This finding had been controversial for many years (Geist, 2000, 2001; Okal and Synolakis, 2001) and remained so until Borrero (2002) investigated and documented historical submarine landslides in conjunction with an inundation mapping study underway for the California Office of Emergency Services. He introduced an innovative analysis of tsunami waves from landslide sources by use of a hydrodynamic model to assign initial landslide

conditions. Borrero found that the waves generated by catastrophic failures during historical events in the Santa Barbara Channel, Santa Monica and Redondo Canyons, and off the Palos Verdes Peninsula caused high, but localized inundation and runup. The approach, while empirical, was gaining acceptance through preliminary validation, see Synolakis (2003).

Dykstra and Jin (2006) and Moffatt and Nichol (2007) reinvestigated the work of Borrero (2002) and computed tsunamis in the ports of Los Angeles and Long Beach. They looked at tsunamis generated in the near field coupled with two Palos Verdes landslides and three tsunamis generated along the Cascadia subduction zone. The Moffat and Nichol report considered the Cascadia Subduction Zone as the only far–field tsunami source. Uslu (2008) looked at Pacific–wide tsunami scenarios, including those impacting Central and Northern California, to assess a probabilistic return rate of the hazard. His work was complementary to the near–field inundation mapping work of Borrero (2002) in that far–field tsunami sources were investigated.

Prior to the Kuril 2006 earthquake and tsunami, current velocity measurements were not routinely taken inside California harbors. The only data available during and following an event were heights recorded at tide gauge stations. As a result, most studies focused on wave heights as the measure of hazard. Following the 2006 Kuril Islands tsunami, eye witness accounts in Crescent City put the currents in the approximate range of 10 knots inside the protected harbor. This Kuril 2006 tsunami caused greater than $10 million damage to Crescent City (Dengler et al., 2008; Kelley et al., 2006; Uslu, 2008). Observed currents in Crescent City Harbor following this 2006 event showed, contrary to previous studies, that a tsunami generated in the far field has the potential to induce small amplitude waves with large, and consequently, destructive currents in harbors. With this in mind, the goal of this study is to provide a tsunami hazard assessment for the California ports of Los Angeles and Long Beach that includes both maximum amplitudes and current velocities. Earthquake sources in the far field from which tsunamis are generated and expected to have the greatest impact on the activities and economy of the ports are identified.

Chapter 2

Background

2.1 The Tsunami History of California

Studies have shown that tsunamis triggered by similar magnitude earthquakes along dissimilar subduction zones may result in substantially different impact at the same harbor (Dengler et al., 2008; Kelley et al., 2006; Uslu, 2008). The Kuril Islands earthquakes of 1933, 1994, 2006, and 2007 were of similar magnitudes and similar source locations, but produced different far–field impact due to fault orientation differences. The events of 1933 and 2006 were thrust fault earthquakes, and the 2007 earthquake had a normal fault mechanism. The 1994 earthquake was described as a vertical tear in the slab near the Hokkaido corner by Tanioka et al. (1995), but has been successfully modeled as a thrust fault in Uslu (2008); Dengler et al. (2008).

Table 2.1 provides a list of historical earthquakes that generated damaging Pacific–wide tsunamis and had a significant impact on the California coastline since 1868. No data are available during most of these events, but observations recorded at the time of the 1952 Kamchatka, 1960 Chile, 1964 Great Alaska, and 2006 Kuril Islands events are used in the hazard assessment of the ports of Los Angeles and Long Beach. Two of these events, the 1960 Chile and the 1964 Great Alaska, are particularly noteworthy. In 1960, a large M_w 9.5 earthquake in Chile generated a tsunami that propagated northward and caused greater than $1 million in damage to the Port of Los Angeles. The tsunami also struck Santa Barbara and broke the mooring lines of one dozen vessels and destroyed a 50–m dock in San Diego (Lander et al., 1993).

The M_w 9.3 1964 Great Alaska Earthquake and tsunami caused eleven fatalities, ten of which were drowning deaths in the Northern California community of Crescent City. Damage from this tsunami was estimated at greater than $17 million in California (Lander et al., 1993). The waterfront and 29 city blocks of Crescent City were damaged or destroyed, with total damage estimated at $15 million. The tsunami was recorded on tidal gauges statewide and caused

Date	Source	M_w	Damage/Effect
1868	Peru	9.3	Minor flooding in San Pedro and Wilmington
1896	Japan	8.0–8.6	Damage in Santa Cruz
1906	Ecuador	8.3	Ships caught in eddies in San Francisco
1922	Chile	8.3	Strong currents
1923	Kamchatka	8.4	Shipping affected in Los Angeles
1946	Aleutian Islands	8.6	90 cm tsunami in Crescent City, broken moorings in northern California and one fatality.
1952	Kamchatka	9.0	4 boats sunk in Crescent City
1957	Aleutian Islands	8.3–8.6	Damage to ships and docks in San Diego
1960	Chile	9.5	$1 million damage in LA Harbor
1964	Alaska	9.2	$17 million damage+12 fatalities
1965	Aleutian Islands	8.7	60 cm sea level rise in Santa Cruz
1975	Hawaii	7.2	Minor damage to a dock on Catalina Island.
2006	Kuril Islands	8.3	$9.7 million in damage in Crescent City

Table 2.1: List of significant far-field generated tsunamis that have affected California (Lander et al., 1993). Seismic moments updated (Okal, 1992, 2007).

approximately $1 million damage at various marinas inside San Francisco Bay, including Sausalito, San Rafae,l and Berkeley. The tsunami also caused strong surges that tore 75 small vessels from their moorings and sank 3 boats in the ports of Los Angeles and Long Beach even without high waves. Unconfirmed reports from Ventura Harbor suggest that the tsunami damaged several vessels (Synolakis, 2008). There were also reports of strong surges and a water level rise of 2 m in San Diego (Lander et al., 1993).

Other notable events impacting Southern California include the M_w 8.6 1946 Aleutian Islands earthquake. The tsunami carried boats one quarter mile inland in Half Moon Bay, washed away a pier on Catalina Island, broke ship moorings in Los Angeles, and caused minor damage in Santa Cruz. The M_w 9.0 1952 Kamchatka tsunami capsized five small boats and moved a 60–ton mooring buoy in Crescent City. This tsunami also caused damage in Santa Cruz. The M_w 8–8.6 1896 Sanriku earthquake in Japan generated a tsunami that propagated across the pacific. It destroyed a dike and caused damage to a ship anchored in Santa Cruz (Lander et al., 1993).

The 2006 Kuril Islands tsunami clearly impacted the California coastline with the set-up of currents that damaged Docks F, G, and H in the small boat basin within Crescent City harbor, shown in Figure 2.1 (Dengler et al., 2009). In addition, other earthquakes generated tsunamis that caused strong currents. The 1960 Ecuador tsunami has been observed with strong currents in San Diego and San Francisco (Soloviev and Go, 1974), and the 1923 Kamchatka tsunami was

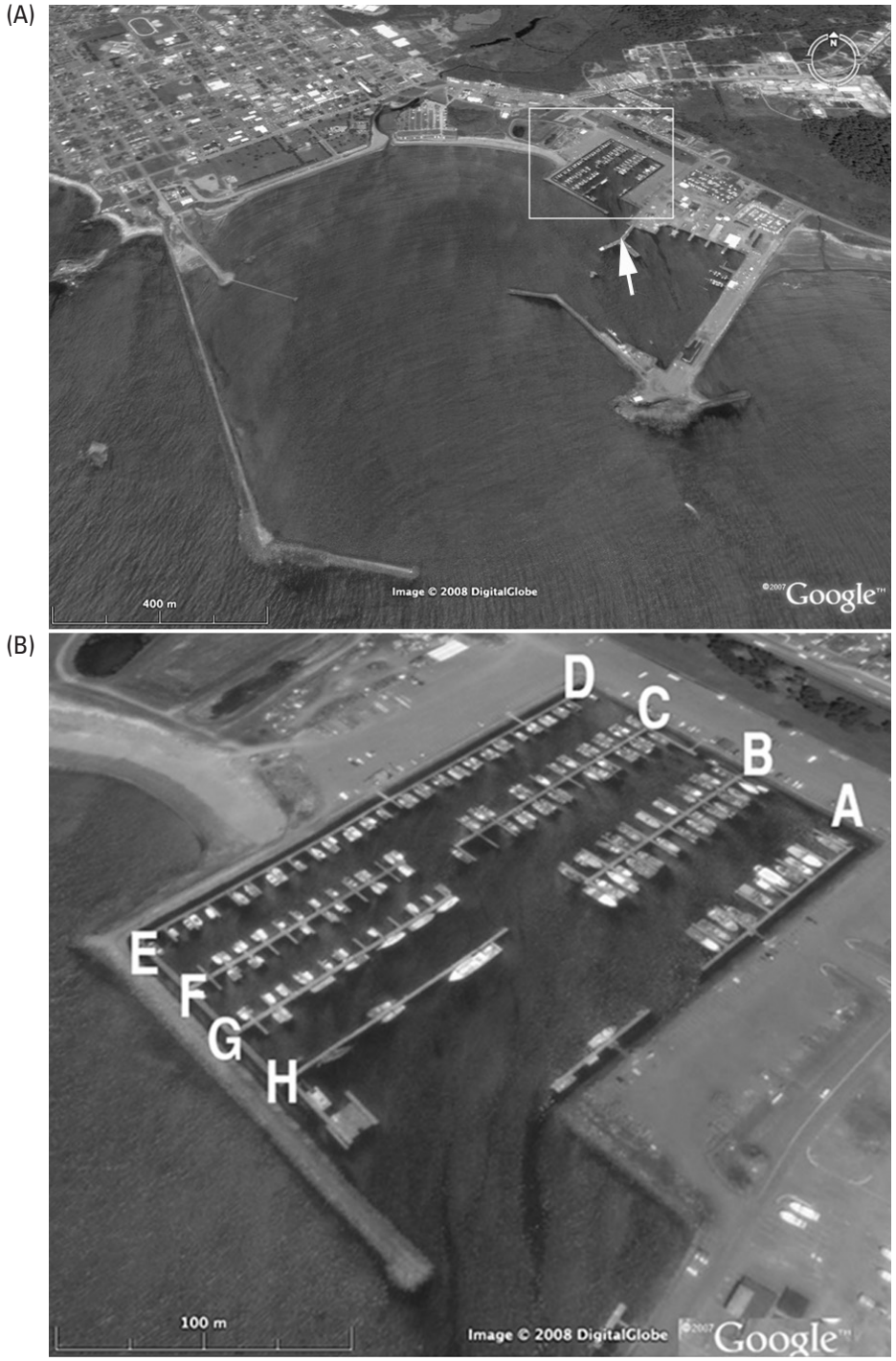

Figure 2.1: A Google Earth view of Crescent City and Crescent City Harbor. The upper figure shows Crescent City with the white box marking the small-boat basin, and the lower figure shows the small boat basin, where the Docks F, G, and H were damaged during the 2006 Kuril Islands Tsunami (Dengler et al., 2009).

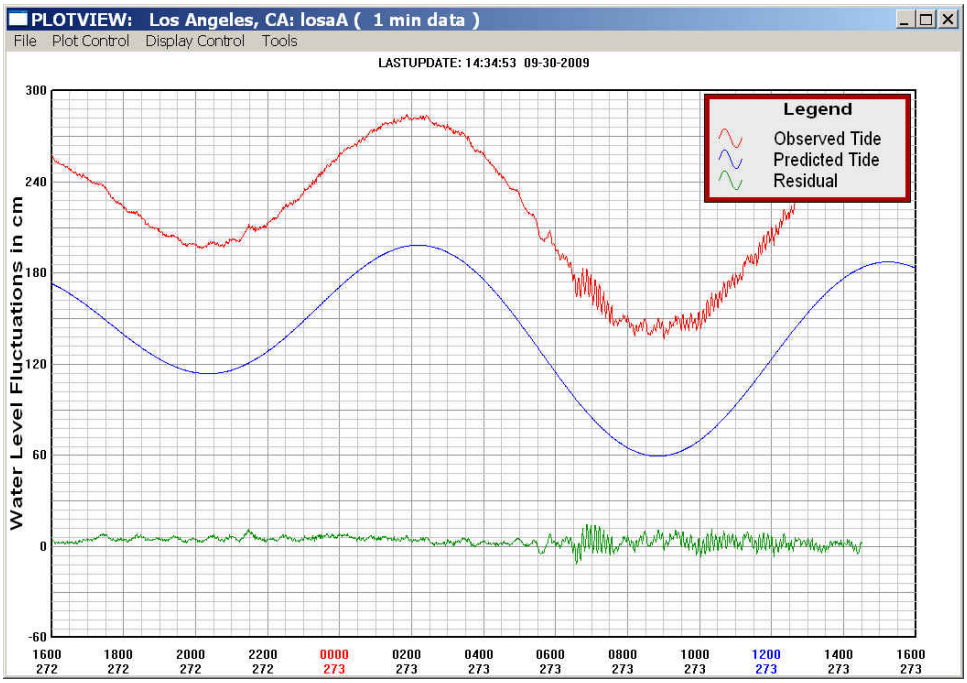

Figure 2.2: 2009 Samoa tsunami recorded at the Los Angeles tide gauge, provided by WCATWC (2009).

recorded with 5 cm in San Diego and 15 cm in San Francisco, and the shipping was greatly affected in Los Angeles because of strong currents (Lander et al., 1993).

On 29 September 2009, a M_w 8.0 earthquake occurred 195 km (125 miles) south of Apia, Samoa at 17:48 UTC (USGS, 2009). The tsunami was recorded at the Los Angeles tide gauge approximately 11 hours later with a height of approximately 25 cm ($\approx$ 10 in), but did not cause any significant damage to the ports of Los Angeles and Long Beach. Figure 2.2, provided by WCATWC (2009), shows the observed tsunami signal following the 2009 Samoa tsunami as recorded at the Los Angeles tide station. The red line is the signal as observed, the blue line shows the predicted tide, and the green line is the de–tided record showing the isolated tsunami signal.

On 15 November 2006, a tsunami generated by a M_w 8.3 earthquake occurring along the Kuril Islands subduction zone caused significant damage to Crescent City. This event was followed closely in time by a M_w 8.1 earthquake and tsunami on 13 January 2007. One decade prior to these events, a tsunami was generated by a M_w 8.3 earthquake that occurred 4 October 1994. Significantly, these earthquakes all had different fault mechanisms even though they occurred adjacent to one another along the Kuril Islands subduction zone. The 2006 event was a classic inter–plate thrust mechanism. The 2007 earthquake

involved normal faulting in the outer rise, probably triggered by stress transfer from the 2006 earthquake. The 1994 earthquake resulted from a slip on a relatively deep (68 km) vertical tear in the slab near Hokkaido, Japan (Tanioka et al., 1995). The difference in earthquake mechanism is particularly significant since all three events generated tsunamis with diverse characteristics. The 1994 Shikotan tsunami ran up locally 5 to 9 m (16–30 ft) and inflicted significant damage to the coast of the southern Kuril Islands (Yeh et al., 1995). A tsunami of amplitude 30 cm (1 ft) was recorded at the Crescent City, California tide gauge following the 1994 event. The 2007 tsunami amplitude was recorded as 25 cm at the Crescent City tide gauge.

The M_w 8.3 15 November 2006 earthquake occurred at approximately 11:14 (UTC) offshore of the central Kuril Islands of Simushir, Rasshua, and Matua, which are uninhabited and inaccessible during the winter months. Therefore, the local tsunami impact on these islands remained unknown until 2007 field work conducted during the summer season revealed runup of up to 21 m (69 ft) on Matua (Bourgeois, 2007; Levin et al., 2008). On Hokkaido Japan, the November 2006 tsunami reached Hanasaki in 64 min and was measured at Japanese tide gauges as 0.5 m ($\approx$ 1.5 ft). As a result, a large tsunami was not anticipated in Alaska nor along the U.S. Pacific coast, yet, on the afternoon of 15 November 2006, Crescent City was hit by a series of strong waves, completely damaging three of the eight docks in the harbor.

The impact on Northern California of tsunamis generated along the Cascadia Subduction Zone has been discussed by Uslu et al. (2007). The Cascadia Subduction Zone extends from Cape Mendocino, California in the south and beyond Vancouver Island in the north, for a total length of 1000 km as shown in Figure 2.3. The Cascadia Subduction Zone is marked by a variable subduction rate, approaching 4 cm/yr where the Juan de Fuca plate dives beneath the North American plate in the vicinity of Washington State (Satake et al., 2003). A slower rate of subduction, 3 cm/yr, is noted at the northern end of the Gorda plate offshore of northern Oregon (Wang et al., 2001). Near the Mendocino triple junction in Northern California where the Gorda Plate terminates, the rate of subduction approaches zero (Clarke and Carver, 1992). A rupture along the Gorda Plate offshore of Southern California poses a great risk to Northern California, but a comparably smaller threat to the coastlines of Central and Southern California.

Satake et al. (1996, 2003) identified a historically reported tsunami in Honshu, Japan in the year 1700. They used coastal subsidence data coupled with numerical simulations to infer that the tsunami was generated at approximately 05:00 (UTC) on 27 January 1700 by a M_w 9.0 Cascadia Subduction Zone earthquake (Uslu et al., 2008). Since there are no direct seismic or geodetic observations to identify the physical behavior of the rupture zone, Wang et al. (2003) combined information about the 1700 A.D. earthquake with relevant data from

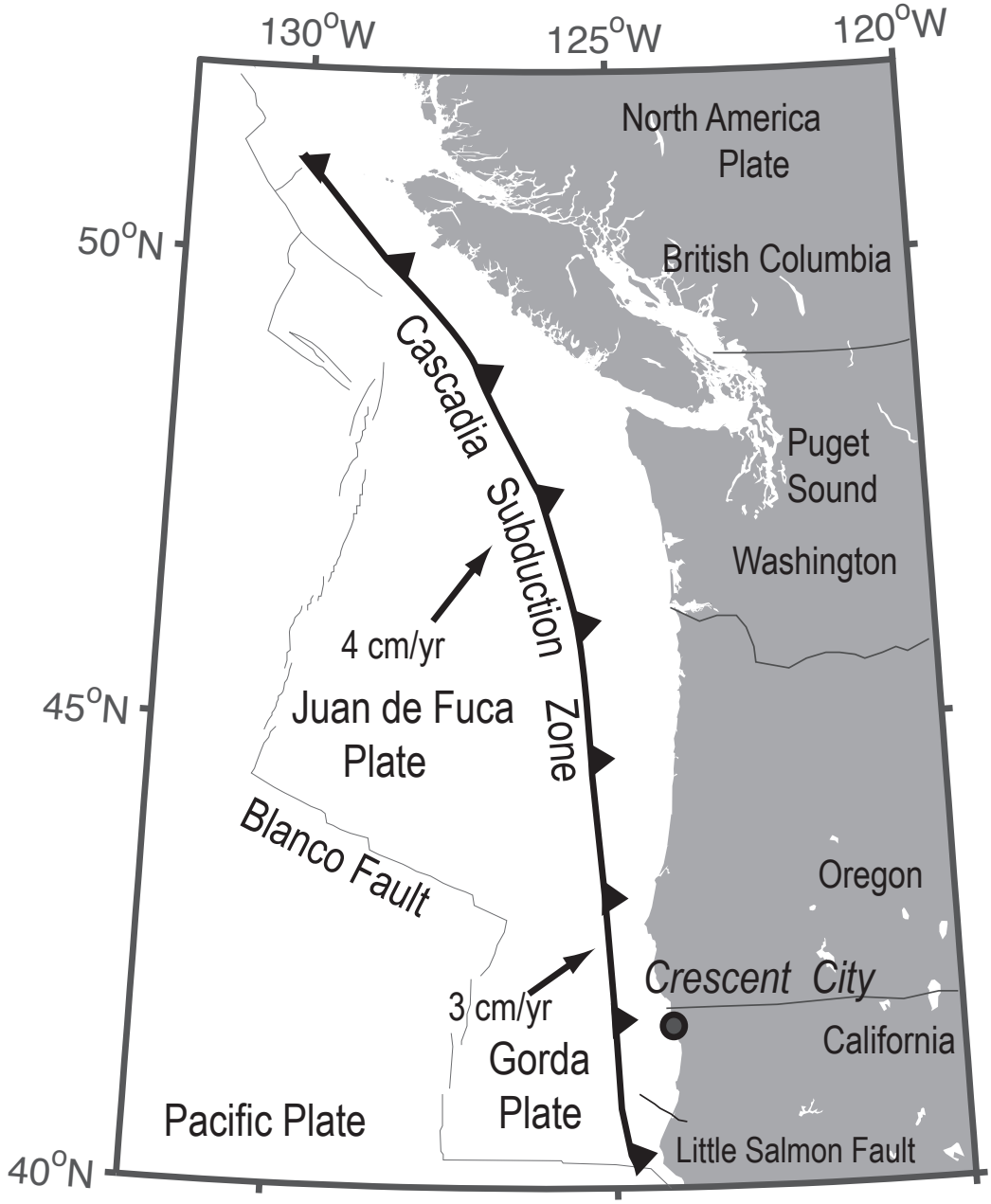

Figure 2.3: Map of the Cascadia Subduction Zone, the Juan de Fuca, Gorda, and Pacific Plates (modified from Satake et al., 2003). Cascadia extends northward from Northern California to just north of Vancouver Island in British Columbia, Canada.

other subduction zones and calculated windows for the potential extent of rupture, strains, rupture velocities, and uplift rates. Their approach assumed a co–seismic rupture over the entire subduction zone with an average recurrence of 500 years, which is a scenario believed to be conservative.

Chapter 3

Tsunami Modeling of California Ports and Harbors

The high–resolution tsunami forecast model used for this study was previously developed for the city of Los Angeles by the NOAA Center for Tsunami Research as part of a tsunami forecasting system under development for use by NOAA's two Tsunami Warning Centers. The high–resolution models capable of simulating wave inundation on land are called inundation models. The ability of the model to reproduce moving boundary conditions (water moving on dry land) is critical to assess the impact of large tsunamis. Therefore, only inundation models should be used for the impact studies, especially if current velocities are to be reproduced, since the inundation dynamics can change the flow velocity substantially. A particular scenario may or may not produce inundation (water actually penetrating onto dry land), but the use of an inundation model is critical, since we cannot predict if this is going to happen or not. Also, the water withdrawal can be tracked only with inundation models. An optimized version of the model is developed to run efficiently in an operational environment without degradation of results. For this hazard assessment study, the high–resolution reference model was applied to the tsunami forecast model and was benchmarked using both available historical data and synthetic scenarios. The study applies the Los Angeles tsunami model to a hazard assessment of the vulnerability of the southern California ports of Los Angeles and Long Beach. Tsunami–induced currents and maximum wave amplitudes are computed following tsunami generation in the far field based on synthetic scenarios selected to quantify the expected worst case.

3.1 Methodology

Tsunamis are triggered by deformation of the seafloor or by impacts sufficient to displace large volumes of water. Underwater earthquakes are the primary

generation mechanism of tsunamis, but other less common events such as volcanic eruptions, landslides, or meteor impacts can also cause tsunami waves. Once generated, a tsunami propagates away from its source throughout the ocean and then inundates vulnerable coastlines. Regardless of the mechanism, once generated, the potential impact of a tsunami to a coastal community, such as that of the southern California coast along which reside the ports of Los Angeles and Long Beach, can be modeled to provide expected wave arrival time and estimates of maximum amplitude, current velocities, and inundation.

A high–resolution inundation model was developed for Los Angeles and used as the basis for development of a complementary optimized tsunami forecast model to provide an estimate of wave arrival time, wave amplitudes, current velocities, and inundation immediately following tsunami generation. Both high–resolution and optimized tsunami forecast models are based on the Method of Splitting Tsunami (MOST) model, which is a suite of numerical simulation codes capable of simulating three processes of tsunami evolution: earthquake, trans–oceanic propagation, and inundation of dry land. Both models were developed previously by the NOAA Center for Tsunami Research and both are used in this study.

The MOST model was validated through a series of laboratory experiments and benchmarked with numerous field surveys (Titov and Synolakis, 1997, 1998). The codes conform to the standards and procedures outlined by Synolakis et al. (2008) and have been used extensively for simulations of historical events prior to this study. Initial water surface elevation, evolution of wave propagation, tsunami inundation, and current velocities are computed by solving the governing non–linear shallow water equations with a finite difference algorithm (Titov and Synolakis, 1997, 1998). The initial displacement of the water surface is of profound significance in calculating the evolution of the resulting waves. It is assumed that displacement is instantaneous so the net seafloor displacement can be considered as an initial condition for the free surface. In this study, an inundation model is necessary for accurate computation of velocities due to overland flow at the coastline. Wave amplitudes and depth–averaged current velocities are computed at each grid point for every modeled time step. Runup onto the shoreline is computed by introducing moving grids to simulate the evolution on initially dry land. To arrive at the governing shallow water equations, total depth is defined as $h = \eta(x, y, t) + d(x, y, t)$, where$\eta(x, y, t)$ is the wave amplitude at the surface, and d(x,y,t) is the undisturbed water depth; $u(x, y, t)$ and $v(x, y, t)$ as the depth–averaged current velocities in the onshore x and long–shore y directions, respectively; and g as the acceleration of gravity, the shallow water equations, then, are:

$$h_t + (uh)_x + (vh)_y = 0, \tag{3.1}$$

$$u_t + uu_x + vu_y + gh_x = gd_x \tag{3.2}$$

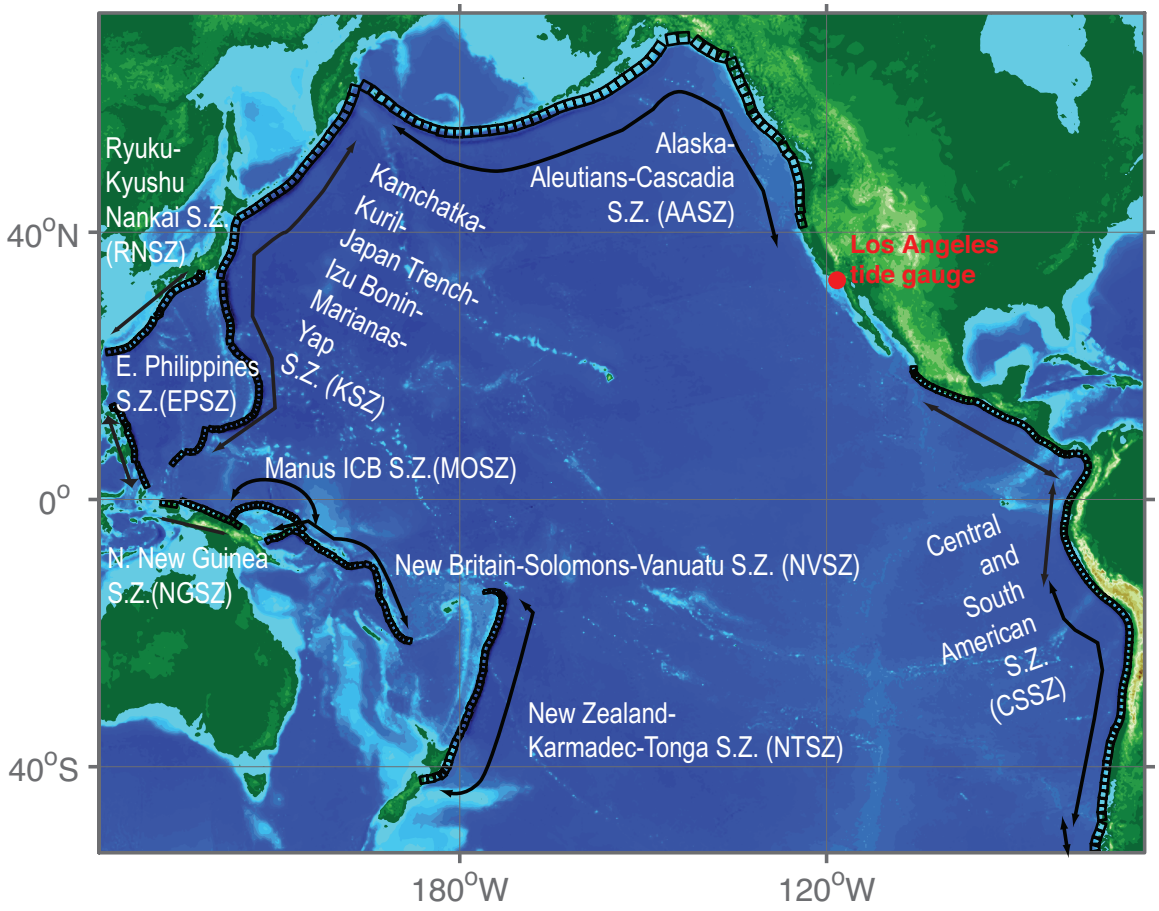

Figure 3.1: Pacific Basin subduction zone propagation database unit sources shown relative to the Los Angeles tide gauge.

and

$$v_t + uv_x + vv_y + gh_y = gd_y. \tag{3.3}$$

3.2 Propagation Database

A pre–computed propagation database consisting of water level and flow velocities over all basin grid points and based on potential seismic unit sources has been developed for the world ocean basins by the NOAA Center for Tsunami Research (Gica et al., 2008). Subduction zones have been broken up into fault segments, or unit sources, each measuring 100 km long by 50 km wide. The propagation database is created from each of these discrete earthquake ruptures segments by computing wave propagation throughout the entire Pacific Basin. There are 403 unit sources from earthquakes of 100 km x 100 km and 1 m rupture. Figure 3.1 shows forecast propagation database locations with

respect to the Los Angeles tide gauge. Heights and currents are computed at the Los Angeles tide station, identified in red in Figure 3.1. The largest earthquake since the turn of the twentieth century was recorded in the Southern Chile region shown in Figure 3.1. Several large earthquakes occurred along the Alaska/Aleutians subduction in the mid–twentieth century, the largest of which was the 1964 Great Alaska earthquake in Prince William Sound. All earthquakes modeled for this study are assumed as occurring from a thrust fault mechanism, with the exception of the 2007 Kuril Islands event. This earthquake was due to a normal fault mechanism, yet was successfully modeled with a negative slip applied to the propagation database. Larger events are modeled by combining unit sources. A M_w 9.3 event can be modeled as a 1000–km × 100–km rupture with a 30–m slip, which is effectively a combination of 10 M_w 7.6 events scaled up 30 times. Detailed source information for each specific subduction zone used for this study appears in Appendix C.

3.3 Numerical Grids

Modeling of the ports of Los Angeles and Long Beach is accomplished by utilizing a previously developed set of three nested grids, referred to as A–, B–, and C–grids, that telescope down from a large spatial extent to a grid that finely defines the two ports in detail. Each of the three grids becomes successively finer in resolution as they telescope from offshore into the port center. The offshore area is covered by the largest and lowest resolution C–grid, while the near-shore details are resolved within the finest scale A–grid to the point that tide gauge observations recorded during historical tsunamis are resolved. The basis for these grids is a high–resolution digital elevation model constructed by the National Geophysical Data Center using best available bathymetric, topographic, and coastal shoreline data. Data were compiled from a variety of sources to produce a digital elevation model referenced to Mean High Water in the vertical and to the World Geodetic System 1984 in the horizontal (http://ngdc.noaa.gov/mgg/ inundation/tsunami/inundation.html). From these digital elevation models, the set of three high–resolution, nested "reference" models was constructed. A detailed discussion of grid preparation is provided by Tang et al. (2008a,b).

The grid setup for the ports of Los Angeles and Long Beach study is shown in Figure 3.2. Tsunami waves pass through each of the two outermost nested grids, arriving at the innermost nested grid that contains the two ports. The resolution of each grid increases from the outer, offshore grid to the inner, harbor grid gradually. The outermost or A–grid includes the Southern California continental shelf. Two sets of model grids are used for this study: one for the high–resolution model and another for the optimized forecast model. The high–resolution model has an outer 30 arc–sec grid, middle 6 arc–sec grid, and an

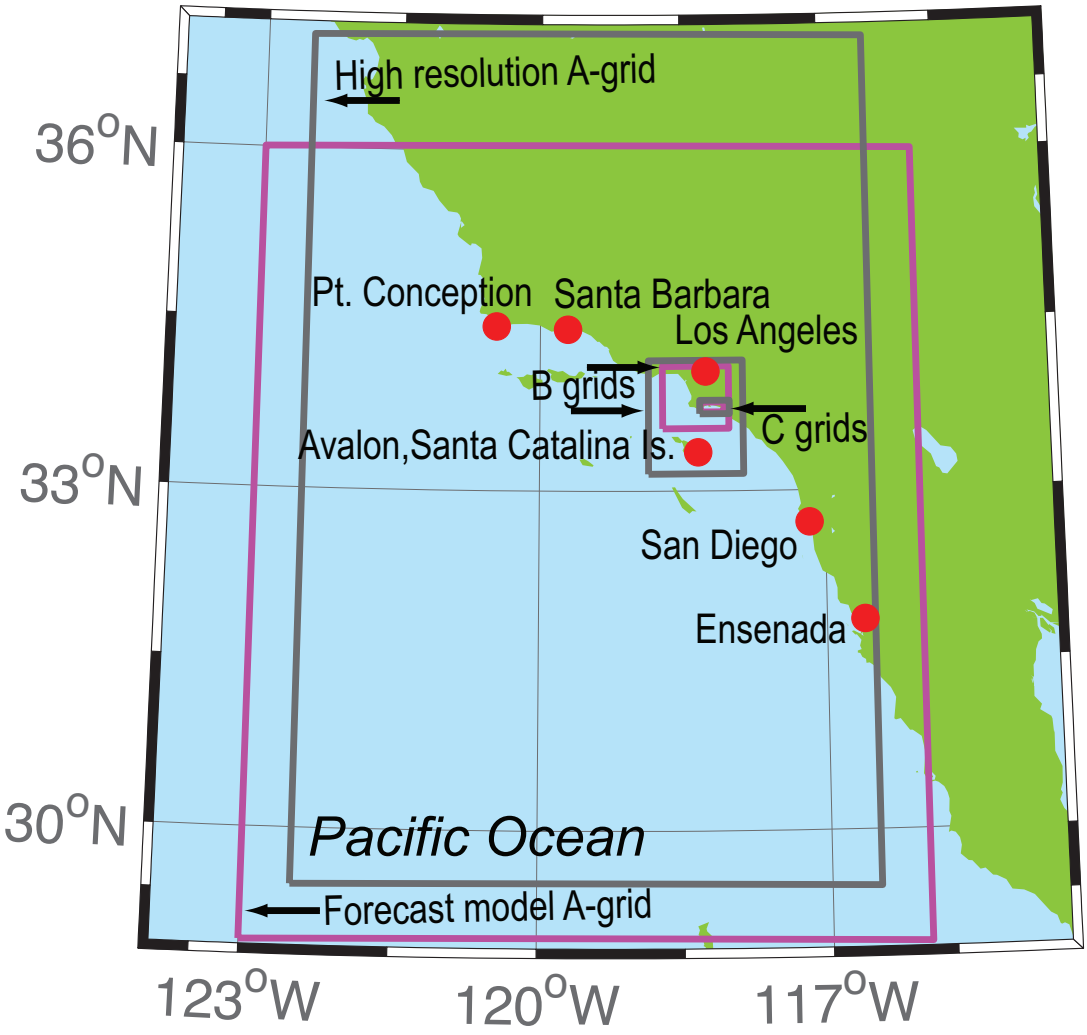

Figure 3.2: Merged nested bathymetry/topography grid locations for Southern California. Magenta boxes demarcate the forecast model grids and the grey boxes show the high resolution reference model grids. The grids are nested; the outer grids are low resolution, and the inner grids are high resolution.

Date	Event	Time (UTC)	M_w	Lat.	Lon.	Source
2006-05-03	Tonga	15:26:39	8.1	20.13N	174.164W	6.6×b29 NTSZ
1964-03-28	Alaska	03:36:14	9.2	61.04N	147.73W	10 × (400km × 290km)+ 10 × (400km×175km)
1960-05-22	Chile	19:11:14	9.5	45.88S	76.29W	20.0 × (a88 − 97 + b88 − 97)CSSZ
1952-11-04	Kamchatka	16:58:26	9.0	52.75N	159.5E	7.0 × (a1 − 7 + b1 − 7) KISZ

Table 3.1: Historic Tsunami Sources recorded at Los Angeles tide station (Uslu, 2008; Borrero et al., 2007; 2006; Tang et al., 2008b;a).

inner 1 arc–sec grid. The resolution of these model grids supports a detailed study of harbor resonance and inundation. The lower resolution forecast model is constructed to provide efficient computational run time, but has been benchmarked against the high–resolution model and compared with available tide gauge records. For the forecast model, the outer grid resolution is 120 arc–sec, the middle grid is 12 arc–sec, and the inner grid is 3 arc–sec. High–resolution model grids (magenta boxes) are distinguished from forecast model grids (gray boxes) in Figure 3.2.

3.4 Using MOST to Simulate Historical Events

The complexity of Southern California's offshore regional bathymetry of the Channel Island, Santa Catalina Island, and the harbor in which reside the ports of Los Angeles and Long Beach pose challenges to the modeling of tsunamis. Numerical modeling of this region, and the investigation of historical events from the most active subduction zones in Alaska/Aleutians and Kurils to the North–Northwest of Southern California and South American subduction zones to the south, has shown that California's offshore geology helps to dissipate tsunami energy.

Four historical tsunamis recorded by the Los Angeles tide gauge, listed in Table 3.1, provided case studies for use as a benchmark for this work. Historical records of wave amplitudes at the tide gauge from these four events, 1952 Kamchatka, 1960 Chile, 1964 Alaska, and 2006 Tonga, are compared to the modeled results of both the high–resolution and forecast model as shown in Figure 3.3. The recent M_w 8.8 Chile earthquake and tsunami provided the opportunity for additional model validation. A comparison between observation at the tide gauge and the model results for 2010 Chile tsunami is provided in Figure 3.4. Computed forecast model and high–resolution model results confirm the accuracy of the forecast model. The maximum wave during the 1952 tsunami is observed as the sixth wave in the series that struck the Los Angeles tide gauge, while the maximum tsunami wave is computed by the model to be the ninth.

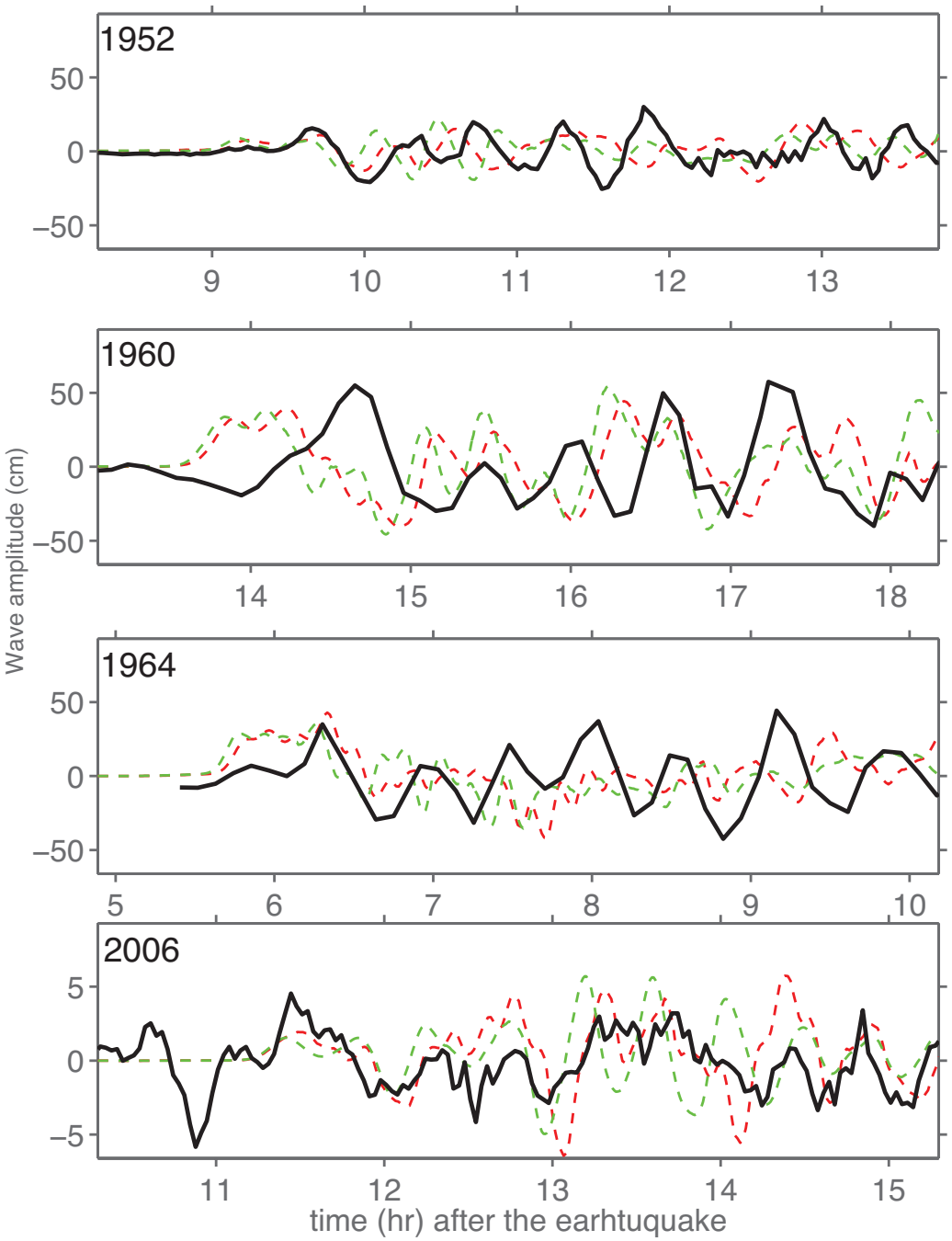

Figure 3.3: Time series of the 1952 Kamchatka, 1960 Chile, 1964 Alaska, and 2006 Tonga tsunamis computed at the Los Angeles tide gauge. The black line shows the time series at the tide gauge while computed time series from the high–resolution reference model and the optimized forecast model are shown in red and green, respectively.

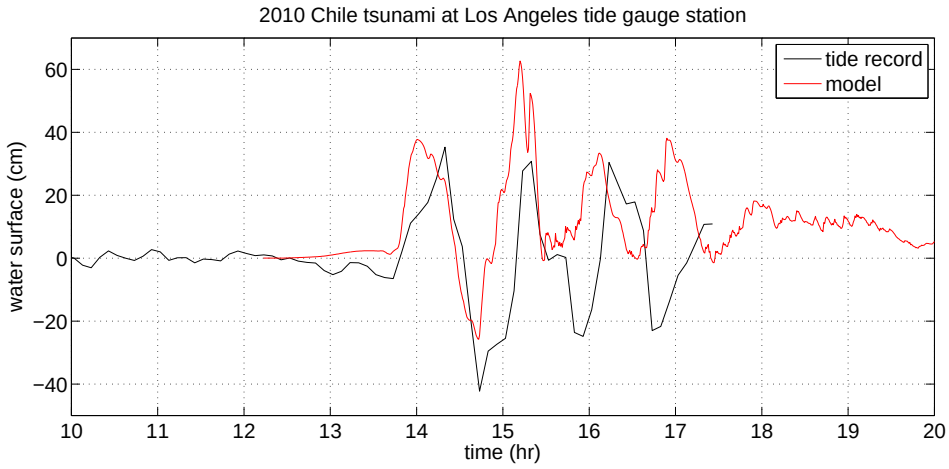

Figure 3.4: Comparison between observations at Los Angeles tide gauge and modeled results during the recent 2010 M_w 8.8 Chile tsunami.

Chapter 4

Results

The results of a deterministic tsunami hazard assessment for the ports of Los Angeles and Long Beach are presented and discussed. The assessment utilized the validated tsunami forecast model developed for Los Angeles as specified in Chapter 3. This assessment of tsunami hazard at the two ports identifies possible worst–case scenarios from 11 far–field source regions selected as subsets of 322 synthetic case scenarios that were investigated.

4.1 Sensitivity of Tsunami Amplitudes at Ports

Maximum computed wave amplitudes at the Los Angeles tide gauge for a total of 322 synthetically generated tsunami source scenarios around the Pacific Basin for a M_w 9.3 earthquake are shown in Figure 4.1. Large waves, in excess of 1.5 m (≈ 5 ft), are computed at the Los Angeles tide gauge for sources in Alaska/Aleutians, Manus, Tonga, and South America. The maximum computed wave amplitude is 1.7 m (≈ 5.5ft) from an Alaska/Aleutian source. Waves exceeding 1 m (3.25 ft) are produced from sources in South America, Manus, New Britain/Vanuatu, and New Zealand/Tonga. There are isolated source locations around the Pacific for which large amplitudes are noted, but Alaska/Aleutian sources consistently return large computed amplitudes at the Los Angeles tide gauge warning point. Kamchatka, Alaska and Chile can produce M_w 9.+ earthquakes, but the potential for Mariana, Manus, and Tonga subduction zones to produce such a great earthquake is questionable. Overall, tsunami waves larger than 1 m (3.25 ft) at the tide gauge are expected in the event of tsunami generation due to a great, far–field earthquake. In addition, computed maximum wave height and current speed results suggest that the Los Angeles tide gauge is located in a protected portion of the harbor, so amplitudes recorded by this gauge are not representative of other harbor locations and, most importantly, underestimate amplitudes expected elsewhere in the harbor. Predicted tsunami amplitudes on the order of 1 m (3.25 ft) at the tide gauge would likely translate

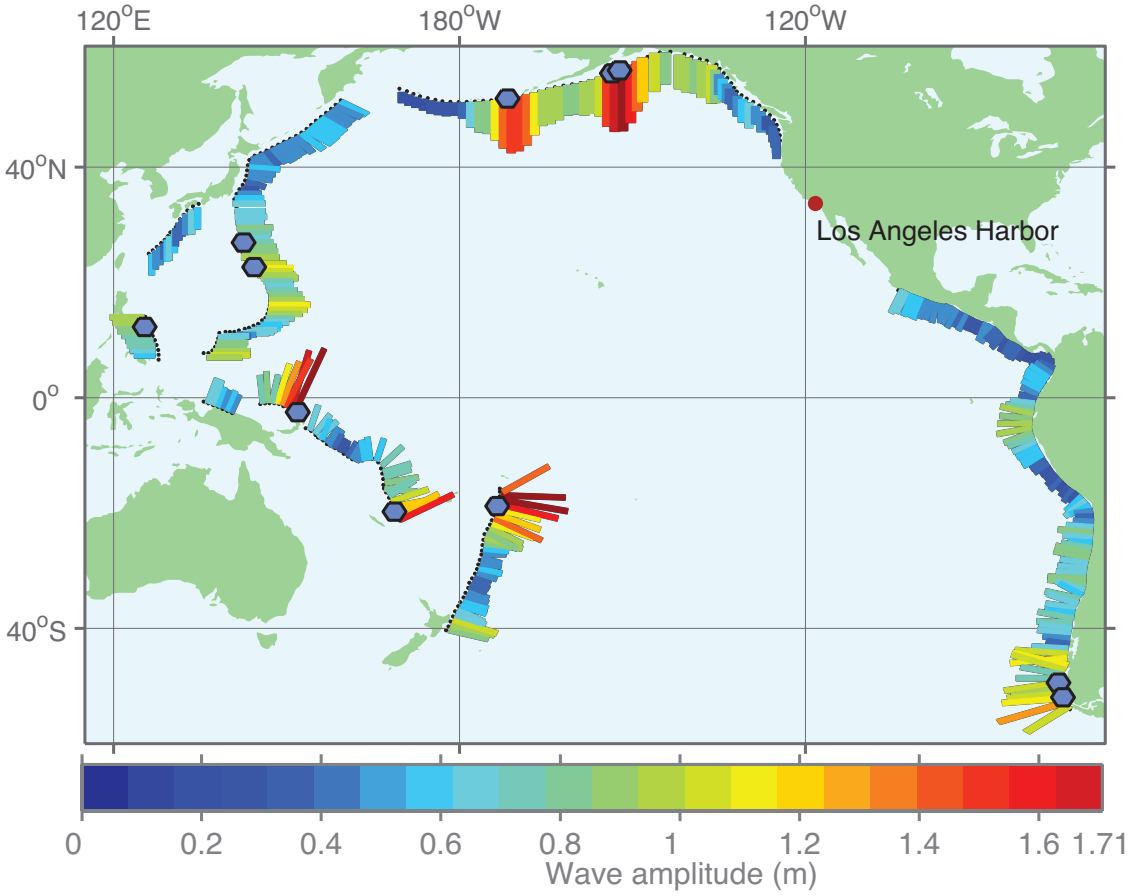

Figure 4.1: The maximum amplitude at the Los Angeles tide gauge from tsunamis triggered by synthetic M_w 9.3 earthquakes along subduction zones around the Pacific Basin as modeled with the Los Angeles tsunami forecast model.

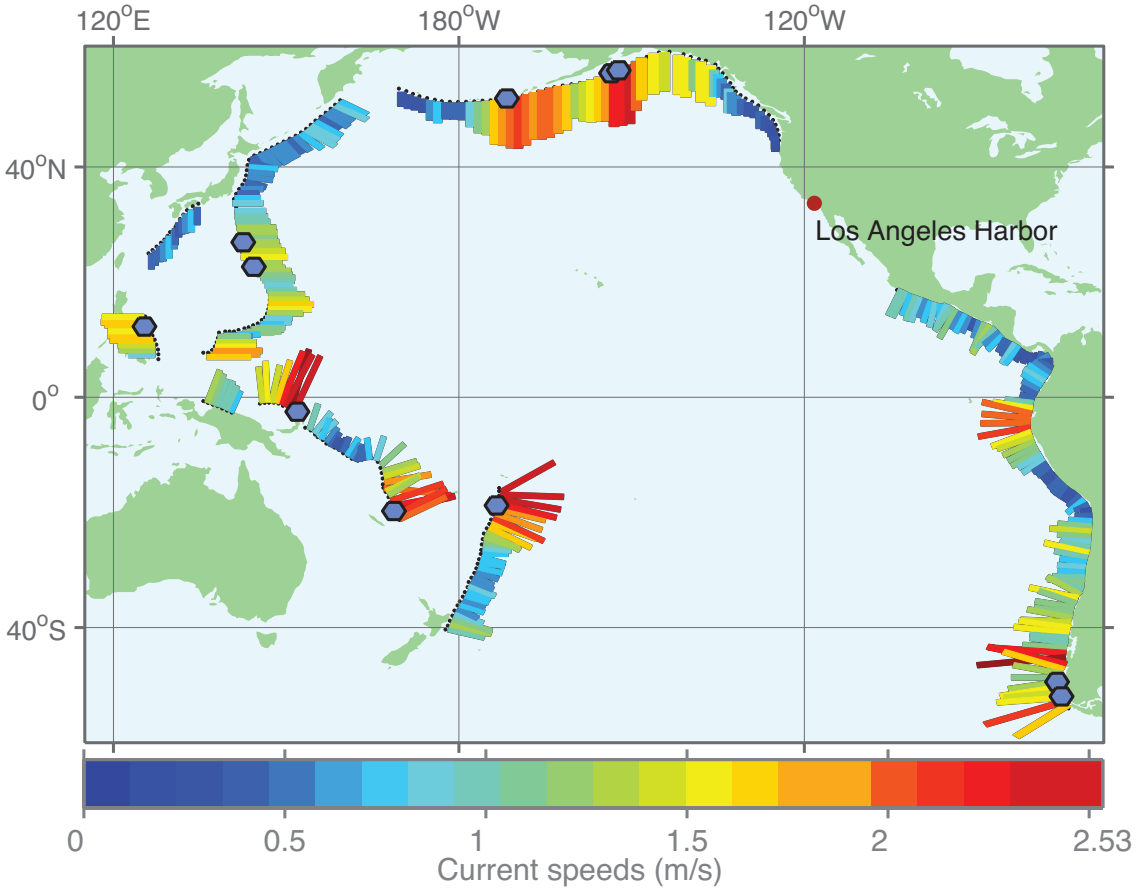

Figure 4.2: The maximum current velocities at the Los Angeles tide gauge, in meters/sec, from tsunamis triggered by synthetic M_w 9.3 earthquakes along subduction zones around the Pacific Basin as modeled with the Los Angeles tsunami forecast model.

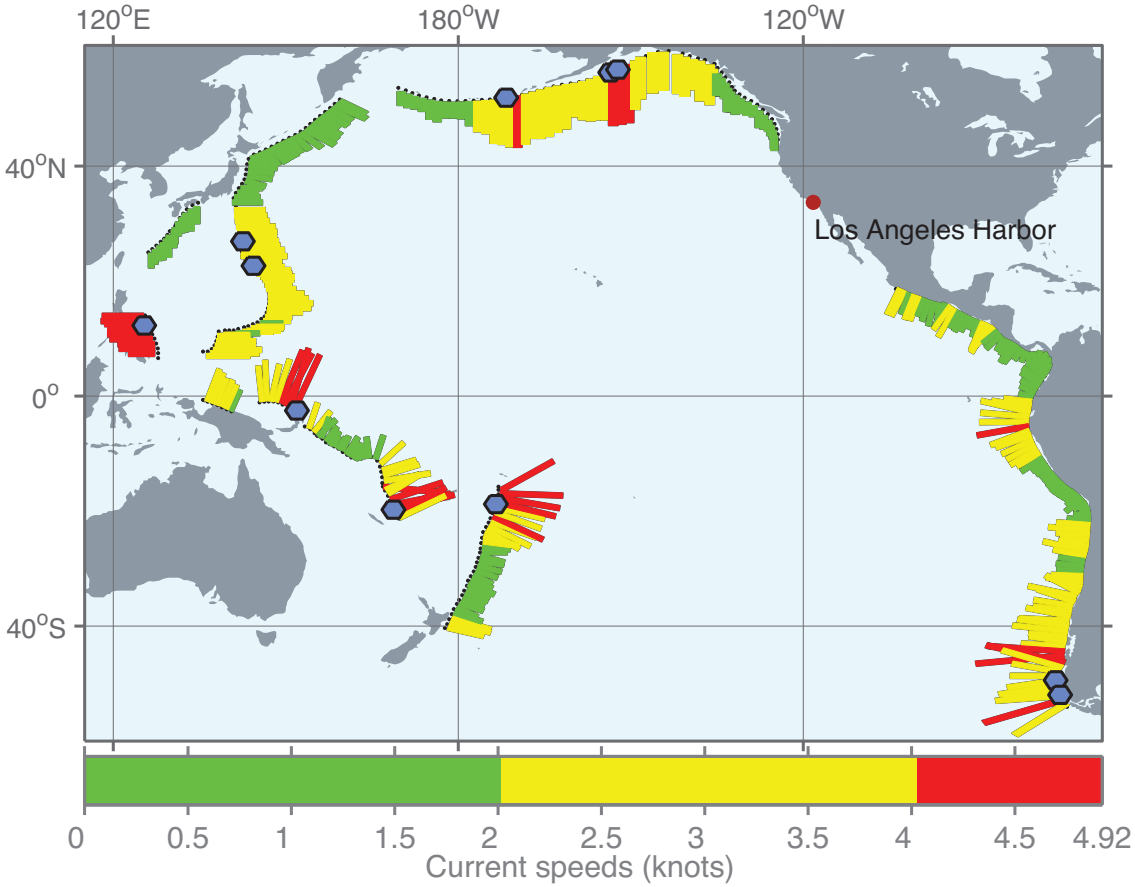

Figure 4.3: The maximum current velocities at the Los Angeles tide gauge, in knots, from tsunamis triggered by synthetic M_w 9.3 earthquakes along subduction zones around the Pacific Basin as modeled with the Los Angeles tsunami forecast model.

to larger amplitudes expected at other harbor locations.

Current velocities computed at the Los Angeles tide gauge for a total of 322 synthetically generated tsunami source scenarios around the Pacific Basin for a M_w 9.3 earthquake are shown in Figure 4.2. For convenience of interpretation, current velocities are presented in m/s as well as in knots in Figures 4.2 and 4.3, respectively. Currents in Figure 4.3 are categorized into three empirical groups: green represents the least risk, corresponding to less than 2 knots; yellow identifies currents in the range of 2–4 knots; and red is reserved for currents in excess of 4 knots, which are considered dangerous. Currents in this red category are computed from sources in the Philippines, Manus, New Guinea, Tonga, Chile, and Alaska/Aleutians. A M_w 9.3 Alaska/Aleutians source resulted in 4.9 knots ($\approx$ 2.53 m/s) at the Los Angeles tide station. Maximum calculated current velocities presented here are revised upward in the following discussion of possible worst–case scenarios.

A comparison of the maximum amplitude results with those of current velocities shows that the greatest qualitative difference is found in distribution. The numerical model results show that even though a few scenarios have big amplitudes at the tide gauge, the scenarios from neighbor segments are relatively smaller. However, in the numerical model a wider distribution with similar currents is observed. This suggests that an earthquake from a similar region is more likely to have similar impacts and be less sensitive to segments in terms of currents than wave amplitudes.

4.2 Potential Worst–Case Scenarios

Based on an examination of the results obtained from all 322 synthetic case scenarios computed, 11 synthetic scenarios, shown as pentagons in Figures 4.1, 4.2 and 4.3, are identified as posing a significant risk to the ports of Los Angeles and Long Beach and, therefore, represent possible worst–case scenarios. These scenarios are specific to Alaska, Chile, Philippines, Manus, New Zealand, and Vanuatu. In Figure 4.4, both a high–resolution reference model and an optimized tsunami forecast model time series at the Los Angeles tide gauge are shown to be consistent with one another. Even though the maximum computed wave amplitude is from Manus Trench, tsunamis originating from Alaska, South America, Tonga, and Vanuatu produce similar amplitude waves in the ports. This result lends further credibility to the validity of the forecast model and the appropriateness of its use under time constraints.

The high resolution results, as presented in Appendix B, suggest that a tsunami triggered by a M_w 9.3 earthquake in the Alaska/Aleutians does not necessarily impact the same region in the ports of Los Angeles and Long Beach as a tsunami triggered by a M_w 9.3 earthquake in Kamchatka or the Philippines.

Scenarios	Subduction Zone	Tsunami Source
ACSZ 15–24	Alaska–Aleutians–Cascadia	A15–24, B15–24
ACSZ 28–37	Alaska–Aleutians–Cascadia	A28–37, B28–37
ACSZ 29–38	Alaska–Aleutians–Cascadia	A29–38, B29–38
CSSZ 101–110	Central and South America	A101–110, B101–110
CSSZ 104–113	Central and South America	A104–113, B104–130
EPSZ 09-18	East Philippines	A9–18, B9–18
KISZ 35–44	Kuril-Kamchatka–Japan	A35–44, B35–44
KISZ 40–49	Kuril-Kamchatka–Japan	A40–49, B40–49
MOSZ 01-10	Manus OCB	A1–10, B1–10
NTSZ 27–36	New Zealand-Kermadec-Tonga	A27–36, B27–36
NVSZ 28–37	New Britain-Solomons-Vanuatu	A28–37, B28–37

Table 4.1: The list of 11 tsunami sources considered for potential worst–case scenarios at the ports of Los Angeles and Long Beach used in high–resolution simulations from earthquakes triggered by a rupture of a 30–m horizontal slip over an area of 1000 km × 100 km.

Because of the directivity of the waves, they have different impact zones in the harbors, and this may mislead port and emergency managers during the future events. In addition, consideration should be paid to the relative location of the tide gauge used as a warning point in this study. Model results at this site are not necessarily the maximum in the ports suggesting that larger waves could occur in other Port regions than those predicted or observed at the tide gauge location.

4.3 A Potential Tsunami from Alaska

The results of this study suggest that tsunamis generated in Manus, Vanuatu, Tonga, South America, and Alaska–Aleutian–Cascadia subduction zones can be potentially dangerous to the ports of Los Angeles and Long Beach. No historical data for M_w 9.3 earthquakes originating along Manus, Vanuatu, and Tonga are available. The likeliest potential worst–case candidate tsunami, however, is not expected from these source regions, but is instead expected to be generated by an earthquake from the Alaska–Aleutian–Cascadia subduction zone. Propagation database segments 29–38 are combined for the worst–case tsunami source. The maximum expected wave amplitudes and current velocities from this source are shown in Figure 4.5, and are also presented in larger scale in Appendix B, B.5, and B.6. Based on the results shown in Figure 4.5, a M_w 9.3 earthquake from Alaska will potentially trigger a tsunami capable of producing wave amplitudes up to 2 m (≈ 6.5 ft) and current velocities exceeding 4 m/s (≈ 8 knots) in the ports of Los Angeles and Long Beach.

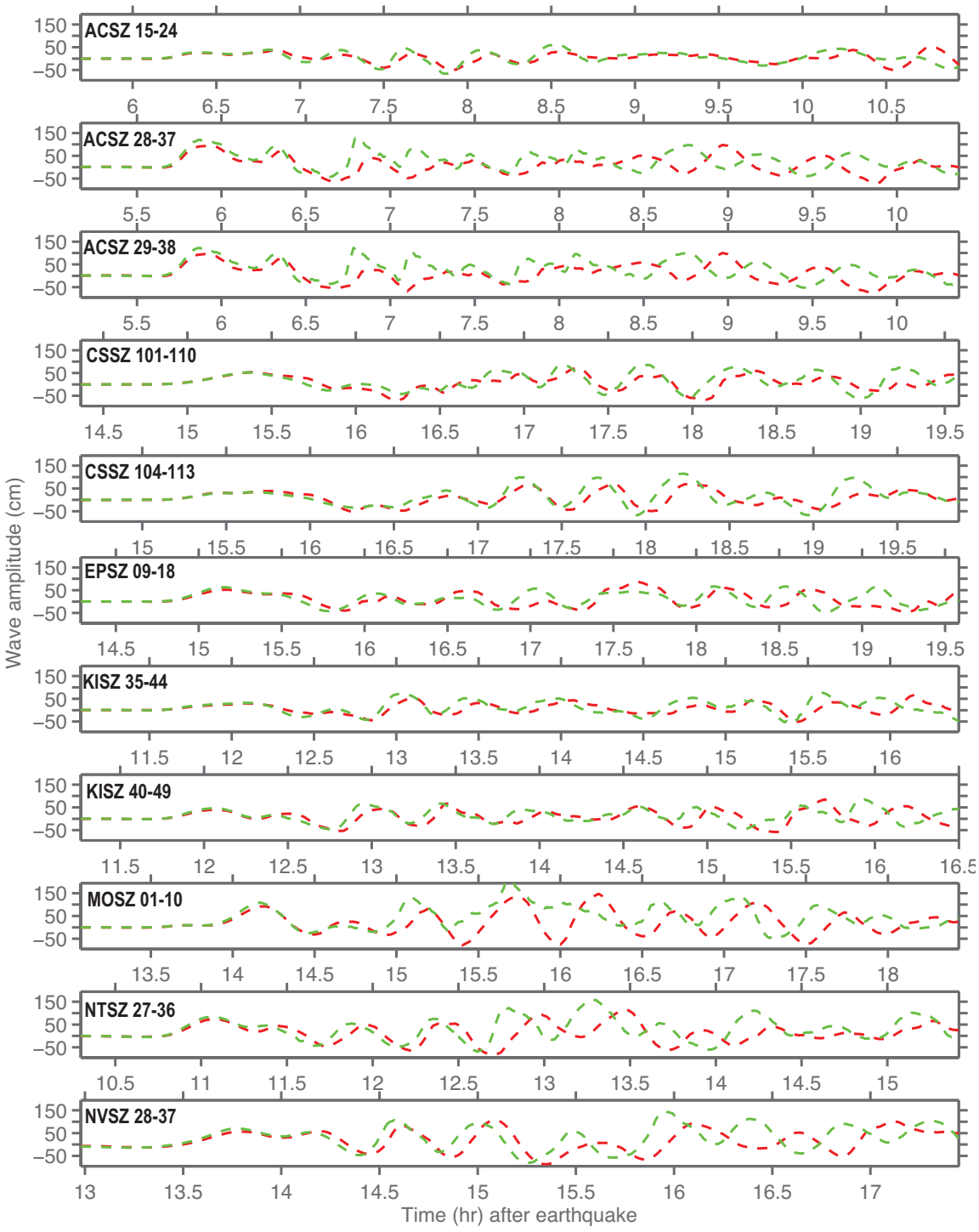

Figure 4.4: Comparison of the time series of the different synthetic tsunami events for Ports of Los Angeles and Long Beach, California from high resolution model (red) and forecast model (green). Sources are given in the left hand side of each time series.

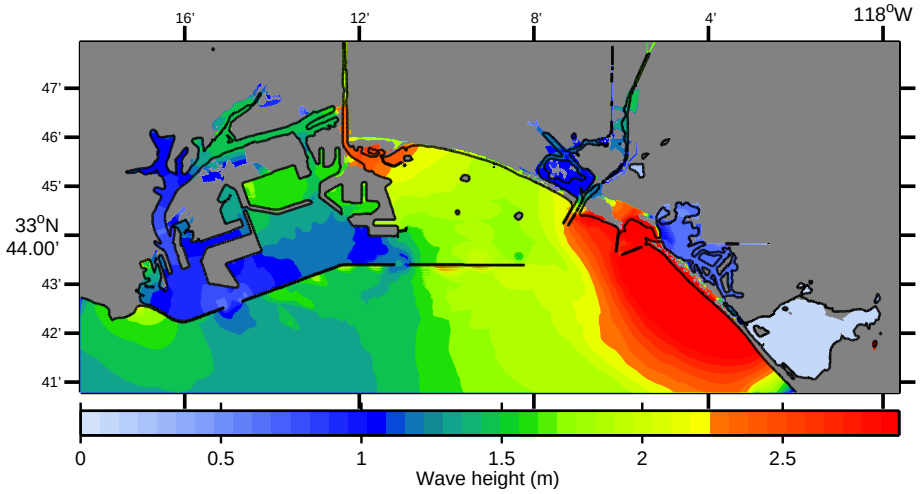

(a)

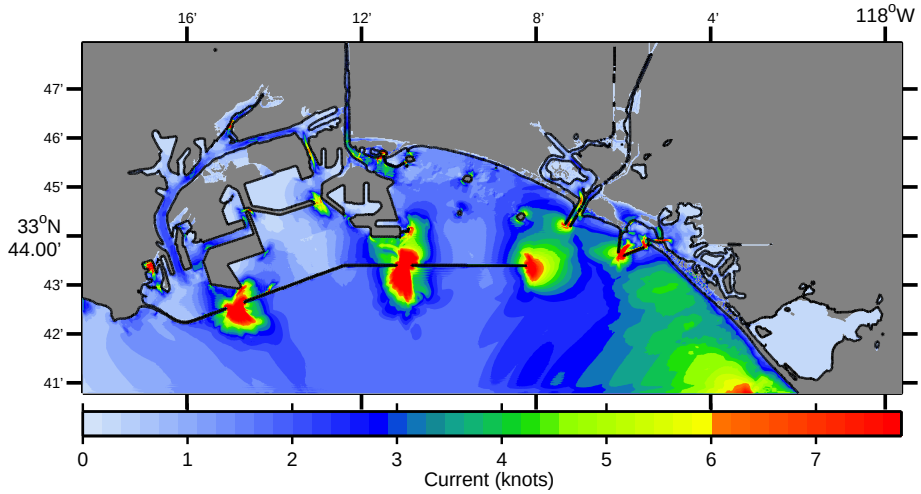

(b)

Figure 4.5: Maximum wave amplitudes (a) and currents (b) at Port of Los Angeles and Long Beach from the synthetic tsunami ACSZ 29. The figure is presented in larger scale in Appendix as Figures B.5 and B.6, together with the results from rest of the Synthetic scenarios.

Chapter 5

Conclusion

Tsunami waves propagate in a complex and highly directional pattern away from the source region of generation. Propagation and wave energy patterns reflect bathymetry encountered by tsunami waves as they transit the ocean basins. The location of tsunami generation and bathymetry between the source and a given harbor might result in one source posing a significantly greater danger than another source even though they are within close proximity of one another. Seismic characteristics and faulting mechanisms also play an important role in the impact potential that a generated tsunami poses to coastal communities. Studies have shown that tsunamis triggered by similar magnitude earthquakes from different subduction zones may result in substantially different impact at the same harbor.

The southern California region including the ports of Los Angeles and Long Beach has a well documented seismic history. For this reason, a detailed hazard assessment has been conducted for the ports of Los Angeles and Long Beach. Of 322 synthetic scenarios investigated in this study, 11 source regions in Alaska, Chile, Philippines, Manus, New Zealand, and Vanuatu are identified as having the potential to generate a tsunami significant to the ports of Los Angeles and Long Beach. Summary of range of likely travel times from sources to the ports are presented in Table 5.1 for each subduction zone to the Los Angeles tide station. The earliest tsunami is detected at the tide gauge in 2 hours and 15 minutes from Alaska–Aleutians–Cascadia Subduction Zone, the latest is from North New Guinea in 15 hours and 1 minute. Findings show that tsunamis generated along far–field subduction zones pose considerably more danger to the ports of Los Angeles and Long Beach than previously thought. Far–field source generation of a tsunami from M_w 9.3 earthquakes can potentially impact the two ports with wave amplitudes reaching up to 2 m ($\approx$ 6.5 ft) and currents exceeding 4 m/s ($\approx$ 8 knots). Currents exceeding 2 m/s ($\approx$ 4 knots) are known to break mooring lines and damage harbor piers and other structures. Depending on the magnitude of the earthquake and the initial condition of the source, then, it

Earliest Expected Arrival			
Subduction Zone	Time (hr)	Tsunami Source	Computed Amplitude the Tide Station
Alaska–Aleutians–Cascadia	2hr 15min 56sec	ACSZ 56-65	46(cm)
Central and South America	3hr 40min 25sec	CSSZ 1–10	69(cm)
East Philippines	14hr 51min 26sec	EPSZ 9–18	90 (cm)
Kuril–Kamchatka–Japan	9hr 2min 29sec	KISZ 1–10	56(cm)
Manus OCB	13hr 53min 42sec	MOSZ 1–10	176 (cm)
North New Guinea	14hr 55min 31sec	NGSZ 2–11	58(cm)
New Zealand–Kermadec–Tonga	10hr 50min 21sec	NTSZ 27–36	152 (cm)
New Britain–Solomons–Vanuatu	12hr 41min 20sec	NVSZ 16–25	63 (cm)
Ryukus–Kyushu–Nankai	12hr 38min 38sec	RNSZ 13–22	58(cm)
Latest Expected Arrival			
Subduction Zone	Time	Tsunami Source	Computed Amplitude at the Tide Station
Alaska–Aleutians–Cascadia	7hr 46min 33sec	ACSZ 1-10	28 (cm)
Central and South America	15hr 30min 21sec	CSSZ 106–115	100 (cm)
East Philippines	15hr 6min 54sec	EPSZ 1–10	57 (cm)
Kuril–Kamchatka–Japan	13hr 53min 49sec	KISZ 66–75	95 (cm)
Manus OCB	14hr 2min 15sec	MOSZ 8–17	77 (cm)
North New Guinea	15hr 1min 0sec	NGSZ 6–15	72 (cm)
New Zealand–Kermadec–Tonga	13hr 20min 20sec	NTSZ 1–10	86 (cm)
New Britain–Solomons–Vanuatu	14hr 20min 8sec	NVSZ 6–15	55 (cm)
Ryukus–Kyushu–Nankai	14hr 10min 6sec	RNSZ 3–12	48 (cm)

Table 5.1: Summary of range of likely travel times from sources to the ports computed for each subduction zone to the Los Angeles tide station. Earliest and latest arrival times are provided.

is recommended that tsunamis from subduction zones in the Alaska/Aleutians, Central and South America, Eastern Philippines, Kuril Islands–Mariana, Manus, New Zealand/Tonga, and New Britain/Vanuatu be assessed immediately following generation. Due to their importance to United States commerce, the hazard posed by tsunami is of great concern because the potential devastation and impact would likely interrupt commerce, marine, and tourism activities. Tourist attractions, including the Maritime Museum, Aquarium of the Pacific, and Queen Mary (Figure 1.1), along with the large number of tourists who visit them daily, are potentially at risk.

Bibliography

Borrero, J. C. (2002). *Tsunami Hazards in Southern California.* PhD thesis, University of Southern California, Los Angeles, California.

Borrero, J. C., Dolan, J., and Synolakis, C. E. (2001). Tsunami sources within the Eastern Santa Barbara Channel. *Geophys. Res. Lett.*, 28:643–647.

Borrero, J. C., Legg, M. R., and Synolakis, C. E. (2004). Tsunami sources in the Southern California bight. *Geophys. Res. Lett.*, 31:L13211.1–L13211.4.

Bourgeois, J. (2007). Personal Communication.

Clarke, S. H. and Carver, G. A. (1992). Late holocene tectonics and paleoseismicity, southern Cascadia Subduction Zone. *Science*, 255:188–192.

Coastal Conservancy, (2009). The Los Angeles County Coast Southern Los Angeles Area, Los Angeles Harbor. http://www.scc.ca.gov/webmaster/project_sites/wheel/lapage/6_so_la/harbor/harbor.html.

Dengler, L., Uslu, B., Barberopoulou, A., Yim, S.C., Kelly, A. (2009). TThe November 15, 2006 Kuril Islands-generated tsunami in Crescent City, California. *Pure Appl. Geophys.*, , 166(1–2), 37–53..

Dengler, L., Uslu, B., Barberopoulou, A., Borrero, J., and Synolakis, C. (2008). The vulnerability of crescent city, california to tsunamis generated by earthquakes in the kuril islands region of the northwestern pacific. *Seis. Res. Let.*, page in publication.

Dykstra, D. H. and Jin, W. (2006). Detailed modeling of locally generated tsunami propagation into the ports of Los Angeles and Long Beach. In *30th International Conference on Coastal Engineering*, pages 1603–1616. World Scientific.

Geist, E. L. (2000). Comment on "Origin of the 17 July 1998 Papua New Guinea Tsunami: Earthquake or Landslide?" by E. L. Geist. *Seismol. Res. Lett.* , 71(3):344–351.

Geist, E. L. (2001). Reply to Comments by E. A. Okal and C. E. Synolakis on"Origin of the 17 July 1998 Papua New Guinea Tsunami: Earthquake or Landslide?". *Seismol. Res. Lett.* , 71(3):367–372.

Gica, E., Spillane, M., Titov, V., Chamberlin, C., and Newman, J. (2008). Development of the forecast propagation database for NOAA's Short–term Inundation Forecast for Tsunamis (SIFT). Tech. Memo. OAR PMEL–139 NTIS: PBB2008-109391, NOAA/Pacific Marine Environmental Laboratory, Seattle, WA.

Houston, J. (1980). Type 19 flood insurance study. WES Report HL-80-18, USACE.

Houston, J. and Garcia, A. (1974). Type 16 flood insurance study. WES Report H-74-3, USACE.

Kelley, A., Dengler, L., Uslu, B., Barberopoulou, A., Yim, S., and Bergen, K. (2006). Recent tsunami highlights need for awareness of tsunami duration. *EOS Transactions AGU*, 87(50):566–567.

Lander, J. F., Lockridge, P., and Kozuch, M. (1993). Tsunamis Affecting the West Coast, US 1806-1992. Technical report, U.S. Department of Commerce.

Levin, B. W., Kaistrenko, V. M., Rybin, A. V., Nosov, M. A., Pinegina, T. K., Razzhigaeva, N. G., Sasorova, E. V., Ganzei, K. S., Ivel'Skaya, T. N., Kravchunovskaya, E. A., Kolesov, S. V., Evdokimov, Y. V., Bourgeois, J., Macinnes, B., and Fitzhugh, B. (2008). Manifestations of the tsunami on November 15, 2006, on the central Kuril Islands and results of the runup heights modeling. *Doklady Earth Sciences*, 419:335–338.

McCarthy, R. J., Bernard, E. N., and Legg, M. R., editors (1993). *The Cape Mendocino Earthquake: A Local Tsunami Wakeup Call?*, In Coastal Zone '93 Volume 3, Proceedings of the Eight Symposium on Coastal and Ocean Management, New Orleans, Louisiana. ASCE.

McCulloch, D. (1985). Evaluating tsunami potential. *U.S. Geol. Survey Prof. Paper*, 1360(374-413).

Moffatt and Nichol (2007). Tsunami hazard assessment for the Ports of Long Beach and Los Angeles. Tech. Report M&N File:4839-169, Moffatt and Nichol.

Okal, E. A. (1992). Use of the mantle magnitude M_m for the reassessment of the moment of historical earthquakes. i: shallow events. *Pure and Applied Geophysics*, 139(1):17–57.

Okal, E. A. (2007). Personal Communication.

Okal, E. A. and Synolakis, C. E. (2001). Origin of the 17 July 1998 Papua New Guinea Tsunami: Earthquake or Landslide? . *Seismol. Res. Lett.* , 71(3):362–366.

Port of Long Beach (2009). About the Port. http://www.polb.com.

Port of Los Angeles (2009). FAQs. http://www.portoflosangeles.org/.

Satake, K., Shimazaki, K., Tsuji, Y., and Ueda, K. (1996). Time and size of a giant earthquake in Cascadia inferred from Japanese tsunami records of January 1700. *Nature*, 379:246–249.

Satake, K., Wang, K., and Atwater, B. F. (2003). Fault slip and seismic moment of the 1700 Cascadia earthquake inferred from Japanese tsunami descriptions. *J. Geophys. Res.*, 108(B11):E–7,1–17.

Soloviev, S. L. and Go, C. N. (1974). Catalog of tsunamis on the western shore of the Pacific Ocean. Technical report, Nauka Publishing House, Moscow.

Synolakis, C. E. (1987). The runup of solitary waves. *Journal of Fluid Mechanics*, 185:523–545.

Synolakis, C. E. (2003). *Tsunami and Seiche*, chapter 9, pages 9.1–9.90. Earthquake Engineering. CRC Press LLC, Boca Raton.

Synolakis, C. E. (2006). What went wrong. *Wall Street Journal, Editorial*, page 25 July.

Synolakis, C. E. (2008). Personal Communication.

Synolakis, C. E., Bardet, J.-P., Borrero, J., H. L. Davies E. A. Okal, E. A., Silver, E. A., Sweet, S., and Tappin, D. R. (2002). The slump origin of the 1998 Papua New Guinea tsunami. *Proc. Roy. Soc. London, Ser. A*, 458:763–790.

Synolakis, C. E., Bernard, E., Titov, V., Kânoğlu, U. K., and González, F. (2008). Validation and verification of tsunami numerical models. *Pure Appl. Geophys.*, 165:2197–2228.

Synolakis, C. E., McCarthy, D., Titov, V. V., and Borrero, J. C., editors (1997). *Evaluating the Tsunami Risk in California*, California and the World Ocean '97 Proceeding of the Conference, San Diego, California. ASCE.

Tang, L., Chamberlin, C., and Titov, V. (2008a). Developing tsunami forecast inundation models for Hawaii: procedures and testing. Tech. Memo. OAR PMEL-141, NOAA.

Tang, L., Titov, V., Wei, Y., Mofjeld, H., Spillane, M., Arcas, D., Bernard, E., Chamberlin, C., Gica, E., and Newman, J. (2008b). Tsunami forecast analysis for the may 2006 tonga tsunami. *J. Geophys. Res.*, page C12015.

Tanioka, Y., Ruff, L. J., and Satake, K. (1995). The Great Kuril earthquake of Oct. 4, 1994 tore the slab. *Geophys. Res. Lett.*, 22(13):1661–1664.

Titov, V. V., González, F. I., Bernard, E. N., Eble, M. C., Mofjeld, H. O., Newman, J. C., and Venturato, A. J. (2005a). Real-time tsunami forecasting: Challenges and solutions. *Natural Hazards*, 35(1):35–41.

Titov, V. V., Rabinovich, A. B., Mofjeld, H. O., Thomson, R. E., and González, F. I. (2005b). The global reach of the 26 December 2004 Sumatra Tsunami. *Science*, 309:2045–2048.

Titov, V. V. and Synolakis, C. E. (1997). Extreme inundation flows during the Hokkaido-Nansei-Oki tsunami. *Geophys. Res. Lett.*, 24(11):1315–1318.

Titov, V. V. and Synolakis, C. E. (1998). Numerical modelling of tidal wave runup. *J. Waterw. Port Coast. Ocean Eng.*, 124:157–171.

USGS, Earthquake Hazards Program (2009). *http://earthquake.usgs.gov*.

Uslu, B. (2008). *Deterministic and Probabilistic tsunami studies in California from near and farfield sources*. PhD thesis, University of Southern California, Los Angeles, California.

Uslu, B., Borrero, J. C., Dengler, L., and Synolakis, C. E. (2007). Tsunami inundation at Crescent City generated by earthquakes along the Cascadia Subduction Zone. *Geophys. Res. Lett.*, 34:L20601.

Uslu, B., Borrero, J. C., Dengler, L., Synolakis, C. E., and Barberopoulou, A. (2008). Tsunami inundation from great earthquakes on the Cascadia Subduction Zone along the northern California coast. In *Solutions to Coastal Disasters*. ASCE.

Wang, K., He, J., Dragert, H., and James, T. S. (2001). Three-dimensional viscoelastic interseismic deformation model for the Cascadia subduction zone. *Earth, Planets, and Space*, 53:295–306.

Wang, K., Wells, R., Mazzotti, S., Hyndman, R. D., and Sagiya, T. (2003). A revised dislocation model of interseismic deformation of the Cascadia Subduction Zone. *J. Geophys. Res*, 108(B1):ETG_9, 13 pp.

WCATWC, West Coast and Alaska Tsunami Warning Center (2009). *http://wcatwc.arh.noaa.gov/*.

Yeh, H., Titov, V. V., Gusiakov, V., Pelinovsky, E., Khramushin, V., and Kaistrenkov, V. M. (1995). The 1994 Shikotan earthquake tsunamis. *Pure and Applied Geophysics*, 144:855–874.

Appendix A

Glossary

Arrival time The time when the first tsunami wave is observed at a particular location, typically given in local and/or universal time, but also commonly noted in minutes or hours relative to the time of the earthquake.

Bathymetry The measurement of water depth of an undisturbed body of water.

Cascadia Subduction Zone Fault that extends from Cape Mendocino in Northern California northward to mid-Vancouver Island Canada. The fault marks the convergence boundary where the Juan de Fuca tectonic plate is being subducted under the margin of the North America plate.

Current speed The scalar rate of water motion measured as distance/time.

Current velocity Movement of water expressed as a vector quantity. Velocity is the distance of movement per time coupled with direction of motion.

Digital Elevation Model (DEM) A digital representation of bathymetry or topography based on regional survey data or satellite imagery. Data are arrays of regularly spaced elevations referenced to a map projection of the geographic coordinate system.

Epicenter The point on the surface of the earth that is directly above the focus of an earthquake.

Focus The point beneath the surface of the earth where a rupture or energy release occurs due to a buildup of stress or the movement of earth's tectonic plates relative to one another.

Inundation The horizontal inland extent of land that a tsunami penetrates, generally measured perpendicularly to a shoreline.

Marigram Tide gauge recording of wave level as a function of time at a particular location. The instrument used for recording is termed a marigraph.

Moment Magnitude (M_W) The magnitude of an earthquake on a logarithmic scale in terms of the energy released. Moment magnitude is based on the size and characteristics of a fault rupture as determined from long-period seismic waves.

Method of Splitting Tsunamis (MOST) A suite of numerical simulation codes used to provide estimates of the three processes of tsunami evolution: tsunami generation, propagation, and inundation.

Near–field A particular location at which the earth's deformation due to energy release affects the modeling solution.

Propagation database A basin-wide database of pre-computed water elevations and flow velocities at uniformly spaced grid points throughout the world oceans. Values are computed from tsunamis generated by earthquakes with a fault rupture at any one of discrete 100 × 50 km unit sources along worldwide subduction zones.

Runup Vertical difference between the elevation of tsunami inundation and the sea level at the time of a tsunami. Runup is the elevation of the highest point of land inundated by a tsunami as measured relative to a stated datum, such as mean sea level.

Short-term Inundation Forecasting for Tsunamis (SIFT) A tsunami forecast system that integrates tsunami observations in the deep-ocean with numerical models to provide an estimate of tsunami wave arrival and amplitude at specific coastal locations while a tsunami propagates across an ocean basin.

Subduction zone A submarine region of the earth's crust at which two or more tectonic plates converge to cause one plate to sink under another, overriding plate. Subduction zones are regions of high seismic activity.

Synthetic event Hypothetical events based on computer simulations or theory of possible or even likely future scenarios.

Tidal wave Term frequently used incorrectly as a synonym for tsunami. A tsunami is unrelated to the predictable periodic rise and fall of sea level due to the gravitational attractions of the moon and sun: the tide.

Tide The predictable rise and fall of a body of water (ocean, sea, bay, etc.) due to the gravitational attractions of the moon and sun.

Tide gauge An instrument for measuring the rise and fall of a column of water over time at a particular location.

Tele–tsunami or distant tsunami or far–field tsunami Most commonly, a tsunami originating from a source greater than 1000 km away from a particular location. In some contexts, a tele-tsunami is one that propagates through deep-ocean before reaching a particular location without regard to distance separation.

Travel time The time it takes for a tsunami to travel from the generating source to a particular location.

tsunami A Japanese term that literally translates to "harbor wave." Tsunamis are a series of long–period shallow water waves that are generated by the sudden displacement of water due to subsea disturbances such as earthquakes, submarine landslides, or volcanic eruptions. Less commonly, meteoric impact to the ocean or meteorological forcing can generate a tsunami.

Tsunami Hazard Assessment A systematic investigation of seismically active regions of the world oceans to determine their potential tsunami impact at a particular location. Numerical models are typically used to characterize tsunami generation, propagation, and inundation, and to quantify the risk posed to a particular community from tsunamis generated in each source region investigated.

Tsunami Propagation The directional movement of a tsunami wave outward from the source of generation. The speed at which a tsunami propagates depends on the depth of the water column in which the wave is traveling. Tsunamis travel at a speed of 700 km/hr (450 mi/hr) over the average depth of 4000 m in the open deep Pacific Ocean.

Tsunami source Location of tsunami origin, most typically an underwater earthquake epicenter. Tsunamis are also generated by submarine landslides, underwater volcanic eruptions, or, less commonly, by meteoric impact of the ocean.

Wave amplitude The maximum vertical rise or drop of a column of water as measured from wave crest (peak) or trough to a defined mean water level state.

Wave crest or peak The highest part of a wave or maximum rise above a defined mean water level state, such as mean lower low water.

Wave height The vertical difference between the highest part of a specific wave (crest) and it's corresponding lowest point (trough).

Wavelength The horizontal distance between two successive wave crests or troughs.

Wave period The length of time between the passage of two successive wave crests or troughs as measured at a fixed location.

Wave trough The lowest part of a wave or the maximum drop below a defined mean water level state, such as mean lower low water.

Appendix B

Results from Synthetic Tsunamis

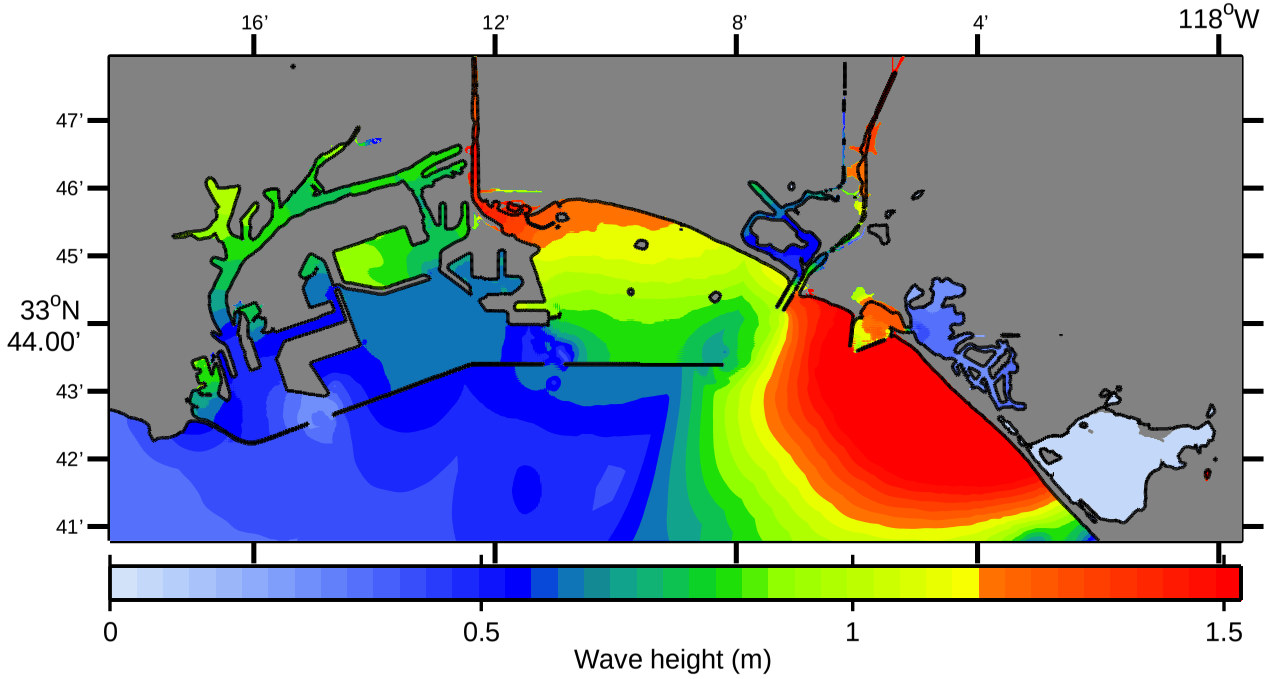

Figure B.1: Maximum wave amplitudes at Port of Los Angeles and Long Beach from the artificial tsunami ACSZ 15–24.

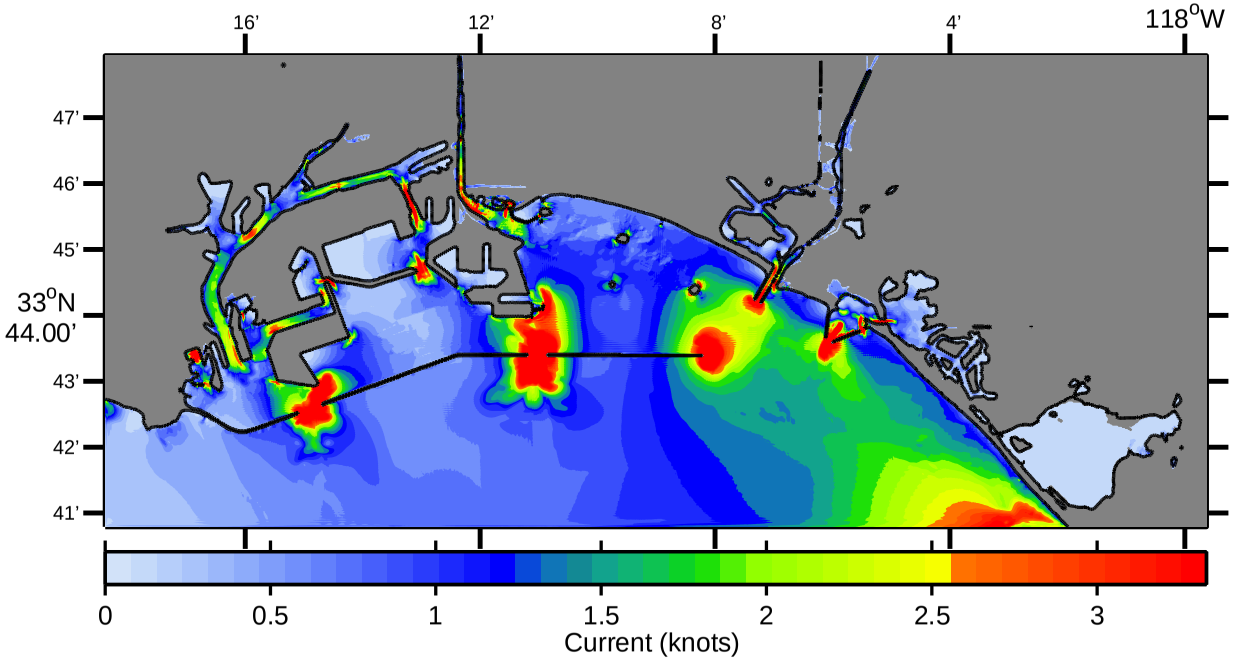

Figure B.2: Maximum current velocities at Port of Los Angeles and Long Beach from the artificial tsunami ACSZ 15–24.

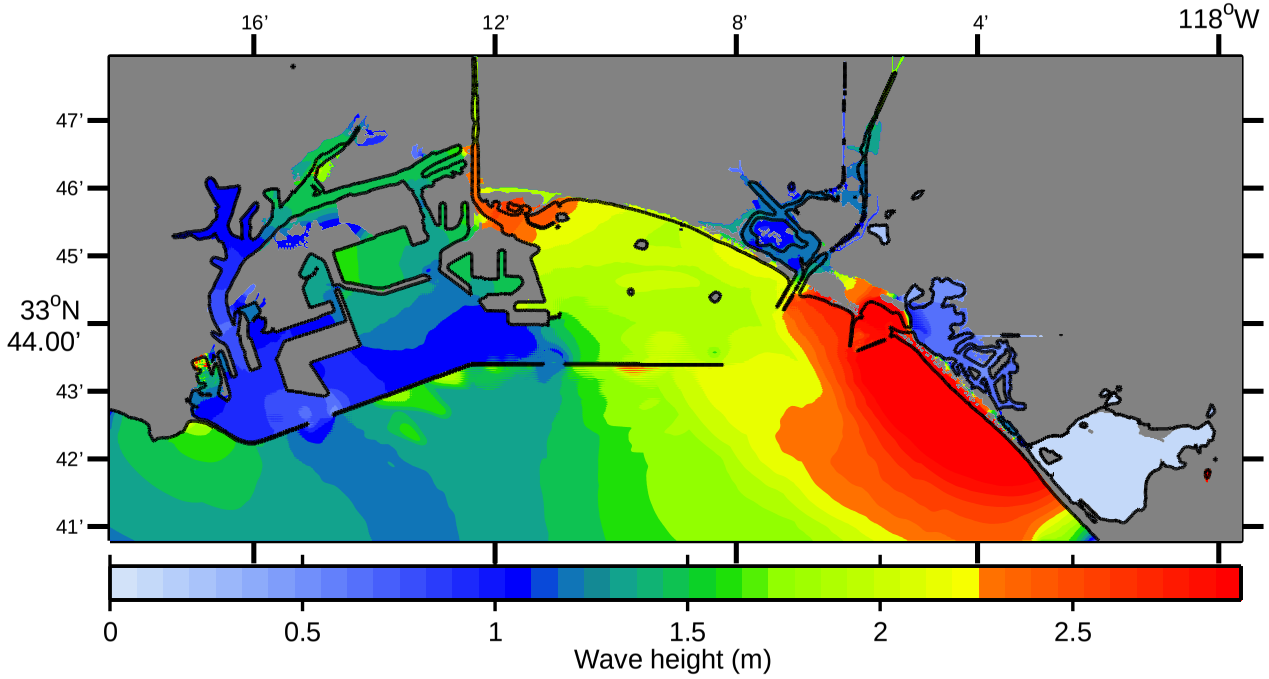

Figure B.3: Maximum wave amplitudes at Port of Los Angeles and Long Beach from the artificial tsunami ACSZ 28–37.

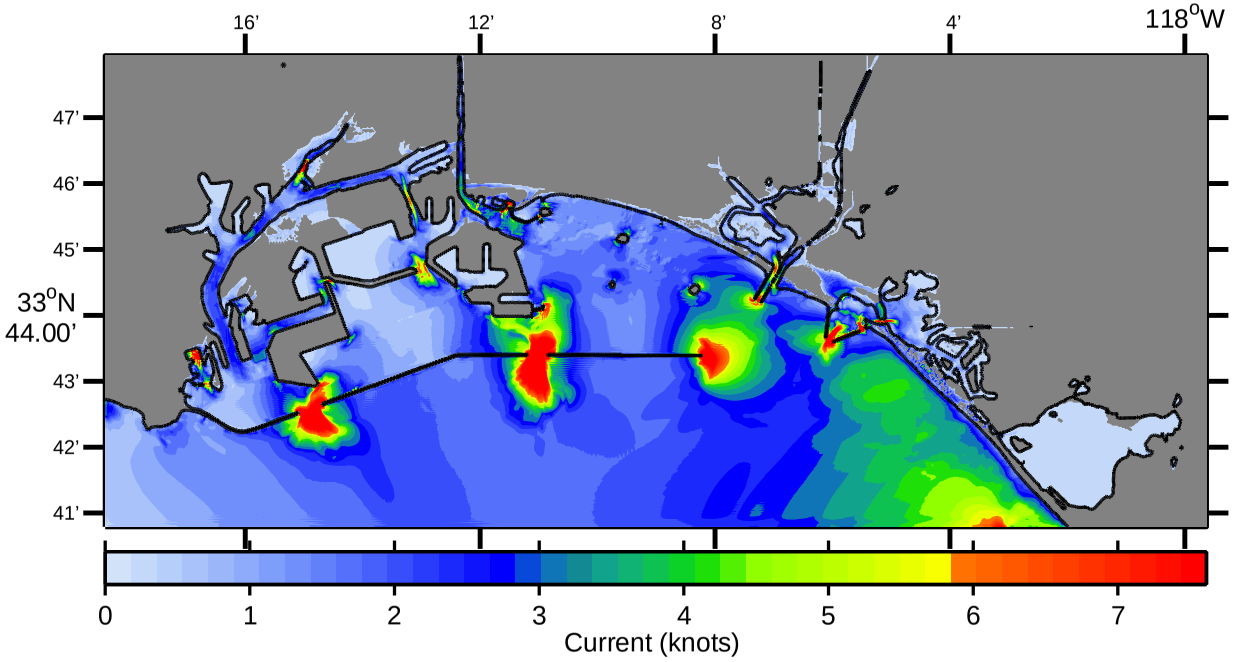

Figure B.4: Maximum current velocities at Port of Los Angeles and Long Beach from the artificial tsunami ACSZ 28–37.

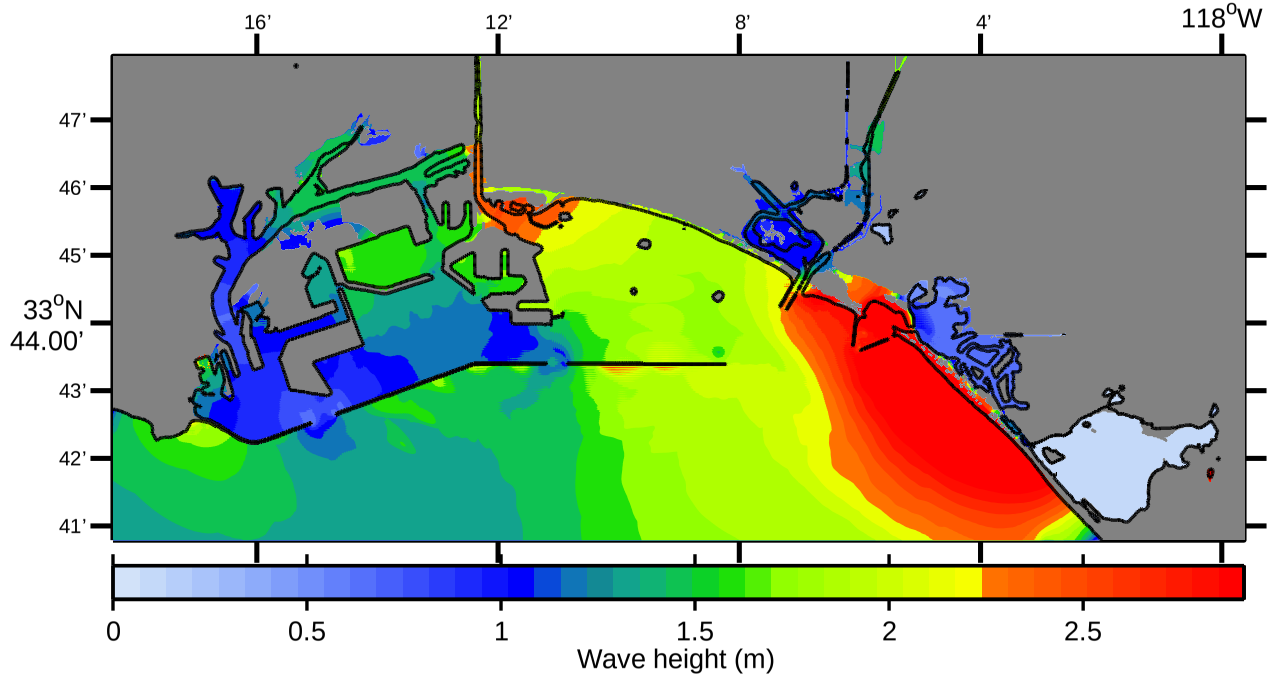

Figure B.5: Maximum wave amplitudes at Port of Los Angeles and Long Beach from the artificial tsunami ACSZ 29–38. This is already presented in Figure 4.5.

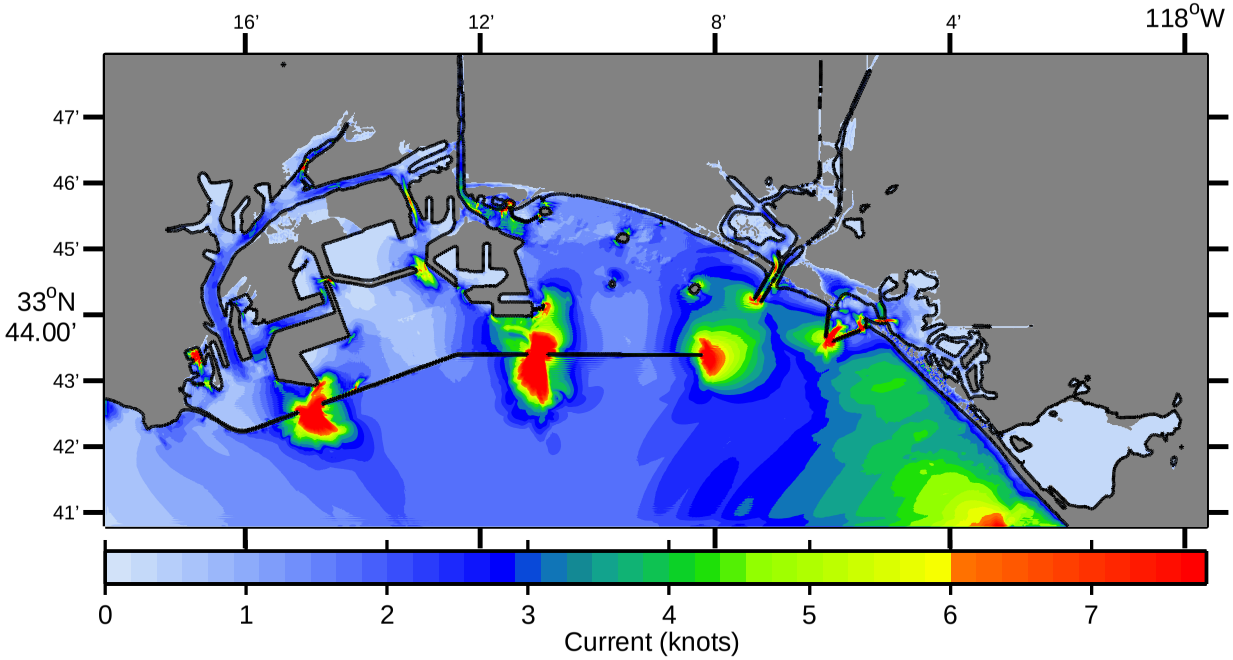

Figure B.6: Maximum current velocities at Port of Los Angeles and Long Beach from the artificial tsunami ACSZ 29–38. This is already presented in Figure 4.5.

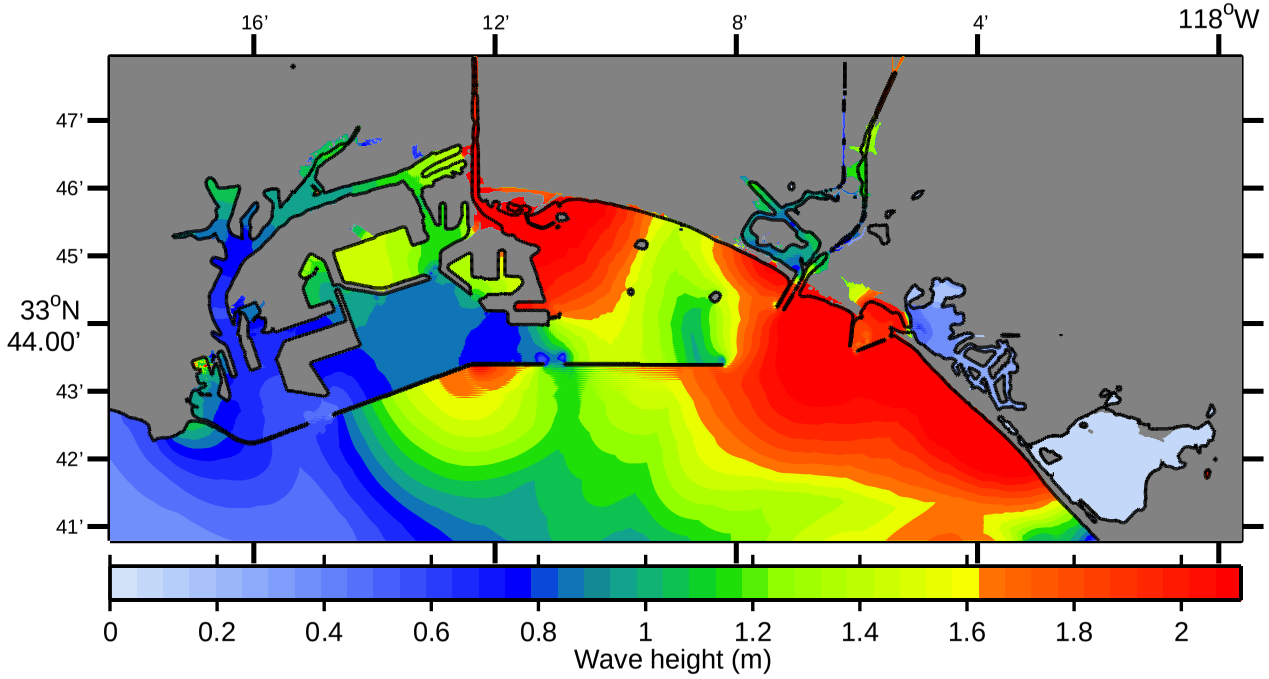

Figure B.7: Maximum wave amplitudes at Port of Los Angeles and Long Beach from the artificial tsunami CSSZ 101–110.

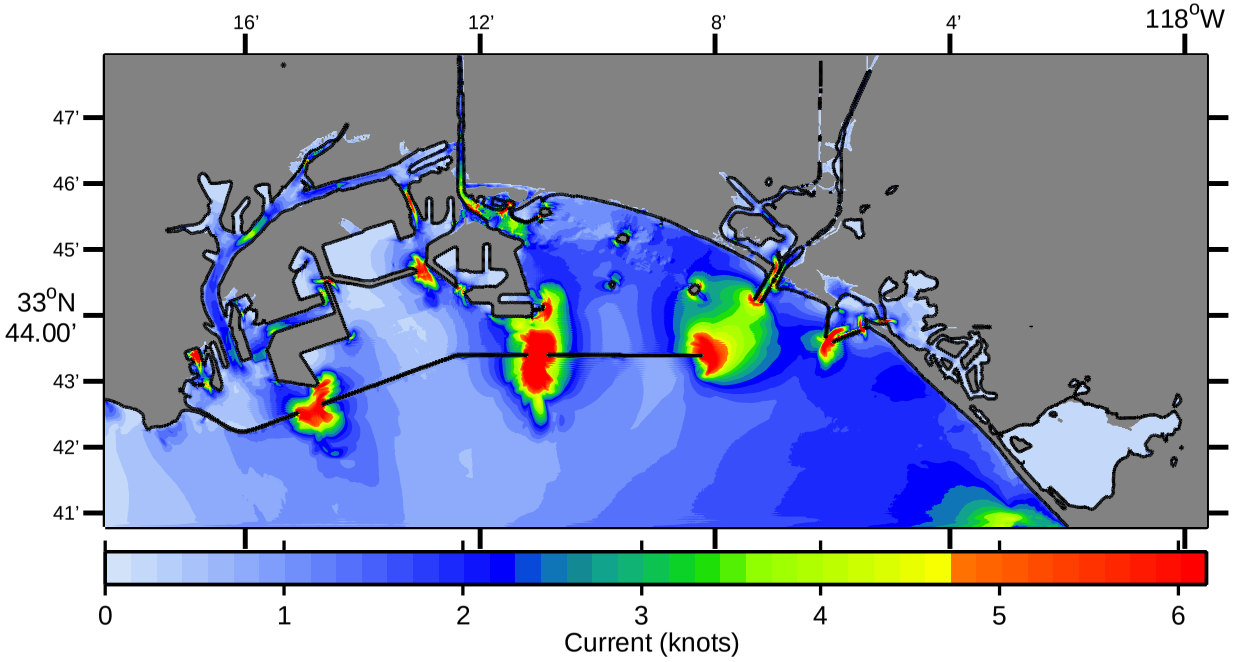

Figure B.8: Maximum current velocities at Port of Los Angeles and Long Beach from the artificial tsunami CSSZ 101–110.

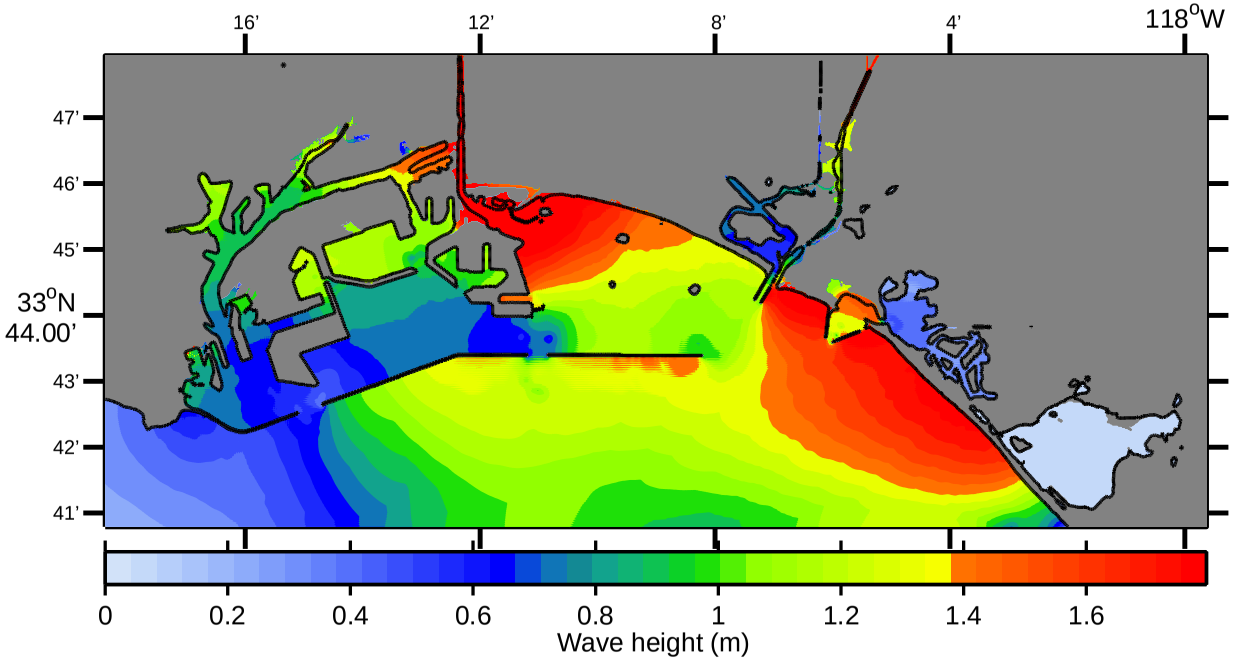

Figure B.9: Maximum wave amplitudes at Port of Los Angeles and Long Beach from the artificial tsunami CSSZ 104–113.

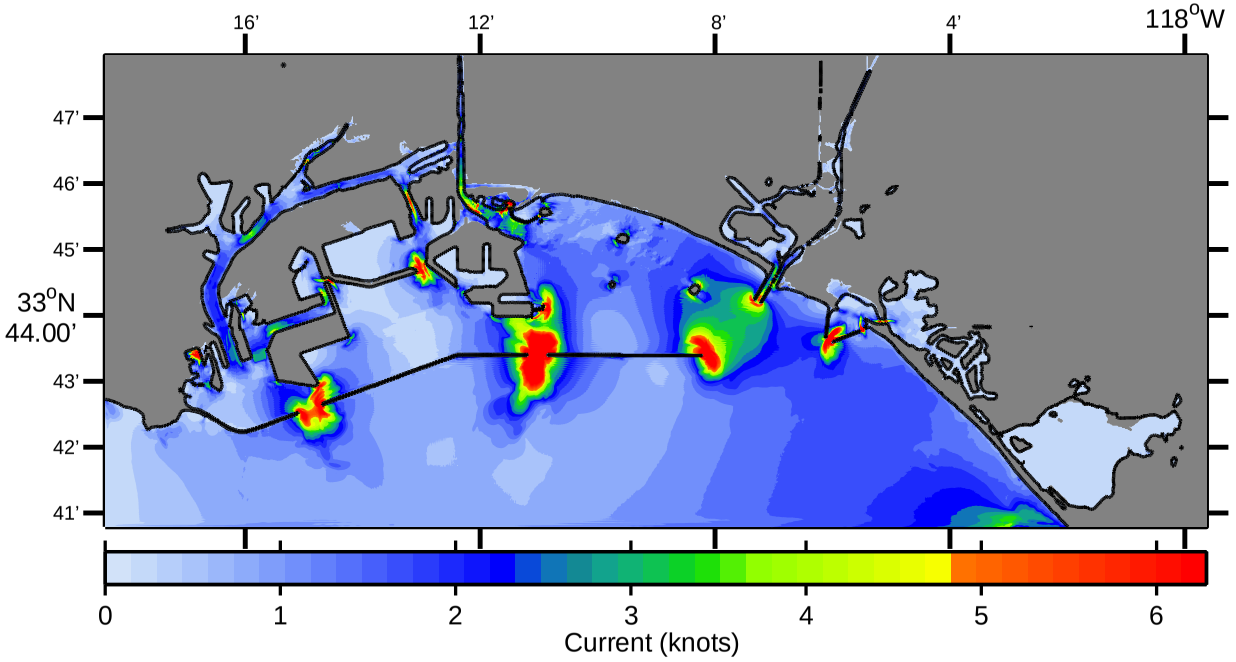

Figure B.10: Maximum current velocities at Port of Los Angeles and Long Beach from the artificial tsunami CSSZ 104–113.

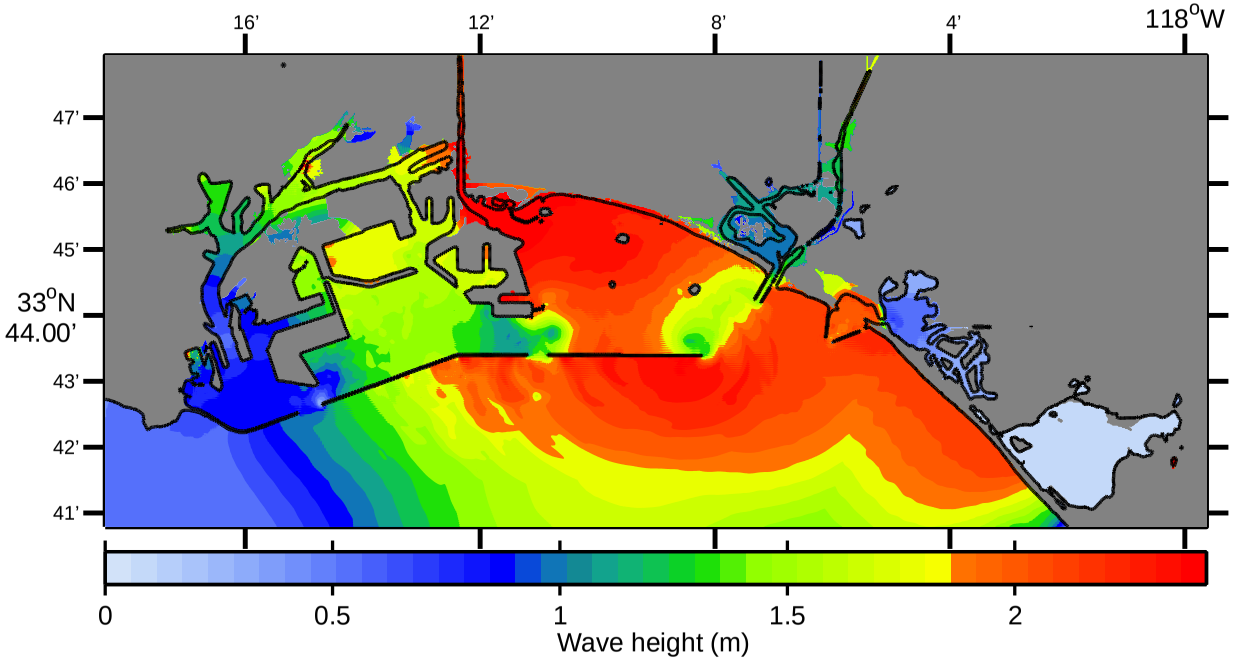

Figure B.11: Maximum wave amplitudes at Port of Los Angeles and Long Beach from the artificial tsunami EPSZ 09–18.

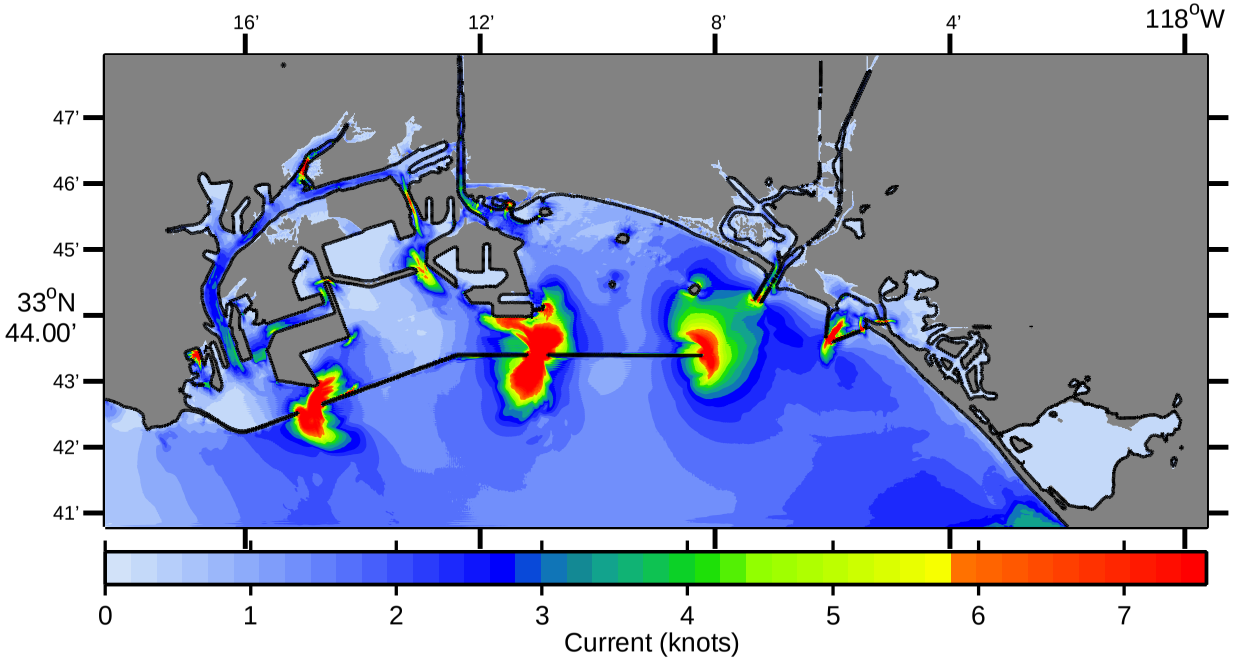

Figure B.12: Maximum current velocities at Port of Los Angeles and Long Beach from the artificial tsunami EPSZ 09–18.

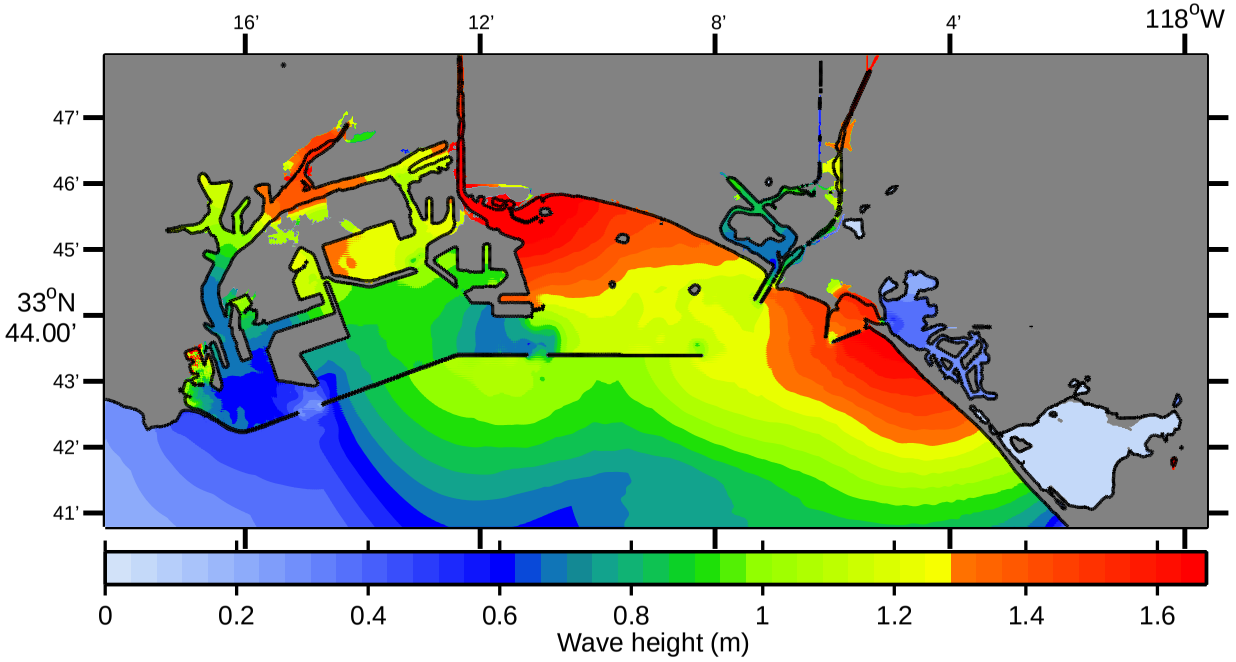

Figure B.13: Maximum wave amplitudes at Port of Los Angeles and Long Beach from the artificial tsunami KISZ 35–44.

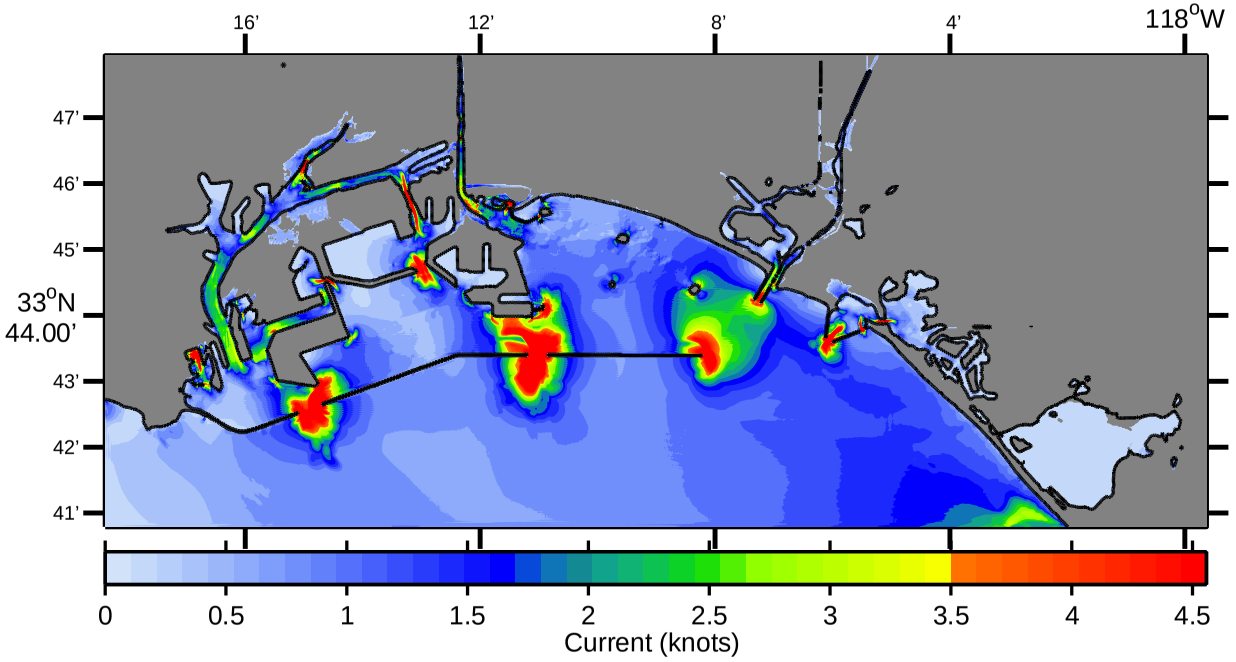

Figure B.14: Maximum current velocities at Port of Los Angeles and Long Beach from the artificial tsunami KISZ 35–44.

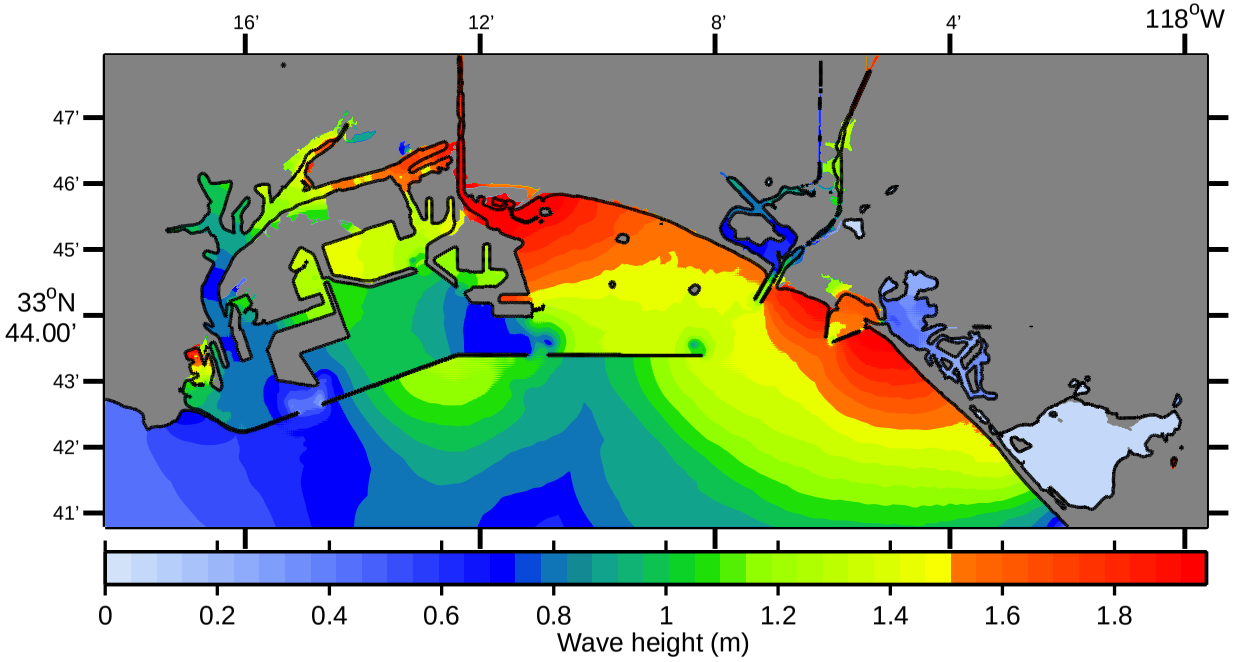

Figure B.15: Maximum wave amplitudes at Port of Los Angeles and Long Beach from the artificial tsunami KISZ 40–49.

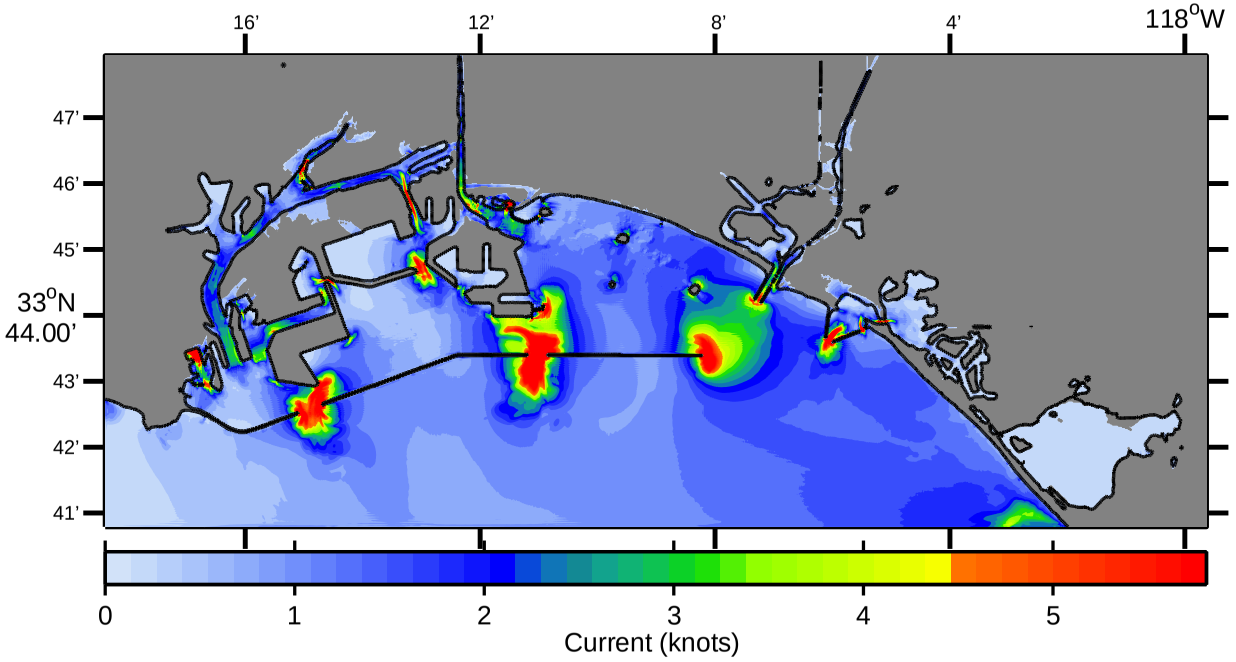

Figure B.16: Maximum current velocities at Port of Los Angeles and Long Beach from the artificial tsunami KISZ 40–49.

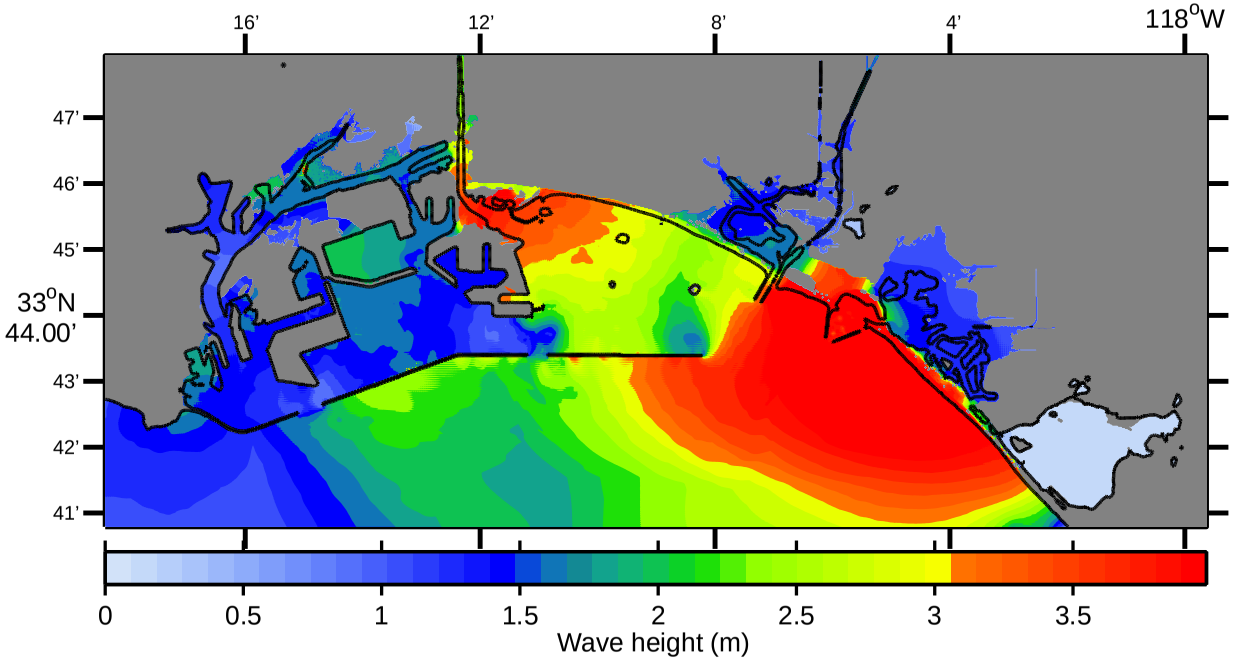

Figure B.17: Maximum wave amplitudes at Port of Los Angeles and Long Beach from the artificial tsunami MOSZ 01–10.

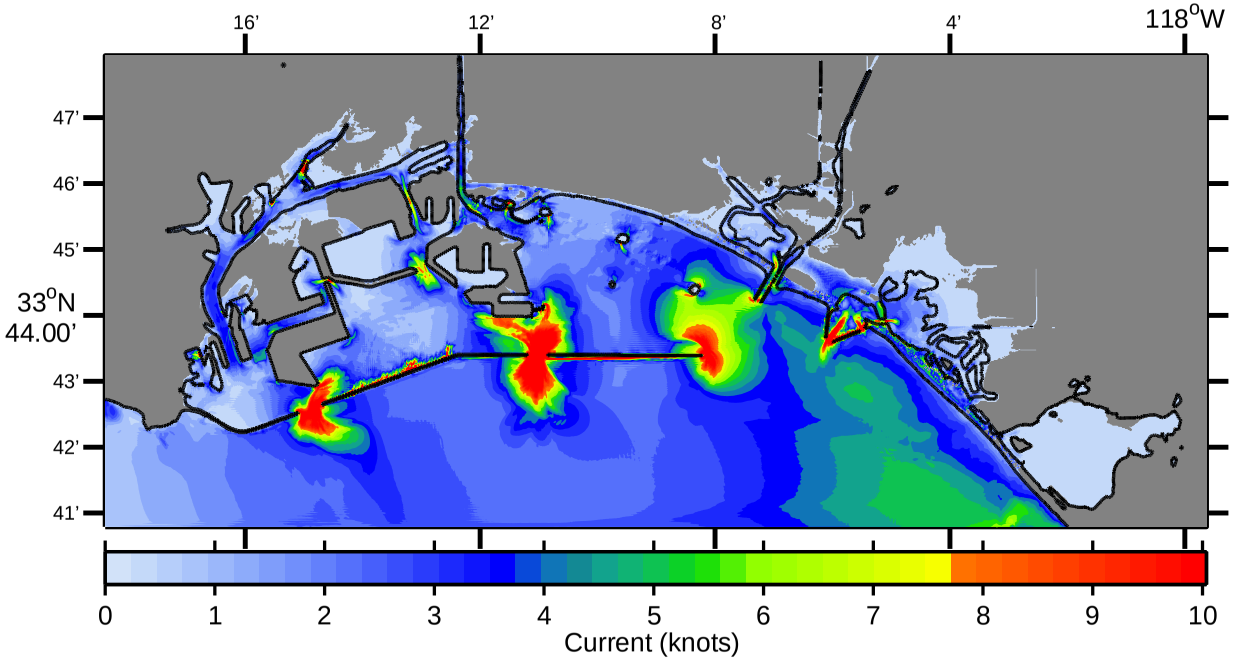

Figure B.18: Maximum current velocities at Port of Los Angeles and Long Beach from the artificial tsunami MOSZ 01–10.

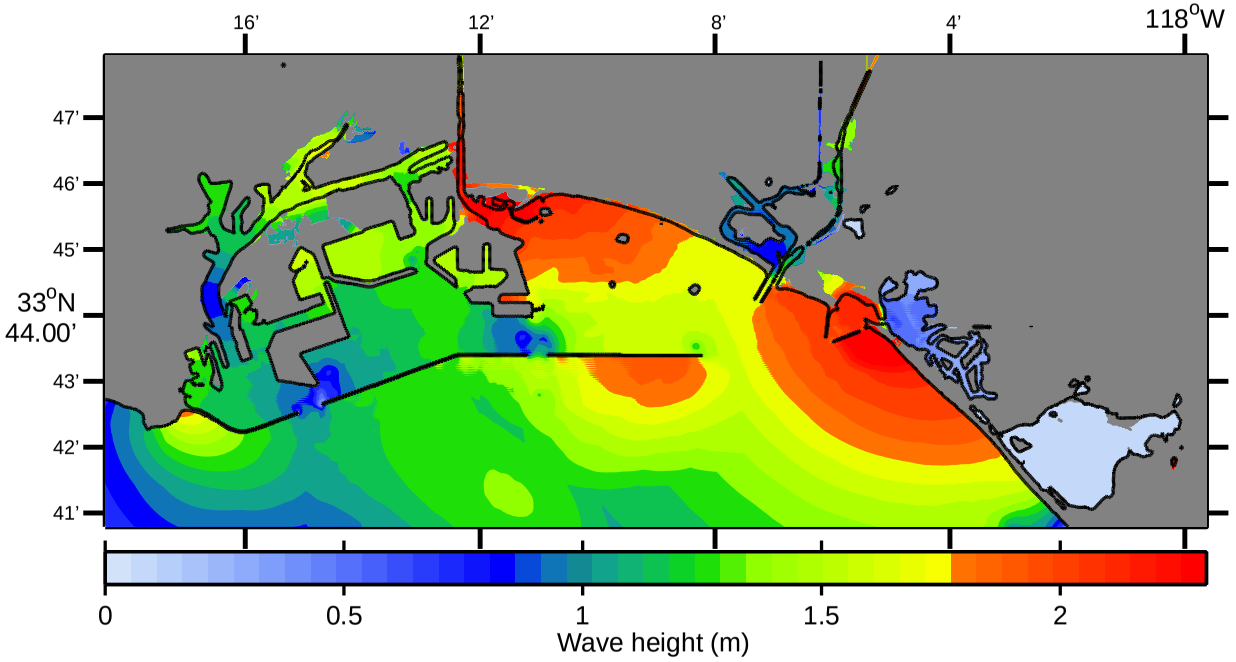

Figure B.19: Maximum wave amplitudes at Port of Los Angeles and Long Beach from the artificial tsunami NTSZ 27–36.

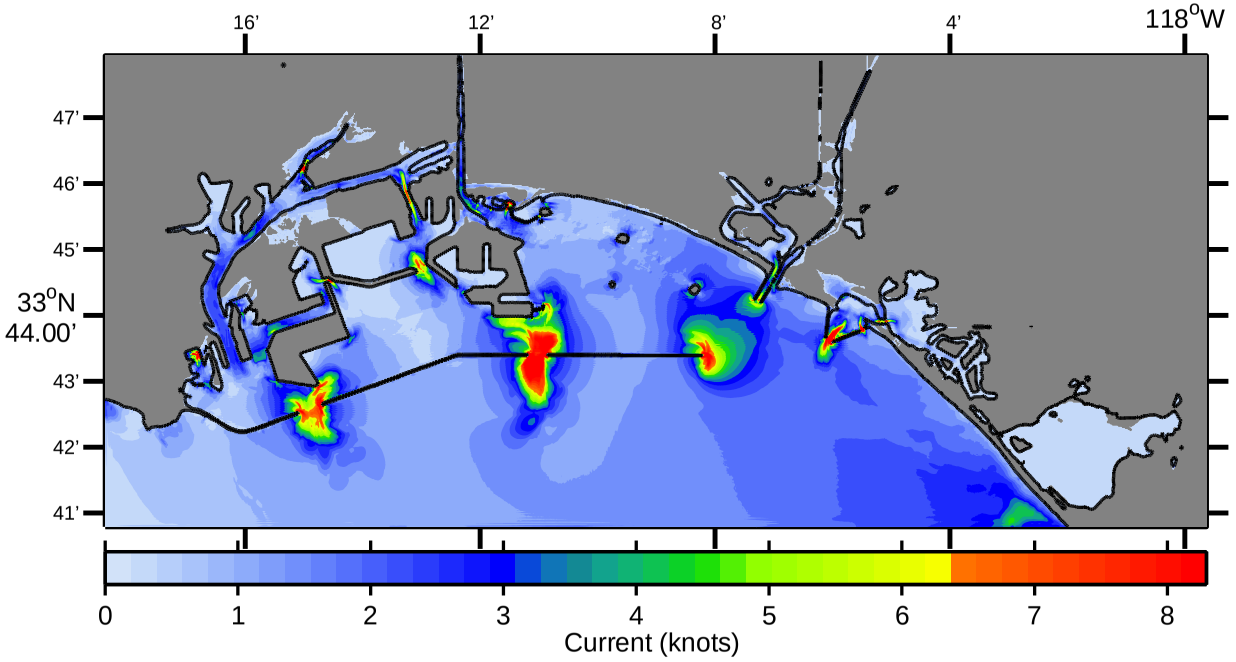

Figure B.20: Maximum current velocities at Port of Los Angeles and Long Beach from the artificial tsunami NTSZ 27–36.

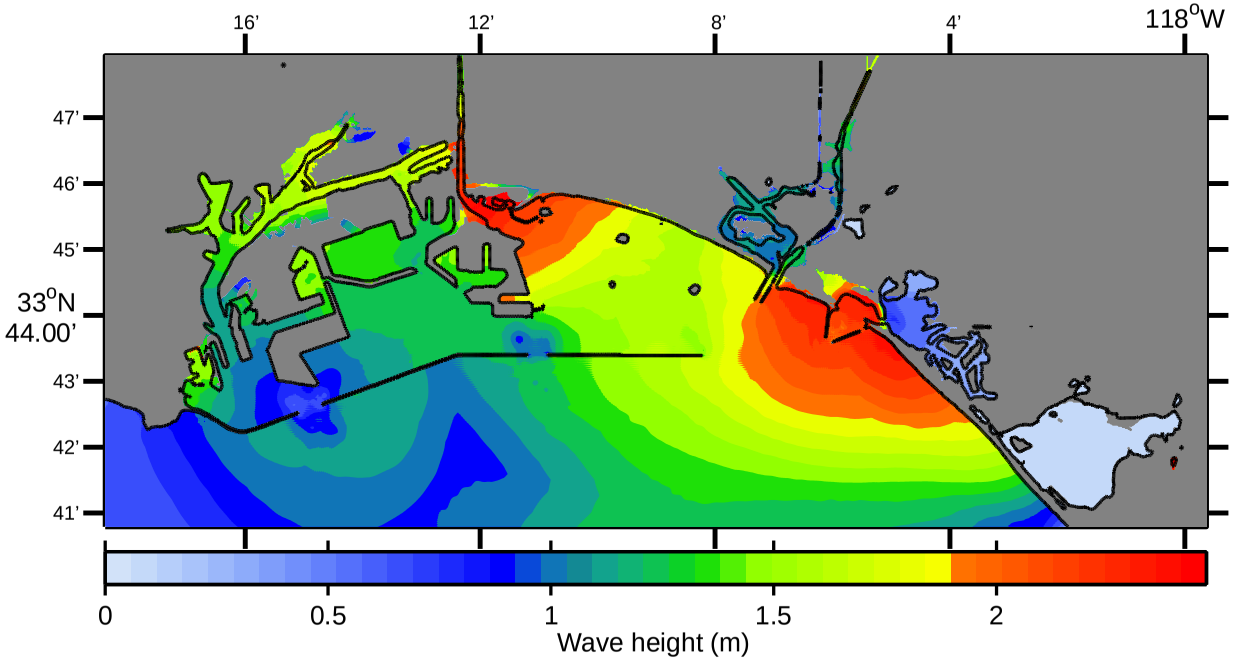

Figure B.21: Maximum wave amplitudes at Port of Los Angeles and Long Beach from the artificial tsunami NVSZ 28–36.

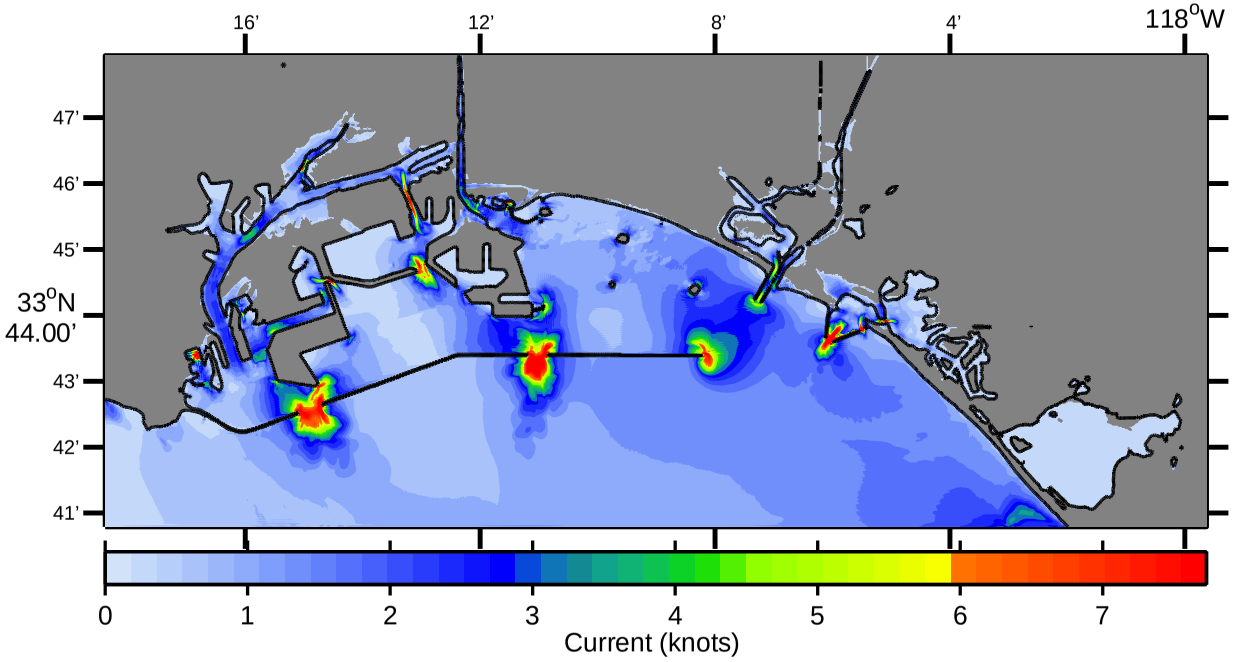

Figure B.22: Maximum current velocities at Port of Los Angeles and Long Beach from the artificial tsunami NVSZ 28–36.

Appendix C

Propagation Database Unit Sources

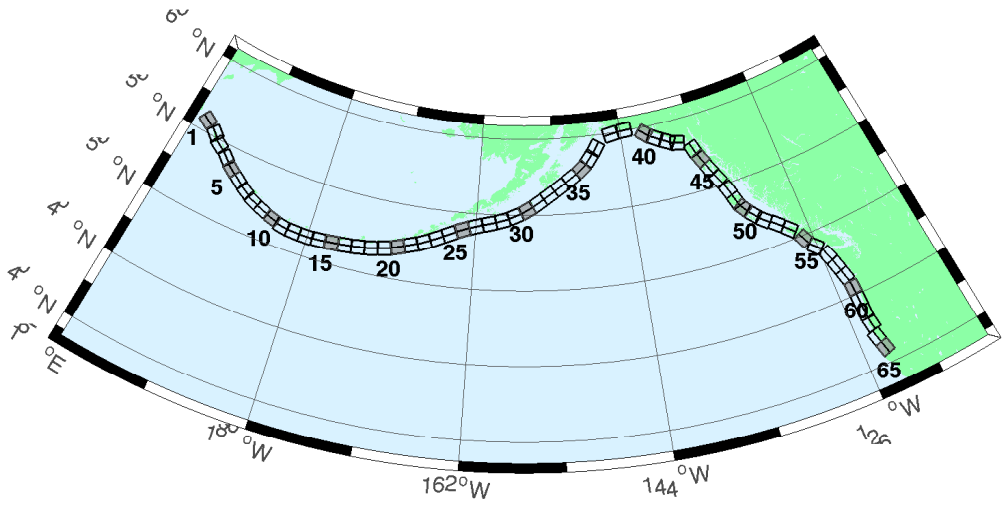

Figure C.1: Alaska–Aleutians/Cascadia Subduction Zone unit sources.

Segment	Description	Longitude(°E)	Latitude(°N)	Strike(°)	Dip(°)	Depth (km)
aasz–1a	Alaska–Aleutians/Cascadia	164.7994	55.9606	299	17	19.61
aasz–1b	Alaska–Aleutians/Cascadia	164.4310	55.5849	299	17	5
aasz–2a	Alaska–Aleutians/Cascadia	166.3418	55.4016	310.2	17	19.61
aasz–2b	Alaska–Aleutians/Cascadia	165.8578	55.0734	310.2	17	5
aasz–3a	Alaska–Aleutians/Cascadia	167.2939	54.8919	300.2	23.36	24.82
aasz–3b	Alaska–Aleutians/Cascadia	166.9362	54.5356	300.2	23.36	5
aasz–4a	Alaska–Aleutians/Cascadia	168.7131	54.2852	310.2	38.51	25.33
aasz–4b	Alaska–Aleutians/Cascadia	168.3269	54.0168	310.2	24	5
aasz–5a	Alaska–Aleutians/Cascadia	169.7447	53.7808	302.8	37.02	23.54
aasz–5b	Alaska–Aleutians/Cascadia	169.4185	53.4793	302.8	21.77	5
aasz–6a	Alaska–Aleutians/Cascadia	171.0144	53.3054	303.2	35.31	22.92

Continued on next page

Table C.1 – continued from previous page

Segment	Description	Longitude(°E)	Latitude(°N)	Strike(°)	Dip(°)	Depth (km)
aasz–6b	Alaska–Aleutians/Cascadia	170.6813	52.9986	303.2	21	5
aasz–7a	Alaska–Aleutians/Cascadia	172.1500	52.8528	298.2	35.56	20.16
aasz–7b	Alaska–Aleutians/Cascadia	171.8665	52.5307	298.2	17.65	5
aasz–8a	Alaska–Aleutians/Cascadia	173.2726	52.4579	290.8	37.92	20.35
aasz–8b	Alaska–Aleutians/Cascadia	173.0681	52.1266	290.8	17.88	5
aasz–9a	Alaska–Aleutians/Cascadia	174.5866	52.1434	289	39.09	21.05
aasz–9b	Alaska–Aleutians/Cascadia	174.4027	51.8138	289	18.73	5
aasz–10a	Alaska–Aleutians/Cascadia	175.8784	51.8526	286.1	40.51	20.87
aasz–10b	Alaska–Aleutians/Cascadia	175.7265	51.5245	286.1	18.51	5
aasz–11a	Alaska–Aleutians/Cascadia	177.1140	51.6488	280	15	17.94
aasz–11b	Alaska–Aleutians/Cascadia	176.9937	51.2215	280	15	5
aasz–12a	Alaska–Aleutians/Cascadia	178.4500	51.5690	273	15	17.94
aasz–12b	Alaska–Aleutians/Cascadia	178.4130	51.1200	273	15	5
aasz–13a	Alaska–Aleutians/Cascadia	179.8550	51.5340	271	15	17.94
aasz–13b	Alaska–Aleutians/Cascadia	179.8420	51.0850	271	15	5
aasz–14a	Alaska–Aleutians/Cascadia	181.2340	51.5780	267	15	17.94
aasz–14b	Alaska–Aleutians/Cascadia	181.2720	51.1290	267	15	5
aasz–15a	Alaska–Aleutians/Cascadia	182.6380	51.6470	265	15	17.94
aasz–15b	Alaska–Aleutians/Cascadia	182.7000	51.2000	265	15	5
aasz–16a	Alaska–Aleutians/Cascadia	184.0550	51.7250	264	15	17.94
aasz–16b	Alaska–Aleutians/Cascadia	184.1280	51.2780	264	15	5
aasz–17a	Alaska–Aleutians/Cascadia	185.4560	51.8170	262	15	17.94
aasz–17b	Alaska–Aleutians/Cascadia	185.5560	51.3720	262	15	5
aasz–18a	Alaska–Aleutians/Cascadia	186.8680	51.9410	261	15	17.94
aasz–18b	Alaska–Aleutians/Cascadia	186.9810	51.4970	261	15	5
aasz–19a	Alaska–Aleutians/Cascadia	188.2430	52.1280	257	15	17.94
aasz–19b	Alaska–Aleutians/Cascadia	188.4060	51.6900	257	15	5
aasz–20a	Alaska–Aleutians/Cascadia	189.5810	52.3550	251	15	17.94
aasz–20b	Alaska–Aleutians/Cascadia	189.8180	51.9300	251	15	5
aasz–21a	Alaska–Aleutians/Cascadia	190.9570	52.6470	251	15	17.94
aasz–21b	Alaska–Aleutians/Cascadia	191.1960	52.2220	251	15	5
aasz–22a	Alaska–Aleutians/Cascadia	192.2940	52.9430	247	15	17.94
aasz–22b	Alaska–Aleutians/Cascadia	192.5820	52.5300	247	15	5
aasz–23a	Alaska–Aleutians/Cascadia	193.6270	53.3070	245	15	17.94
aasz–23b	Alaska–Aleutians/Cascadia	193.9410	52.9000	245	15	5
aasz–24a	Alaska–Aleutians/Cascadia	194.9740	53.6870	245	15	17.94
aasz–24b	Alaska–Aleutians/Cascadia	195.2910	53.2800	245	15	5
aasz–25a	Alaska–Aleutians/Cascadia	196.4340	54.0760	250	15	17.94
aasz–25b	Alaska–Aleutians/Cascadia	196.6930	53.6543	250	15	5
aasz–26a	Alaska–Aleutians/Cascadia	197.8970	54.3600	253	15	17.94
aasz–26b	Alaska–Aleutians/Cascadia	198.1200	53.9300	253	15	5
aasz–27a	Alaska–Aleutians/Cascadia	199.4340	54.5960	256	15	17.94
aasz–27b	Alaska–Aleutians/Cascadia	199.6200	54.1600	256	15	5
aasz–28a	Alaska–Aleutians/Cascadia	200.8820	54.8300	253	15	17.94
aasz–28b	Alaska–Aleutians/Cascadia	201.1080	54.4000	253	15	5
aasz–29a	Alaska–Aleutians/Cascadia	202.2610	55.1330	247	15	17.94
aasz–29b	Alaska–Aleutians/Cascadia	202.5650	54.7200	247	15	5
aasz–30a	Alaska–Aleutians/Cascadia	203.6040	55.5090	240	15	17.94
aasz–30b	Alaska–Aleutians/Cascadia	203.9970	55.1200	240	15	5
aasz–31a	Alaska–Aleutians/Cascadia	204.8950	55.9700	236	15	17.94
aasz–31b	Alaska–Aleutians/Cascadia	205.3400	55.5980	236	15	5
aasz–32a	Alaska–Aleutians/Cascadia	206.2080	56.4730	236	15	17.94
aasz–32b	Alaska–Aleutians/Cascadia	206.6580	56.1000	236	15	5
aasz–33a	Alaska–Aleutians/Cascadia	207.5370	56.9750	236	15	17.94
aasz–33b	Alaska–Aleutians/Cascadia	207.9930	56.6030	236	15	5
aasz–34a	Alaska–Aleutians/Cascadia	208.9371	57.5124	236	15	17.94
aasz–34b	Alaska–Aleutians/Cascadia	209.4000	57.1400	236	15	5
aasz–35a	Alaska–Aleutians/Cascadia	210.2597	58.0441	230	15	17.94
aasz–35b	Alaska–Aleutians/Cascadia	210.8000	57.7000	230	15	5
aasz–36a	Alaska–Aleutians/Cascadia	211.3249	58.6565	218	15	17.94
aasz–36b	Alaska–Aleutians/Cascadia	212.0000	58.3800	218	15	5

Continued on next page

Table C.1 – continued from previous page

Segment	Description	Longitude(°E)	Latitude(°N)	Strike(°)	Dip(°)	Depth (km)
aasz–37a	Alaska–Aleutians/Cascadia	212.2505	59.2720	213.7	15	17.94
aasz–37b	Alaska–Aleutians/Cascadia	212.9519	59.0312	213.7	15	5
aasz–38a	Alaska–Aleutians/Cascadia	214.6555	60.1351	260.1	0	15
aasz–38b	Alaska–Aleutians/Cascadia	214.8088	59.6927	260.1	0	15
aasz–39a	Alaska–Aleutians/Cascadia	216.5607	60.2480	267	0	15
aasz–39b	Alaska–Aleutians/Cascadia	216.6068	59.7994	267	0	15
aasz–40a	Alaska–Aleutians/Cascadia	219.3069	59.7574	310.9	0	15
aasz–40b	Alaska–Aleutians/Cascadia	218.7288	59.4180	310.9	0	15
aasz–41a	Alaska–Aleutians/Cascadia	220.4832	59.3390	300.7	0	15
aasz–41b	Alaska–Aleutians/Cascadia	220.0382	58.9529	300.7	0	15
aasz–42a	Alaska–Aleutians/Cascadia	221.8835	58.9310	298.9	0	15
aasz–42b	Alaska–Aleutians/Cascadia	221.4671	58.5379	298.9	0	15
aasz–43a	Alaska–Aleutians/Cascadia	222.9711	58.6934	282.3	0	15
aasz–43b	Alaska–Aleutians/Cascadia	222.7887	58.2546	282.3	0	15
aasz–44a	Alaska–Aleutians/Cascadia	224.9379	57.9054	340.9	12	11.09
aasz–44b	Alaska–Aleutians/Cascadia	224.1596	57.7617	340.9	7	5
aasz–45a	Alaska–Aleutians/Cascadia	225.4994	57.1634	334.1	12	11.09
aasz–45b	Alaska–Aleutians/Cascadia	224.7740	56.9718	334.1	7	5
aasz–46a	Alaska–Aleutians/Cascadia	226.1459	56.3552	334.1	12	11.09
aasz–46b	Alaska–Aleutians/Cascadia	225.4358	56.1636	334.1	7	5
aasz–47a	Alaska–Aleutians/Cascadia	226.7731	55.5830	332.3	12	11.09
aasz–47b	Alaska–Aleutians/Cascadia	226.0887	55.3785	332.3	7	5
aasz–48a	Alaska–Aleutians/Cascadia	227.4799	54.6763	339.4	12	11.09
aasz–48b	Alaska–Aleutians/Cascadia	226.7713	54.5217	339.4	7	5
aasz–49a	Alaska–Aleutians/Cascadia	227.9482	53.8155	341.2	12	11.09
aasz–49b	Alaska–Aleutians/Cascadia	227.2462	53.6737	341.2	7	5
aasz–50a	Alaska–Aleutians/Cascadia	228.3970	53.2509	324.5	12	11.09
aasz–50b	Alaska–Aleutians/Cascadia	227.8027	52.9958	324.5	7	5
aasz–51a	Alaska–Aleutians/Cascadia	229.1844	52.6297	318.4	12	11.09
aasz–51b	Alaska–Aleutians/Cascadia	228.6470	52.3378	318.4	7	5
aasz–52a	Alaska–Aleutians/Cascadia	230.0306	52.0768	310.9	12	11.09
aasz–52b	Alaska–Aleutians/Cascadia	229.5665	51.7445	310.9	7	5
aasz–53a	Alaska–Aleutians/Cascadia	231.1735	51.5258	310.9	12	11.09
aasz–53b	Alaska–Aleutians/Cascadia	230.7150	51.1935	310.9	7	5
aasz–54a	Alaska–Aleutians/Cascadia	232.2453	50.8809	314.1	12	11.09
aasz–54b	Alaska–Aleutians/Cascadia	231.7639	50.5655	314.1	7	5
aasz–55a	Alaska–Aleutians/Cascadia	233.3066	49.9032	333.7	12	11.09
aasz–55b	Alaska–Aleutians/Cascadia	232.6975	49.7086	333.7	7	5
aasz–56a	Alaska–Aleutians/Cascadia	234.0588	49.1702	315	11	12.82
aasz–56b	Alaska–Aleutians/Cascadia	233.5849	48.8584	315	9	5
aasz–57a	Alaska–Aleutians/Cascadia	234.9041	48.2596	341	11	12.82
aasz–57b	Alaska–Aleutians/Cascadia	234.2797	48.1161	341	9	5
aasz–58a	Alaska–Aleutians/Cascadia	235.3021	47.3812	344	11	12.82
aasz–58b	Alaska–Aleutians/Cascadia	234.6776	47.2597	344	9	5
aasz–59a	Alaska–Aleutians/Cascadia	235.6432	46.5082	345	11	12.82
aasz–59b	Alaska–Aleutians/Cascadia	235.0257	46.3941	345	9	5
aasz–60a	Alaska–Aleutians/Cascadia	235.8640	45.5429	356	11	12.82
aasz–60b	Alaska–Aleutians/Cascadia	235.2363	45.5121	356	9	5
aasz–61a	Alaska–Aleutians/Cascadia	235.9106	44.6227	359	11	12.82
aasz–61b	Alaska–Aleutians/Cascadia	235.2913	44.6150	359	9	5
aasz–62a	Alaska–Aleutians/Cascadia	235.9229	43.7245	359	11	12.82
aasz–62b	Alaska–Aleutians/Cascadia	235.3130	43.7168	359	9	5
aasz–63a	Alaska–Aleutians/Cascadia	236.0220	42.9020	350	11	12.82
aasz–63b	Alaska–Aleutians/Cascadia	235.4300	42.8254	350	9	5
aasz–64a	Alaska–Aleutians/Cascadia	235.9638	41.9818	345	11	12.82
aasz–64b	Alaska–Aleutians/Cascadia	235.3919	41.8677	345	9	5
aasz–65a	Alaska–Aleutians/Cascadia	236.2643	41.1141	345	11	12.82
aasz–65b	Alaska–Aleutians/Cascadia	235.7000	41.0000	345	9	5

Table C.1: Earthquake parameters for Alaska–Aleutians/Cascadia Subduction Zone unit sources.

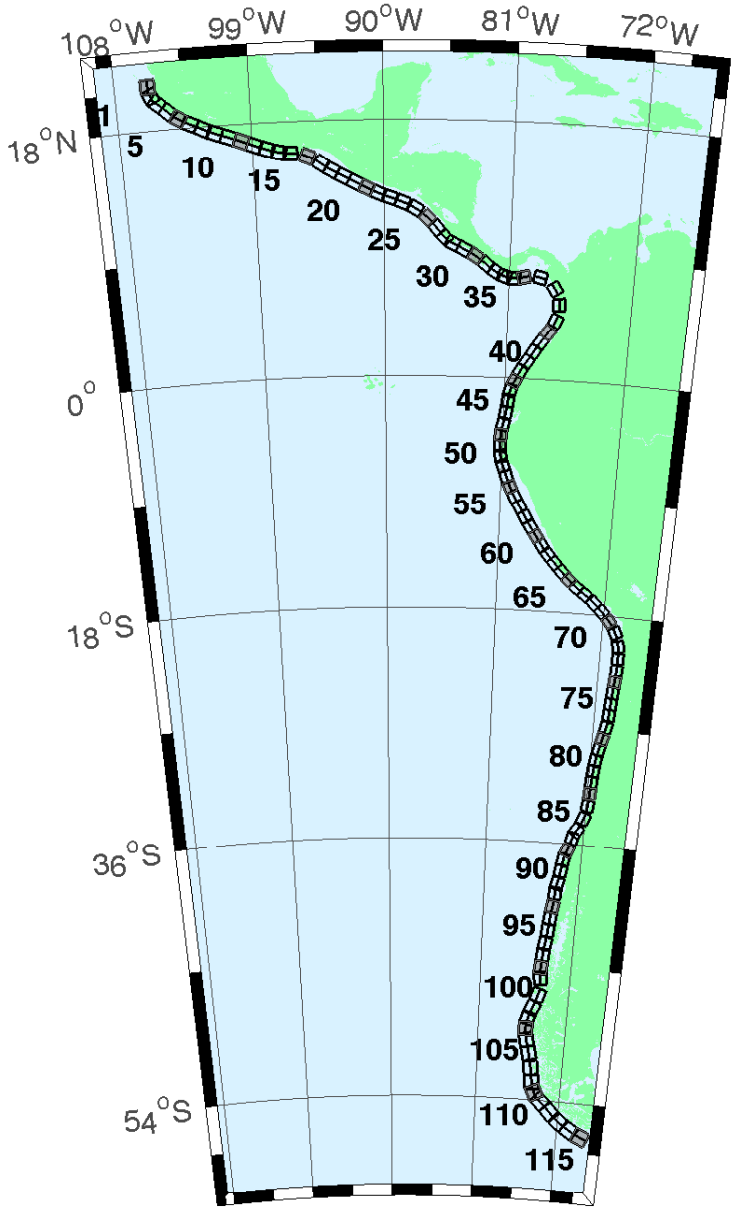

Figure C.2: Central and South America Subduction Zone unit sources.

Segment	Description	Longitude(°E)	Latitude(°N)	Strike(°)	Dip(°)	Depth (km)
cssz–1a	Central and South America	254.4573	20.8170	359	19	15.4
cssz–1b	Central and South America	254.0035	20.8094	359	12	5
cssz–2a	Central and South America	254.5765	20.2806	336.8	19	15.4
cssz–2b	Central and South America	254.1607	20.1130	336.8	12	5
cssz–3a	Central and South America	254.8789	19.8923	310.6	18.31	15.27
cssz–3b	Central and South America	254.5841	19.5685	310.6	11.85	5
cssz–4a	Central and South America	255.6167	19.2649	313.4	17.62	15.12
cssz–4b	Central and South America	255.3056	18.9537	313.4	11.68	5
cssz–5a	Central and South America	256.2240	18.8148	302.7	16.92	15
cssz–5b	Central and South America	255.9790	18.4532	302.7	11.54	5
cssz–6a	Central and South America	256.9425	18.4383	295.1	16.23	14.87
cssz–6b	Central and South America	256.7495	18.0479	295.1	11.38	5
cssz–7a	Central and South America	257.8137	18.0339	296.9	15.54	14.74
cssz–7b	Central and South America	257.6079	17.6480	296.9	11.23	5
cssz–8a	Central and South America	258.5779	17.7151	290.4	14.85	14.61
cssz–8b	Central and South America	258.4191	17.3082	290.4	11.08	5
cssz–9a	Central and South America	259.4578	17.4024	290.5	14.15	14.47
cssz–9b	Central and South America	259.2983	16.9944	290.5	10.92	5
cssz–10a	Central and South America	260.3385	17.0861	290.8	13.46	14.34
cssz–10b	Central and South America	260.1768	16.6776	290.8	10.77	5
cssz–11a	Central and South America	261.2255	16.7554	291.8	12.77	14.21
cssz–11b	Central and South America	261.0556	16.3487	291.8	10.62	5
cssz–12a	Central and South America	262.0561	16.4603	288.9	12.08	14.08
cssz–12b	Central and South America	261.9082	16.0447	288.9	10.46	5
cssz–13a	Central and South America	262.8638	16.2381	283.2	11.38	13.95
cssz–13b	Central and South America	262.7593	15.8094	283.2	10.31	5
cssz–14a	Central and South America	263.6066	16.1435	272.1	10.69	13.81
cssz–14b	Central and South America	263.5901	15.7024	272.1	10.15	5
cssz–15a	Central and South America	264.8259	15.8829	293	10	13.68
cssz–15b	Central and South America	264.6462	15.4758	293	10	5
cssz–16a	Central and South America	265.7928	15.3507	304.9	15	15.82
cssz–16b	Central and South America	265.5353	14.9951	304.9	12.5	5
cssz–17a	Central and South America	266.4947	14.9019	299.5	20	17.94
cssz–17b	Central and South America	266.2797	14.5346	299.5	15	5
cssz–18a	Central and South America	267.2827	14.4768	298	21.5	17.94
cssz–18b	Central and South America	267.0802	14.1078	298	15	5
cssz–19a	Central and South America	268.0919	14.0560	297.6	23	17.94
cssz–19b	Central and South America	267.8943	13.6897	297.6	15	5
cssz–20a	Central and South America	268.8929	13.6558	296.2	24	17.94
cssz–20b	Central and South America	268.7064	13.2877	296.2	15	5
cssz–21a	Central and South America	269.6797	13.3031	292.6	25	17.94
cssz–21b	Central and South America	269.5187	12.9274	292.6	15	5
cssz–22a	Central and South America	270.4823	13.0079	288.6	25	17.94
cssz–22b	Central and South America	270.3492	12.6221	288.6	15	5
cssz–23a	Central and South America	271.3961	12.6734	292.4	25	17.94
cssz–23b	Central and South America	271.2369	12.2972	292.4	15	5
cssz–24a	Central and South America	272.3203	12.2251	300.2	25	17.94
cssz–24b	Central and South America	272.1107	11.8734	300.2	15	5
cssz–25a	Central and South America	273.2075	11.5684	313.8	25	17.94
cssz–25b	Central and South America	272.9200	11.2746	313.8	15	5
cssz–26a	Central and South America	273.8943	10.8402	320.4	25	17.94
cssz–26b	Central and South America	273.5750	10.5808	320.4	15	5
cssz–27a	Central and South America	274.4569	10.2177	316.1	25	17.94
cssz–27b	Central and South America	274.1590	9.9354	316.1	15	5
cssz–28a	Central and South America	274.9586	9.8695	297.1	22	14.54
cssz–28b	Central and South America	274.7661	9.4988	297.1	11	5
cssz–29a	Central and South America	275.7686	9.4789	296.6	19	11.09
cssz–29b	Central and South America	275.5759	9.0992	296.6	7	5
cssz–30a	Central and South America	276.6346	8.9973	302.2	19	9.36
cssz–30b	Central and South America	276.4053	8.6381	302.2	5	5
cssz–31a	Central and South America	277.4554	8.4152	309.1	19	7.62

Continued on next page

Table C.2 – continued from previous page

Segment	Description	Longitude(°E)	Latitude(°N)	Strike(°)	Dip(°)	Depth (km)
cssz–31b	Central and South America	277.1851	8.0854	309.1	3	5
cssz–32a	Central and South America	278.1112	7.9425	303	18.67	8.49
cssz–32b	Central and South America	277.8775	7.5855	303	4	5
cssz–33a	Central and South America	278.7082	7.6620	287.6	18.33	10.23
cssz–33b	Central and South America	278.5785	7.2555	287.6	6	5
cssz–34a	Central and South America	279.3184	7.5592	269.5	18	17.94
cssz–34b	Central and South America	279.3223	7.1320	269.5	15	5
cssz–35a	Central and South America	280.0039	7.6543	255.9	17.67	14.54
cssz–35b	Central and South America	280.1090	7.2392	255.9	11	5
cssz–36a	Central and South America	281.2882	7.6778	282.5	17.33	11.09
cssz–36b	Central and South America	281.1948	7.2592	282.5	7	5
cssz–37a	Central and South America	282.5252	6.8289	326.9	17	10.23
cssz–37b	Central and South America	282.1629	6.5944	326.9	6	5
cssz–38a	Central and South America	282.9469	5.5973	355.4	17	10.23
cssz–38b	Central and South America	282.5167	5.5626	355.4	6	5
cssz–39a	Central and South America	282.7236	4.3108	24.13	17	10.23
cssz–39b	Central and South America	282.3305	4.4864	24.13	6	5
cssz–40a	Central and South America	282.1940	3.3863	35.28	17	10.23
cssz–40b	Central and South America	281.8427	3.6344	35.28	6	5
cssz–41a	Central and South America	281.6890	2.6611	34.27	17	10.23
cssz–41b	Central and South America	281.3336	2.9030	34.27	6	5
cssz–42a	Central and South America	281.2266	1.9444	31.29	17	10.23
cssz–42b	Central and South America	280.8593	2.1675	31.29	6	5
cssz–43a	Central and South America	280.7297	1.1593	33.3	17	10.23
cssz–43b	Central and South America	280.3706	1.3951	33.3	6	5
cssz–44a	Central and South America	280.3018	0.4491	28.8	17	10.23
cssz–44b	Central and South America	279.9254	0.6560	28.8	6	5
cssz–45a	Central and South America	279.9083	-0.3259	26.91	10	8.49
cssz–45b	Central and South America	279.5139	-0.1257	26.91	4	5
cssz–46a	Central and South America	279.6461	-0.9975	15.76	10	8.49
cssz–46b	Central and South America	279.2203	-0.8774	15.76	4	5
cssz–47a	Central and South America	279.4972	-1.7407	6.9	10	8.49
cssz–47b	Central and South America	279.0579	-1.6876	6.9	4	5
cssz–48a	Central and South America	279.3695	-2.6622	8.96	10	8.49
cssz–48b	Central and South America	278.9321	-2.5933	8.96	4	5
cssz–49a	Central and South America	279.1852	-3.6070	13.15	10	8.49
cssz–49b	Central and South America	278.7536	-3.5064	13.15	4	5
cssz–50a	Central and South America	279.0652	-4.3635	4.78	10.33	9.64
cssz–50b	Central and South America	278.6235	-4.3267	4.78	5.33	5
cssz–51a	Central and South America	279.0349	-5.1773	359.4	10.67	10.81
cssz–51b	Central and South America	278.5915	-5.1817	359.4	6.67	5
cssz–52a	Central and South America	279.1047	-5.9196	349.8	11	11.96
cssz–52b	Central and South America	278.6685	-5.9981	349.8	8	5
cssz–53a	Central and South America	279.3044	-6.6242	339.2	10.25	11.74
cssz–53b	Central and South America	278.8884	-6.7811	339.2	7.75	5
cssz–54a	Central and South America	279.6256	-7.4907	340.8	9.5	11.53
cssz–54b	Central and South America	279.2036	-7.6365	340.8	7.5	5
cssz–55a	Central and South America	279.9348	-8.2452	335.4	8.75	11.74
cssz–55b	Central and South America	279.5269	-8.4301	335.4	7.75	5
cssz–56a	Central and South America	280.3172	-8.9958	331.6	8	11.09
cssz–56b	Central and South America	279.9209	-9.2072	331.6	7	5
cssz–57a	Central and South America	280.7492	-9.7356	328.7	8.6	10.75
cssz–57b	Central and South America	280.3640	-9.9663	328.7	6.6	5
cssz–58a	Central and South America	281.2275	-10.5350	330.5	9.2	10.4
cssz–58b	Central and South America	280.8348	-10.7532	330.5	6.2	5
cssz–59a	Central and South America	281.6735	-11.2430	326.2	9.8	10.05
cssz–59b	Central and South America	281.2982	-11.4890	326.2	5.8	5
cssz–60a	Central and South America	282.1864	-11.9946	326.5	10.4	9.71
cssz–60b	Central and South America	281.8096	-12.2384	326.5	5.4	5
cssz–61a	Central and South America	282.6944	-12.7263	325.5	11	9.36
cssz–61b	Central and South America	282.3218	-12.9762	325.5	5	5

Continued on next page

Table C.2 – continued from previous page

Segment	Description	Longitude(°E)	Latitude(°N)	Strike(°)	Dip(°)	Depth (km)
cssz–62a	Central and South America	283.1980	-13.3556	319	11	9.79
cssz–62b	Central and South America	282.8560	-13.6451	319	5.5	5
cssz–63a	Central and South America	283.8032	-14.0147	317.9	11	10.23
cssz–63b	Central and South America	283.4661	-14.3106	317.9	6	5
cssz–64a	Central and South America	284.4144	-14.6482	315.7	13	11.96
cssz–64b	Central and South America	284.0905	-14.9540	315.7	8	5
cssz–65a	Central and South America	285.0493	-15.2554	313.2	15	13.68
cssz–65b	Central and South America	284.7411	-15.5715	313.2	10	5
cssz–66a	Central and South America	285.6954	-15.7816	307.7	14.5	13.68
cssz–66b	Central and South America	285.4190	-16.1258	307.7	10	5
cssz–67a	Central and South America	286.4127	-16.2781	304.3	14	13.68
cssz–67b	Central and South America	286.1566	-16.6381	304.3	10	5
cssz–68a	Central and South America	287.2481	-16.9016	311.8	14	13.68
cssz–68b	Central and South America	286.9442	-17.2264	311.8	10	5
cssz–69a	Central and South America	287.9724	-17.5502	314.9	14	13.68
cssz–69b	Central and South America	287.6496	-17.8590	314.9	10	5
cssz–70a	Central and South America	288.6731	-18.2747	320.4	14	13.25
cssz–70b	Central and South America	288.3193	-18.5527	320.4	9.5	5
cssz–71a	Central and South America	289.3089	-19.1854	333.2	14	12.82
cssz–71b	Central and South America	288.8968	-19.3820	333.2	9	5
cssz–72a	Central and South America	289.6857	-20.3117	352.4	14	12.54
cssz–72b	Central and South America	289.2250	-20.3694	352.4	8.67	5
cssz–73a	Central and South America	289.7731	-21.3061	358.9	14	12.24
cssz–73b	Central and South America	289.3053	-21.3142	358.9	8.33	5
cssz–74a	Central and South America	289.7610	-22.2671	3.06	14	11.96
cssz–74b	Central and South America	289.2909	-22.2438	3.06	8	5
cssz–75a	Central and South America	289.6982	-23.1903	4.83	14.09	11.96
cssz–75b	Central and South America	289.2261	-23.1536	4.83	8	5
cssz–76a	Central and South America	289.6237	-24.0831	4.67	14.18	11.96
cssz–76b	Central and South America	289.1484	-24.0476	4.67	8	5
cssz–77a	Central and South America	289.5538	-24.9729	4.3	14.27	11.96
cssz–77b	Central and South America	289.0750	-24.9403	4.3	8	5
cssz–78a	Central and South America	289.4904	-25.8621	3.86	14.36	11.96
cssz–78b	Central and South America	289.0081	-25.8328	3.86	8	5
cssz–79a	Central and South America	289.3491	-26.8644	11.34	14.45	11.96
cssz–79b	Central and South America	288.8712	-26.7789	11.34	8	5
cssz–80a	Central and South America	289.1231	-27.7826	14.16	14.54	11.96
cssz–80b	Central and South America	288.6469	-27.6762	14.16	8	5
cssz–81a	Central and South America	288.8943	-28.6409	13.19	14.63	11.96
cssz–81b	Central and South America	288.4124	-28.5417	13.19	8	5
cssz–82a	Central and South America	288.7113	-29.4680	9.68	14.72	11.96
cssz–82b	Central and South America	288.2196	-29.3950	9.68	8	5
cssz–83a	Central and South America	288.5944	-30.2923	5.36	14.81	11.96
cssz–83b	Central and South America	288.0938	-30.2517	5.36	8	5
cssz–84a	Central and South America	288.5223	-31.1639	3.8	14.9	11.96
cssz–84b	Central and South America	288.0163	-31.1351	3.8	8	5
cssz–85a	Central and South America	288.4748	-32.0416	2.55	15	11.96
cssz–85b	Central and South America	287.9635	-32.0223	2.55	8	5
cssz–86a	Central and South America	288.3901	-33.0041	7.01	15	11.96
cssz–86b	Central and South America	287.8768	-32.9512	7.01	8	5
cssz–87a	Central and South America	288.1050	-34.0583	19.4	15	11.96
cssz–87b	Central and South America	287.6115	-33.9142	19.4	8	5
cssz–88a	Central and South America	287.5309	-35.0437	32.81	15	11.96
cssz–88b	Central and South America	287.0862	-34.8086	32.81	8	5
cssz–89a	Central and South America	287.2380	-35.5993	14.52	16.67	11.96
cssz–89b	Central and South America	286.7261	-35.4914	14.52	8	5
cssz–90a	Central and South America	286.8442	-36.5645	22.64	18.33	11.96
cssz–90b	Central and South America	286.3548	-36.4004	22.64	8	5
cssz–91a	Central and South America	286.5925	-37.2488	10.9	20	11.96
cssz–91b	Central and South America	286.0721	-37.1690	10.9	8	5
cssz–92a	Central and South America	286.4254	-38.0945	8.23	20	11.96

Continued on next page

Table C.2 – continued from previous page

Segment	Description	Longitude(°E)	Latitude(°N)	Strike(°)	Dip(°)	Depth (km)
cssz–92b	Central and South America	285.8948	-38.0341	8.23	8	5
cssz–93a	Central and South America	286.2047	-39.0535	13.46	20	11.96
cssz–93b	Central and South America	285.6765	-38.9553	13.46	8	5
cssz–94a	Central and South America	286.0772	-39.7883	3.4	20	11.96
cssz–94b	Central and South America	285.5290	-39.7633	3.4	8	5
cssz–95a	Central and South America	285.9426	-40.7760	9.84	20	11.96
cssz–95b	Central and South America	285.3937	-40.7039	9.84	8	5
cssz–96a	Central and South America	285.7839	-41.6303	7.6	20	11.96
cssz–96b	Central and South America	285.2245	-41.5745	7.6	8	5
cssz–97a	Central and South America	285.6695	-42.4882	5.3	20	11.96
cssz–97b	Central and South America	285.0998	-42.4492	5.3	8	5
cssz–98a	Central and South America	285.5035	-43.4553	10.53	20	11.96
cssz–98b	Central and South America	284.9322	-43.3782	10.53	8	5
cssz–99a	Central and South America	285.3700	-44.2595	4.86	20	11.96
cssz–99b	Central and South America	284.7830	-44.2237	4.86	8	5
cssz–100a	Central and South America	285.2713	-45.1664	5.68	20	11.96
cssz–100b	Central and South America	284.6758	-45.1246	5.68	8	5
cssz–101a	Central and South America	285.3080	-45.8607	352.6	20	9.36
cssz–101b	Central and South America	284.7067	-45.9152	352.6	5	5
cssz–102a	Central and South America	285.2028	-47.1185	17.72	5	9.36
cssz–102b	Central and South America	284.5772	-46.9823	17.72	5	5
cssz–103a	Central and South America	284.7075	-48.0396	23.37	7.5	11.53
cssz–103b	Central and South America	284.0972	-47.8630	23.37	7.5	5
cssz–104a	Central and South America	284.3440	-48.7597	14.87	10	13.68
cssz–104b	Central and South America	283.6962	-48.6462	14.87	10	5
cssz–105a	Central and South America	284.2312	-49.4198	0.25	9.67	13.4
cssz–105b	Central and South America	283.5518	-49.4179	0.25	9.67	5
cssz–106a	Central and South America	284.3730	-50.1117	347.5	9.25	13.04
cssz–106b	Central and South America	283.6974	-50.2077	347.5	9.25	5
cssz–107a	Central and South America	284.7130	-50.9714	346.5	9	12.82
cssz–107b	Central and South America	284.0273	-51.0751	346.5	9	5
cssz–108a	Central and South America	285.0378	-51.9370	352	8.67	12.54
cssz–108b	Central and South America	284.3241	-51.9987	352	8.67	5
cssz–109a	Central and South America	285.2635	-52.8439	353.1	8.33	12.24
cssz–109b	Central and South America	284.5326	-52.8974	353.1	8.33	5
cssz–110a	Central and South America	285.5705	-53.4139	334.2	8	11.96
cssz–110b	Central and South America	284.8972	-53.6076	334.2	8	5
cssz–111a	Central and South America	286.1627	-53.8749	313.8	8	11.96
cssz–111b	Central and South America	285.6382	-54.1958	313.8	8	5
cssz–112a	Central and South America	287.3287	-54.5394	316.4	8	11.96
cssz–112b	Central and South America	286.7715	-54.8462	316.4	8	5
cssz–113a	Central and South America	288.3409	-55.0480	307.6	8	11.96
cssz–113b	Central and South America	287.8647	-55.4002	307.6	8	5
cssz–114a	Central and South America	289.5342	-55.5026	301.5	8	11.96
cssz–114b	Central and South America	289.1221	-55.8819	301.5	8	5
cssz–115a	Central and South America	290.7682	-55.8485	292.7	8	11.96
cssz–115b	Central and South America	290.4608	-56.2588	292.7	8	5

Table C.2: Earthquake parameters for Central and South America Subduction Zone unit sources.

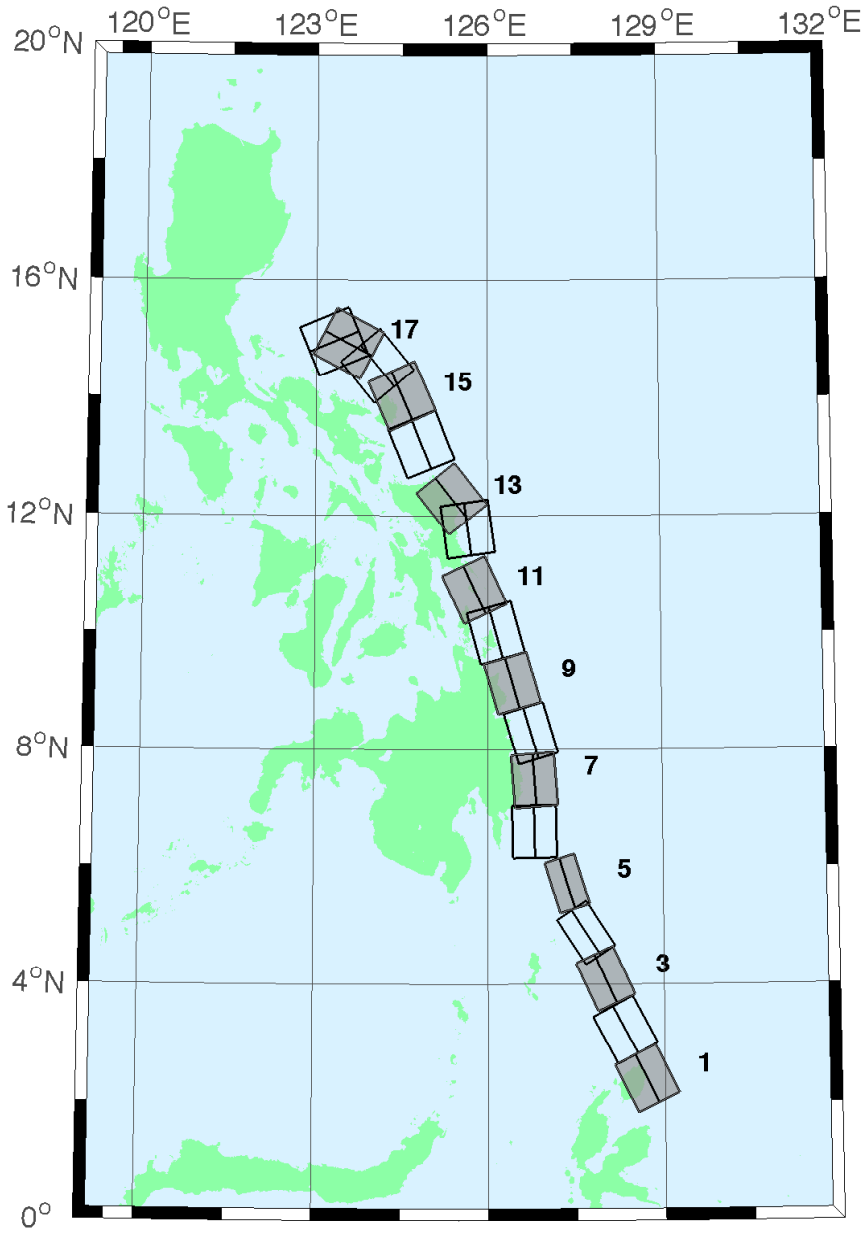

Figure C.3: Eastern Philippines Subduction Zone unit sources.

Segment	Description	Longitude(^{o}E)	Latitude(^{o}N)	Strike(^{o})	Dip(^{o})	Depth (km)
epsz–1a	Eastern Philippines	128.5521	2.3289	153.6	44.2	27.62
epsz–1b	Eastern Philippines	128.8408	2.4720	153.6	26.9	5
epsz–2a	Eastern Philippines	128.1943	3.1508	151.9	45.9	32.44
epsz–2b	Eastern Philippines	128.4706	3.2979	151.9	32.8	5.35
epsz–3a	Eastern Philippines	127.8899	4.0428	155.2	57.3	40.22
epsz–3b	Eastern Philippines	128.1108	4.1445	155.2	42.7	6.31
epsz–4a	Eastern Philippines	127.6120	4.8371	146.8	71.4	48.25
epsz–4b	Eastern Philippines	127.7324	4.9155	146.8	54.8	7.39
epsz–5a	Eastern Philippines	127.3173	5.7040	162.9	79.9	57.4
epsz–5b	Eastern Philippines	127.3930	5.7272	162.9	79.4	8.25
epsz–6a	Eastern Philippines	126.6488	6.6027	178.9	48.6	45.09
epsz–6b	Eastern Philippines	126.9478	6.6085	178.9	48.6	7.58
epsz–7a	Eastern Philippines	126.6578	7.4711	175.8	50.7	45.52
epsz–7b	Eastern Philippines	126.9439	7.4921	175.8	50.7	6.83
epsz–8a	Eastern Philippines	126.6227	8.2456	163.3	56.7	45.6
epsz–8b	Eastern Philippines	126.8614	8.3164	163.3	48.9	7.92
epsz–9a	Eastern Philippines	126.2751	9.0961	164.1	47	43.59
epsz–9b	Eastern Philippines	126.5735	9.1801	164.1	44.9	8.3
epsz–10a	Eastern Philippines	125.9798	9.9559	164.5	43.1	42.25
epsz–10b	Eastern Philippines	126.3007	10.0438	164.5	43.1	8.09
epsz–11a	Eastern Philippines	125.6079	10.6557	155	37.8	38.29
epsz–11b	Eastern Philippines	125.9353	10.8059	155	37.8	7.64
epsz–12a	Eastern Philippines	125.4697	11.7452	172.1	36	37.01
epsz–12b	Eastern Philippines	125.8374	11.7949	172.1	36	7.62
epsz–13a	Eastern Philippines	125.2238	12.1670	141.5	32.4	33.87
epsz–13b	Eastern Philippines	125.5278	12.4029	141.5	32.4	7.08
epsz–14a	Eastern Philippines	124.6476	13.1365	158.2	23	25.92
epsz–14b	Eastern Philippines	125.0421	13.2898	158.2	23	6.38
epsz–15a	Eastern Philippines	124.3107	13.9453	156.1	24.1	26.51
epsz–15b	Eastern Philippines	124.6973	14.1113	156.1	24.1	6.09
epsz–16a	Eastern Philippines	123.8998	14.4025	140.3	19.5	21.69
epsz–16b	Eastern Philippines	124.2366	14.6728	140.3	19.5	5
epsz–17a	Eastern Philippines	123.4604	14.7222	117.6	15.3	18.19
epsz–17b	Eastern Philippines	123.6682	15.1062	117.6	15.3	5
epsz–18a	Eastern Philippines	123.3946	14.7462	67.4	15	17.94
epsz–18b	Eastern Philippines	123.2219	15.1467	67.4	15	5

Table C.3: Earthquake parameters for Eastern Philippines Subduction Zone unit sources.

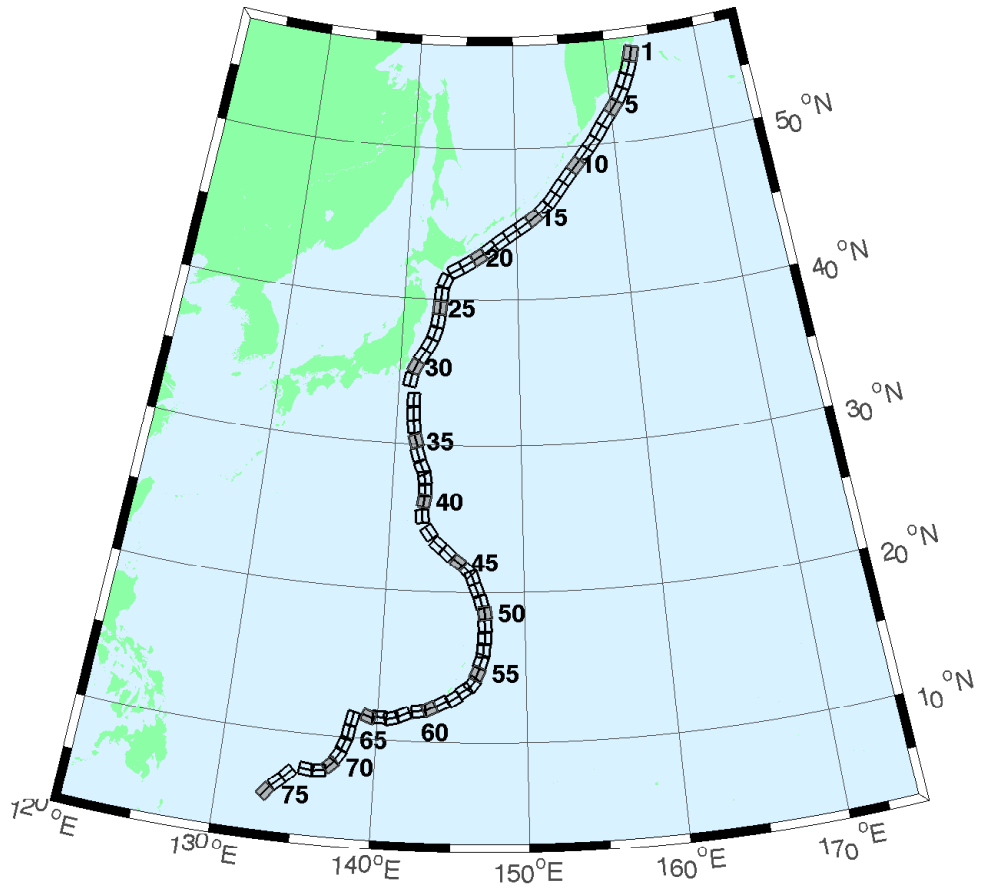

Figure C.4: Kuril Islands/Japan, and Mariana Subduction Zone unit sources.

Segment	Description	Longitude(°E)	Latitude(°N)	Strike(°)	Dip(°)	Depth (km)
ksz–1a	Kuril Islands/Japan, and Mariana	162.4318	55.5017	195	29	26.13
ksz–1b	Kuril Islands/Japan, and Mariana	163.1000	55.4000	195	25	5
ksz–2a	Kuril Islands/Japan, and Mariana	161.9883	54.6784	200	29	26.13
ksz–2b	Kuril Islands/Japan, and Mariana	162.6247	54.5440	200	25	5
ksz–3a	Kuril Islands/Japan, and Mariana	161.4385	53.8714	204	29	26.13
ksz–3b	Kuril Islands/Japan, and Mariana	162.0449	53.7116	204	25	5
ksz–4a	Kuril Islands/Japan, and Mariana	160.7926	53.1087	210	29	26.13
ksz–4b	Kuril Islands/Japan, and Mariana	161.3568	52.9123	210	25	5
ksz–5a	Kuril Islands/Japan, and Mariana	160.0211	52.4113	218	29	26.13
ksz–5b	Kuril Islands/Japan, and Mariana	160.5258	52.1694	218	25	5
ksz–6a	Kuril Islands/Japan, and Mariana	159.1272	51.7034	218	29	26.13
ksz–6b	Kuril Islands/Japan, and Mariana	159.6241	51.4615	218	25	5
ksz–7a	Kuril Islands/Japan, and Mariana	158.2625	50.9549	214	29	26.13
ksz–7b	Kuril Islands/Japan, and Mariana	158.7771	50.7352	214	25	5
ksz–8a	Kuril Islands/Japan, and Mariana	157.4712	50.2459	218	31	27.7
ksz–8b	Kuril Islands/Japan, and Mariana	157.9433	50.0089	218	27	5

Continued on next page

Table C.4 – continued from previous page

Segment	Description	Longitude(°E)	Latitude(°N)	Strike(°)	Dip(°)	Depth (km)
ksz–9a	Kuril Islands/Japan, and Mariana	156.6114	49.5583	220	31	27.7
ksz–9b	Kuril Islands/Japan, and Mariana	157.0638	49.3109	220	27	5
ksz–10a	Kuril Islands/Japan, and Mariana	155.7294	48.8804	221	31	27.7
ksz–10b	Kuril Islands/Japan, and Mariana	156.1690	48.6278	221	27	5
ksz–11a	Kuril Islands/Japan, and Mariana	154.8489	48.1821	219	31	27.7
ksz–11b	Kuril Islands/Japan, and Mariana	155.2955	47.9398	219	27	5
ksz–12a	Kuril Islands/Japan, and Mariana	153.9994	47.4729	217	31	27.7
ksz–12b	Kuril Islands/Japan, and Mariana	154.4701	47.2320	217	27	5
ksz–13a	Kuril Islands/Japan, and Mariana	153.2239	46.7564	218	31	27.7
ksz–13b	Kuril Islands/Japan, and Mariana	153.6648	46.5194	218	27	5
ksz–14a	Kuril Islands/Japan, and Mariana	152.3657	46.1514	225	23	24.54
ksz–14b	Kuril Islands/Japan, and Mariana	152.7855	45.8591	225	23	5
ksz–15a	Kuril Islands/Japan, and Mariana	151.4663	45.5963	233	25	23.73
ksz–15b	Kuril Islands/Japan, and Mariana	151.8144	45.2712	233	22	5
ksz–16a	Kuril Islands/Japan, and Mariana	150.4572	45.0977	237	25	23.73
ksz–16b	Kuril Islands/Japan, and Mariana	150.7694	44.7563	237	22	5
ksz–17a	Kuril Islands/Japan, and Mariana	149.3989	44.6084	237	25	23.73
ksz–17b	Kuril Islands/Japan, and Mariana	149.7085	44.2670	237	22	5
ksz–18a	Kuril Islands/Japan, and Mariana	148.3454	44.0982	235	25	23.73
ksz–18b	Kuril Islands/Japan, and Mariana	148.6687	43.7647	235	22	5
ksz–19a	Kuril Islands/Japan, and Mariana	147.3262	43.5619	233	25	23.73
ksz–19b	Kuril Islands/Japan, and Mariana	147.6625	43.2368	233	22	5
ksz–20a	Kuril Islands/Japan, and Mariana	146.3513	43.0633	237	25	23.73
ksz–20b	Kuril Islands/Japan, and Mariana	146.6531	42.7219	237	22	5
ksz–21a	Kuril Islands/Japan, and Mariana	145.3331	42.5948	239	25	23.73
ksz–21b	Kuril Islands/Japan, and Mariana	145.6163	42.2459	239	22	5
ksz–22a	Kuril Islands/Japan, and Mariana	144.3041	42.1631	242	25	23.73
ksz–22b	Kuril Islands/Japan, and Mariana	144.5605	41.8037	242	22	5
ksz–23a	Kuril Islands/Japan, and Mariana	143.2863	41.3335	202	21	21.28
ksz–23b	Kuril Islands/Japan, and Mariana	143.8028	41.1764	202	19	5
ksz–24a	Kuril Islands/Japan, and Mariana	142.9795	40.3490	185	21	21.28
ksz–24b	Kuril Islands/Japan, and Mariana	143.5273	40.3125	185	19	5
ksz–25a	Kuril Islands/Japan, and Mariana	142.8839	39.4541	185	21	21.28
ksz–25b	Kuril Islands/Japan, and Mariana	143.4246	39.4176	185	19	5
ksz–26a	Kuril Islands/Japan, and Mariana	142.7622	38.5837	188	21	21.28
ksz–26b	Kuril Islands/Japan, and Mariana	143.2930	38.5254	188	19	5
ksz–27a	Kuril Islands/Japan, and Mariana	142.5320	37.7830	198	21	21.28
ksz–27b	Kuril Islands/Japan, and Mariana	143.0357	37.6534	198	19	5
ksz–28a	Kuril Islands/Japan, and Mariana	142.1315	37.0265	208	21	21.28
ksz–28b	Kuril Islands/Japan, and Mariana	142.5941	36.8297	208	19	5
ksz–29a	Kuril Islands/Japan, and Mariana	141.5970	36.2640	211	21	21.28
ksz–29b	Kuril Islands/Japan, and Mariana	142.0416	36.0481	211	19	5
ksz–30a	Kuril Islands/Japan, and Mariana	141.0553	35.4332	205	21	21.28
ksz–30b	Kuril Islands/Japan, and Mariana	141.5207	35.2560	205	19	5
ksz–31a	Kuril Islands/Japan, and Mariana	140.6956	34.4789	190	22	22.1
ksz–31b	Kuril Islands/Japan, and Mariana	141.1927	34.4066	190	20	5
ksz–32a	Kuril Islands/Japan, and Mariana	141.0551	33.0921	180	32	23.48
ksz–32b	Kuril Islands/Japan, and Mariana	141.5098	33.0921	180	21.69	5
ksz–33a	Kuril Islands/Japan, and Mariana	141.0924	32.1047	173.8	27.65	20.67
ksz–33b	Kuril Islands/Japan, and Mariana	141.5596	32.1473	173.8	18.27	5
ksz–34a	Kuril Islands/Japan, and Mariana	141.1869	31.1851	172.1	25	18.26
ksz–34b	Kuril Islands/Japan, and Mariana	141.6585	31.2408	172.1	15.38	5
ksz–35a	Kuril Islands/Japan, and Mariana	141.4154	30.1707	163	25	17.12
ksz–35b	Kuril Islands/Japan, and Mariana	141.8662	30.2899	163	14.03	5
ksz–36a	Kuril Islands/Japan, and Mariana	141.6261	29.2740	161.7	25.73	18.71
ksz–36b	Kuril Islands/Japan, and Mariana	142.0670	29.4012	161.7	15.91	5
ksz–37a	Kuril Islands/Japan, and Mariana	142.0120	28.3322	154.7	20	14.54
ksz–37b	Kuril Islands/Japan, and Mariana	142.4463	28.5124	154.7	11	5
ksz–38a	Kuril Islands/Japan, and Mariana	142.2254	27.6946	170.3	20	14.54
ksz–38b	Kuril Islands/Japan, and Mariana	142.6955	27.7659	170.3	11	5
ksz–39a	Kuril Islands/Japan, and Mariana	142.3085	26.9127	177.2	24.23	17.42

Continued on next page

Table C.4 – continued from previous page

Segment	Description	Longitude(°E)	Latitude(°N)	Strike(°)	Dip(°)	Depth (km)
ksz–39b	Kuril Islands/Japan, and Mariana	142.7674	26.9325	177.2	14.38	5
ksz–40a	Kuril Islands/Japan, and Mariana	142.2673	26.1923	189.4	26.49	22.26
ksz–40b	Kuril Islands/Japan, and Mariana	142.7090	26.1264	189.4	20.2	5
ksz–41a	Kuril Islands/Japan, and Mariana	142.1595	25.0729	173.7	22.07	19.08
ksz–41b	Kuril Islands/Japan, and Mariana	142.6165	25.1184	173.7	16.36	5
ksz–42a	Kuril Islands/Japan, and Mariana	142.7641	23.8947	143.5	21.54	18.4
ksz–42b	Kuril Islands/Japan, and Mariana	143.1321	24.1432	143.5	15.54	5
ksz–43a	Kuril Islands/Japan, and Mariana	143.5281	23.0423	129.2	23.02	18.77
ksz–43b	Kuril Islands/Japan, and Mariana	143.8128	23.3626	129.2	15.99	5
ksz–44a	Kuril Islands/Japan, and Mariana	144.2230	22.5240	134.6	28.24	18.56
ksz–44b	Kuril Islands/Japan, and Mariana	144.5246	22.8056	134.6	15.74	5
ksz–45a	Kuril Islands/Japan, and Mariana	145.0895	21.8866	125.8	36.73	22.79
ksz–45b	Kuril Islands/Japan, and Mariana	145.3171	22.1785	125.8	20.84	5
ksz–46a	Kuril Islands/Japan, and Mariana	145.6972	21.3783	135.9	30.75	20.63
ksz–46b	Kuril Islands/Japan, and Mariana	145.9954	21.6469	135.9	18.22	5
ksz–47a	Kuril Islands/Japan, and Mariana	146.0406	20.9341	160.1	29.87	19.62
ksz–47b	Kuril Islands/Japan, and Mariana	146.4330	21.0669	160.1	17	5
ksz–48a	Kuril Islands/Japan, and Mariana	146.3836	20.0690	158	32.75	19.68
ksz–48b	Kuril Islands/Japan, and Mariana	146.7567	20.2108	158	17.07	5
ksz–49a	Kuril Islands/Japan, and Mariana	146.6689	19.3123	164.5	25.07	21.41
ksz–49b	Kuril Islands/Japan, and Mariana	147.0846	19.4212	164.5	19.16	5
ksz–50a	Kuril Islands/Japan, and Mariana	146.9297	18.5663	172.1	22	22.1
ksz–50b	Kuril Islands/Japan, and Mariana	147.3650	18.6238	172.1	20	5
ksz–51a	Kuril Islands/Japan, and Mariana	146.9495	17.7148	175.1	22.06	22.04
ksz–51b	Kuril Islands/Japan, and Mariana	147.3850	17.7503	175.1	19.93	5
ksz–52a	Kuril Islands/Japan, and Mariana	146.9447	16.8869	180	25.51	18.61
ksz–52b	Kuril Islands/Japan, and Mariana	147.3683	16.8869	180	15.79	5
ksz–53a	Kuril Islands/Japan, and Mariana	146.8626	16.0669	185.2	27.39	18.41
ksz–53b	Kuril Islands/Japan, and Mariana	147.2758	16.0309	185.2	15.56	5
ksz–54a	Kuril Islands/Japan, and Mariana	146.7068	15.3883	199.1	28.12	20.91
ksz–54b	Kuril Islands/Japan, and Mariana	147.0949	15.2590	199.1	18.56	5
ksz–55a	Kuril Islands/Japan, and Mariana	146.4717	14.6025	204.3	29.6	26.27
ksz–55b	Kuril Islands/Japan, and Mariana	146.8391	14.4415	204.3	25.18	5
ksz–56a	Kuril Islands/Japan, and Mariana	146.1678	13.9485	217.4	32.04	26.79
ksz–56b	Kuril Islands/Japan, and Mariana	146.4789	13.7170	217.4	25.84	5
ksz–57a	Kuril Islands/Japan, and Mariana	145.6515	13.5576	235.8	37	24.54
ksz–57b	Kuril Islands/Japan, and Mariana	145.8586	13.2609	235.8	23	5
ksz–58a	Kuril Islands/Japan, and Mariana	144.9648	12.9990	237.8	37.72	24.54
ksz–58b	Kuril Islands/Japan, and Mariana	145.1589	12.6984	237.8	23	5
ksz–59a	Kuril Islands/Japan, and Mariana	144.1799	12.6914	242.9	34.33	22.31
ksz–59b	Kuril Islands/Japan, and Mariana	144.3531	12.3613	242.9	20.25	5
ksz–60a	Kuril Islands/Japan, and Mariana	143.3687	12.3280	244.9	30.9	20.62
ksz–60b	Kuril Islands/Japan, and Mariana	143.5355	11.9788	244.9	18.2	5
ksz–61a	Kuril Islands/Japan, and Mariana	142.7051	12.1507	261.8	35.41	25.51
ksz–61b	Kuril Islands/Japan, and Mariana	142.7582	11.7883	261.8	24.22	5
ksz–62a	Kuril Islands/Japan, and Mariana	141.6301	11.8447	245.7	39.86	34.35
ksz–62b	Kuril Islands/Japan, and Mariana	141.7750	11.5305	245.7	35.94	5
ksz–63a	Kuril Islands/Japan, and Mariana	140.8923	11.5740	256.2	42	38.46
ksz–63b	Kuril Islands/Japan, and Mariana	140.9735	11.2498	256.2	42	5
ksz–64a	Kuril Islands/Japan, and Mariana	140.1387	11.6028	269.6	42.48	38.77
ksz–64b	Kuril Islands/Japan, and Mariana	140.1410	11.2716	269.6	42.48	5
ksz–65a	Kuril Islands/Japan, and Mariana	139.4595	11.5883	288.7	44.16	39.83
ksz–65b	Kuril Islands/Japan, and Mariana	139.3541	11.2831	288.7	44.16	5
ksz–66a	Kuril Islands/Japan, and Mariana	138.1823	11.2648	193.1	45	40.36
ksz–66b	Kuril Islands/Japan, and Mariana	138.4977	11.1929	193.1	45	5
ksz–67a	Kuril Islands/Japan, and Mariana	137.9923	10.3398	189.8	45	40.36
ksz–67b	Kuril Islands/Japan, and Mariana	138.3104	10.2856	189.8	45	5
ksz–68a	Kuril Islands/Japan, and Mariana	137.7607	9.6136	201.7	45	40.36
ksz–68b	Kuril Islands/Japan, and Mariana	138.0599	9.4963	201.7	45	5
ksz–69a	Kuril Islands/Japan, and Mariana	137.4537	8.8996	213.5	45	40.36
ksz–69b	Kuril Islands/Japan, and Mariana	137.7215	8.7241	213.5	45	5

Continued on next page

Table C.4 – continued from previous page

Segment	Description	Longitude(^{o}E)	Latitude(^{o}N)	Strike(^{o})	Dip(^{o})	Depth (km)
ksz–70a	Kuril Islands/Japan, and Mariana	137.0191	8.2872	226.5	45	40.36
ksz–70b	Kuril Islands/Japan, and Mariana	137.2400	8.0569	226.5	45	5
ksz–71a	Kuril Islands/Japan, and Mariana	136.3863	7.9078	263.9	45	40.36
ksz–71b	Kuril Islands/Japan, and Mariana	136.4202	7.5920	263.9	45	5
ksz–72a	Kuril Islands/Japan, and Mariana	135.6310	7.9130	276.9	45	40.36
ksz–72b	Kuril Islands/Japan, and Mariana	135.5926	7.5977	276.9	45	5
ksz–73a	Kuril Islands/Japan, and Mariana	134.3296	7.4541	224	45	40.36
ksz–73b	Kuril Islands/Japan, and Mariana	134.5600	7.2335	224	45	5
ksz–74a	Kuril Islands/Japan, and Mariana	133.7125	6.8621	228.1	45	40.36
ksz–74b	Kuril Islands/Japan, and Mariana	133.9263	6.6258	228.1	45	5
ksz–75a	Kuril Islands/Japan, and Mariana	133.0224	6.1221	217.7	45	40.36
ksz–75b	Kuril Islands/Japan, and Mariana	133.2751	5.9280	217.7	45	5

Table C.4: Earthquake parameters for Kuril Islands/Japan, and Mariana Subduction Zone unit sources.

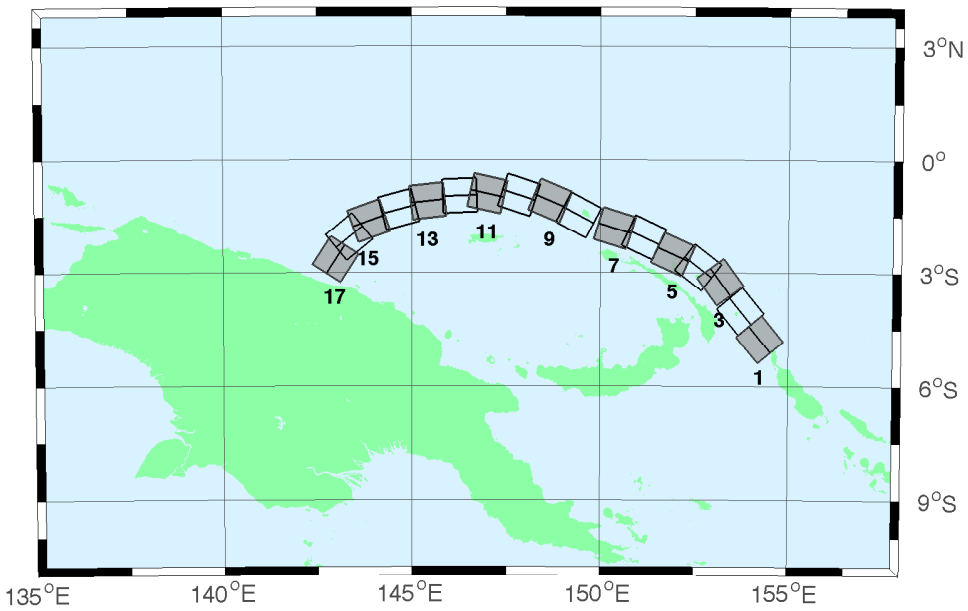

Figure C.5: Manus Subduction Zone unit sources.

Segment	Description	Longitude(°E)	Latitude(°N)	Strike(°)	Dip(°)	Depth (km)
msz–1a	Manus	154.0737	-4.8960	140.2	15	15.88
msz–1b	Manus	154.4082	-4.6185	140.2	15	5
msz–2a	Manus	153.5589	-4.1575	140.2	15	15.91
msz–2b	Manus	153.8931	-3.8800	140.2	15	5.35
msz–3a	Manus	153.0151	-3.3716	143.9	15	16.64
msz–3b	Manus	153.3662	-3.1160	143.9	15	6.31
msz–4a	Manus	152.4667	-3.0241	127.7	15	17.32
msz–4b	Manus	152.7321	-2.6806	127.7	15	7.39
msz–5a	Manus	151.8447	-2.7066	114.3	15	17.57
msz–5b	Manus	152.0235	-2.3112	114.3	15	8.25
msz–6a	Manus	151.0679	-2.2550	115	15	17.66
msz–6b	Manus	151.2513	-1.8618	115	15	7.58
msz–7a	Manus	150.3210	-2.0236	107.2	15	17.73
msz–7b	Manus	150.4493	-1.6092	107.2	15	6.83
msz–8a	Manus	149.3226	-1.6666	117.8	15	17.83
msz–8b	Manus	149.5251	-1.2829	117.8	15	7.92
msz–9a	Manus	148.5865	-1.3017	112.7	15	17.84
msz–9b	Manus	148.7540	-0.9015	112.7	15	8.3
msz–10a	Manus	147.7760	-1.1560	108	15	17.78
msz–10b	Manus	147.9102	-0.7434	108	15	8.09
msz–11a	Manus	146.9596	-1.1226	102.5	15	17.54
msz–11b	Manus	147.0531	-0.6990	102.5	15	7.64
msz–12a	Manus	146.2858	-1.1820	87.48	15	17.29
msz–12b	Manus	146.2667	-0.7486	87.48	15	7.62
msz–13a	Manus	145.4540	-1.3214	83.75	15	17.34
msz–13b	Manus	145.4068	-0.8901	83.75	15	7.08
msz–14a	Manus	144.7151	-1.5346	75.09	15	17.21
msz–14b	Manus	144.6035	-1.1154	75.09	15	6.38

Continued on next page

Table C.5 – continued from previous page

Segment	Description	Longitude(^{o}E)	Latitude(^{o}N)	Strike(^{o})	Dip(^{o})	Depth (km)
msz–15a	Manus	143.9394	-1.8278	70.43	15	16.52
msz–15b	Manus	143.7940	-1.4190	70.43	15	6.09
msz–16a	Manus	143.4850	-2.2118	50.79	15	15.86
msz–16b	Manus	143.2106	-1.8756	50.79	15	5
msz–17a	Manus	143.1655	-2.7580	33	15	16.64
msz–17b	Manus	142.8013	-2.5217	33	15	5

Table C.5: Earthquake parameters for Manus Subduction Zone unit sources.

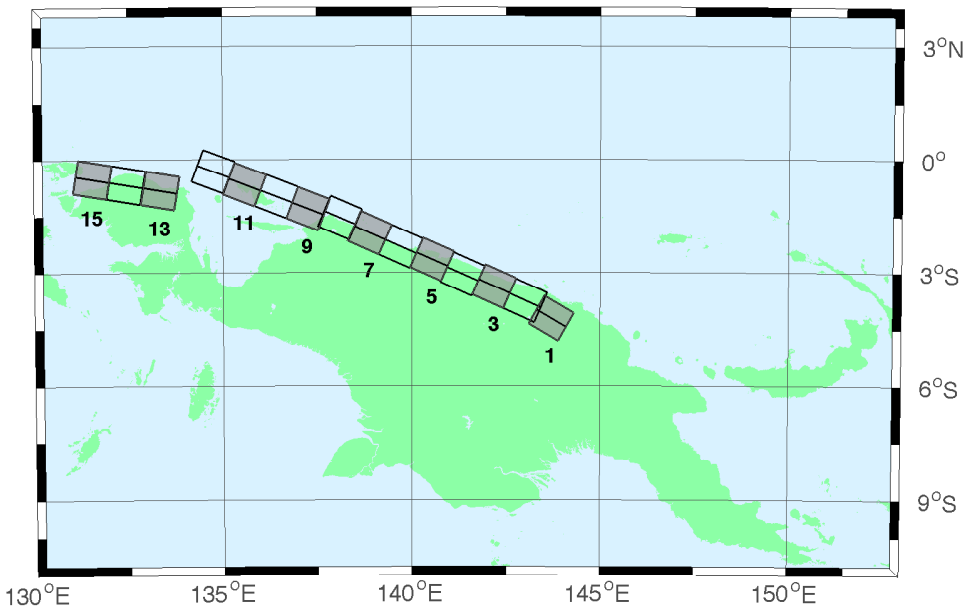

Figure C.6: New Guinea Zone unit sources.

Segment	Description	Longitude(°E)	Latitude(°N)	Strike(°)	Dip(°)	Depth (km)
ngsz–1a	New Guinea	143.6063	-4.3804	120	29	25.64
ngsz–1b	New Guinea	143.8032	-4.0402	120	29	1.4
ngsz–2a	New Guinea	142.9310	-3.9263	114	27.63	20.1
ngsz–2b	New Guinea	143.0932	-3.5628	114	21.72	1.6
ngsz–3a	New Guinea	142.1076	-3.5632	114	20.06	18.73
ngsz–3b	New Guinea	142.2795	-3.1778	114	15.94	5
ngsz–4a	New Guinea	141.2681	-3.2376	114	21	17.76
ngsz–4b	New Guinea	141.4389	-2.8545	114	14.79	5
ngsz–5a	New Guinea	140.4592	-2.8429	114	21.26	16.14
ngsz–5b	New Guinea	140.6296	-2.4605	114	12.87	5
ngsz–6a	New Guinea	139.6288	-2.4960	114	22.72	15.4
ngsz–6b	New Guinea	139.7974	-2.1175	114	12	5
ngsz–7a	New Guinea	138.8074	-2.1312	114	21.39	15.4
ngsz–7b	New Guinea	138.9776	-1.7491	114	12	5
ngsz–8a	New Guinea	138.0185	-1.7353	113.1	18.79	15.14
ngsz–8b	New Guinea	138.1853	-1.3441	113.1	11.7	5
ngsz–9a	New Guinea	137.1805	-1.5037	111	15.24	13.23
ngsz–9b	New Guinea	137.3358	-1.0991	111	9.47	5
ngsz–10a	New Guinea	136.3418	-1.1774	111	13.51	11.09
ngsz–10b	New Guinea	136.4983	-0.7697	111	7	5
ngsz–11a	New Guinea	135.4984	-0.8641	111	11.38	12.49
ngsz–11b	New Guinea	135.6562	-0.4530	111	8.62	5
ngsz–12a	New Guinea	134.6759	-0.5216	110.5	10	13.68
ngsz–12b	New Guinea	134.8307	-0.1072	110.5	10	5
ngsz–13a	New Guinea	133.3065	-1.0298	99.5	10	13.68
ngsz–13b	New Guinea	133.3795	-0.5935	99.5	10	5
ngsz–14a	New Guinea	132.4048	-0.8816	99.5	10	13.68
ngsz–14b	New Guinea	132.4778	-0.4453	99.5	10	5

Continued on next page

Table C.6 – continued from previous page

Segment	Description	Longitude(^{o}E)	Latitude(^{o}N)	Strike(^{o})	Dip(^{o})	Depth (km)
ngsz–15a	New Guinea	131.5141	-0.7353	99.5	10	13.68
ngsz–15b	New Guinea	131.5871	-0.2990	99.5	10	5

Table C.6: Earthquake parameters for New Guinea Subduction Zone unit sources.

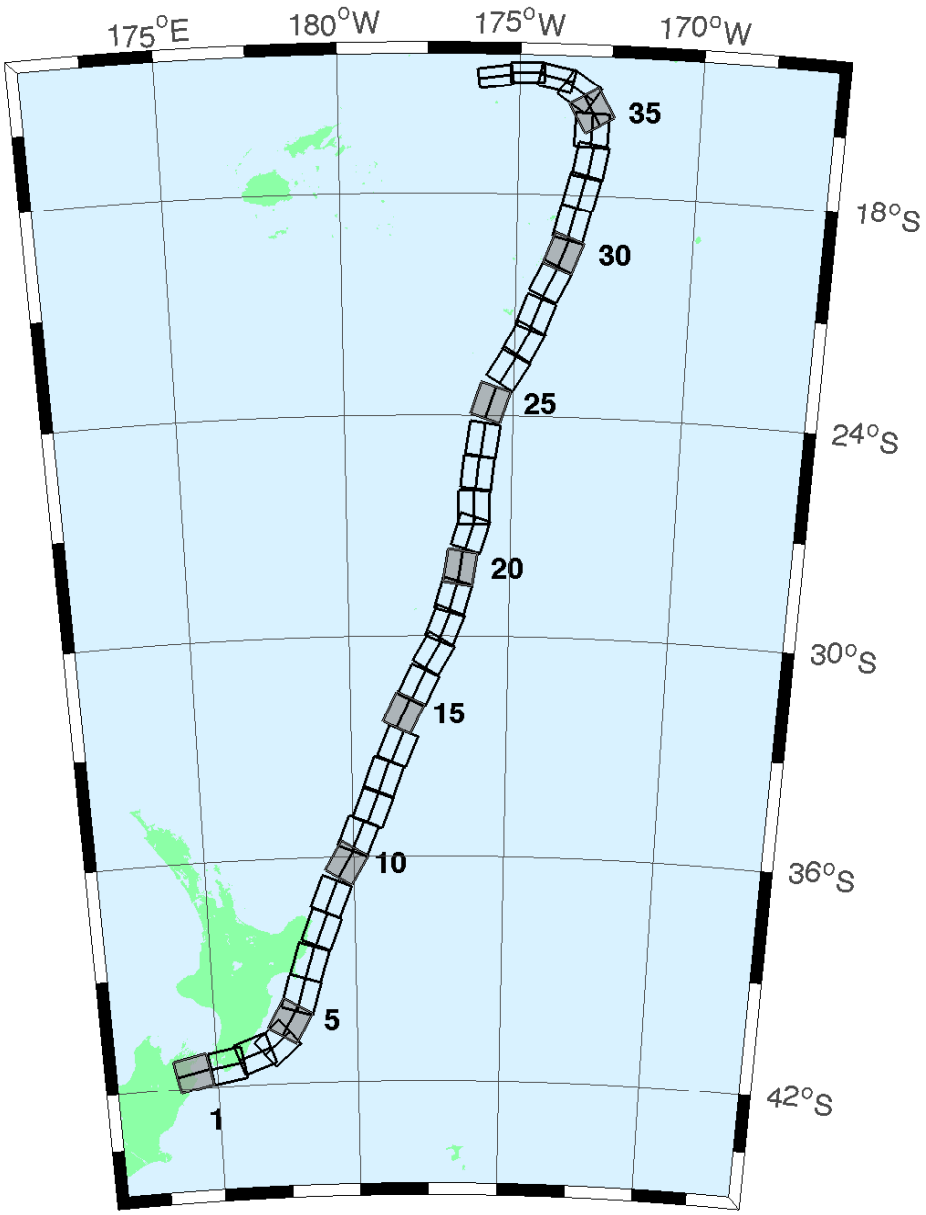

Figure C.7: New Zealand–Tonga Subduction Zone unit sources.

Segment	Description	Longitude(°E)	Latitude(°N)	Strike(°)	Dip(°)	Depth (km)
ntsz–1a	New Zealand–Tonga	174.0985	-41.3951	258.6	24	25.34
ntsz–1b	New Zealand–Tonga	174.2076	-41.7973	258.6	24	5
ntsz–2a	New Zealand–Tonga	175.3289	-41.2592	260.6	29.38	23.17
ntsz–2b	New Zealand–Tonga	175.4142	-41.6454	260.6	21.31	5
ntsz–3a	New Zealand–Tonga	176.2855	-40.9950	250.7	29.54	21.74
ntsz–3b	New Zealand–Tonga	176.4580	-41.3637	250.7	19.56	5
ntsz–4a	New Zealand–Tonga	177.0023	-40.7679	229.4	24.43	18.87
ntsz–4b	New Zealand–Tonga	177.3552	-41.0785	229.4	16.1	5
ntsz–5a	New Zealand–Tonga	177.4114	-40.2396	210	18.8	19.29
ntsz–5b	New Zealand–Tonga	177.8951	-40.4525	210	16.61	5
ntsz–6a	New Zealand–Tonga	177.8036	-39.6085	196.7	18.17	15.8
ntsz–6b	New Zealand–Tonga	178.3352	-39.7310	196.7	12.48	5
ntsz–7a	New Zealand–Tonga	178.1676	-38.7480	197	28.1	17.85
ntsz–7b	New Zealand–Tonga	178.6541	-38.8640	197	14.89	5
ntsz–8a	New Zealand–Tonga	178.6263	-37.8501	201.4	31.47	18.78
ntsz–8b	New Zealand–Tonga	179.0788	-37.9899	201.4	16	5
ntsz–9a	New Zealand–Tonga	178.9833	-36.9770	202.2	29.58	20.02
ntsz–9b	New Zealand–Tonga	179.4369	-37.1245	202.2	17.48	5
ntsz–10a	New Zealand–Tonga	179.5534	-36.0655	210.6	32.1	20.72
ntsz–10b	New Zealand–Tonga	179.9595	-36.2593	210.6	18.32	5
ntsz–11a	New Zealand–Tonga	179.9267	-35.3538	201.7	25	16.09
ntsz–11b	New Zealand–Tonga	180.3915	-35.5040	201.7	12.81	5
ntsz–12a	New Zealand–Tonga	180.4433	-34.5759	201.2	25	15.46
ntsz–12b	New Zealand–Tonga	180.9051	-34.7230	201.2	12.08	5
ntsz–13a	New Zealand–Tonga	180.7990	-33.7707	199.8	25.87	19.06
ntsz–13b	New Zealand–Tonga	181.2573	-33.9073	199.8	16.33	5
ntsz–14a	New Zealand–Tonga	181.2828	-32.9288	202.4	31.28	22.73
ntsz–14b	New Zealand–Tonga	181.7063	-33.0751	202.4	20.77	5
ntsz–15a	New Zealand–Tonga	181.4918	-32.0035	205.4	32.33	22.64
ntsz–15b	New Zealand–Tonga	181.8967	-32.1665	205.4	20.66	5
ntsz–16a	New Zealand–Tonga	181.9781	-31.2535	205.5	34.29	23.59
ntsz–16b	New Zealand–Tonga	182.3706	-31.4131	205.5	21.83	5
ntsz–17a	New Zealand–Tonga	182.4819	-30.3859	210.3	37.6	25.58
ntsz–17b	New Zealand–Tonga	182.8387	-30.5655	210.3	24.3	5
ntsz–18a	New Zealand–Tonga	182.8176	-29.6545	201.6	37.65	26.13
ntsz–18b	New Zealand–Tonga	183.1985	-29.7856	201.6	25	5
ntsz–19a	New Zealand–Tonga	183.0622	-28.8739	195.7	34.41	26.13
ntsz–19b	New Zealand–Tonga	183.4700	-28.9742	195.7	25	5
ntsz–20a	New Zealand–Tonga	183.2724	-28.0967	188.8	38	26.13
ntsz–20b	New Zealand–Tonga	183.6691	-28.1508	188.8	25	5
ntsz–21a	New Zealand–Tonga	183.5747	-27.1402	197.1	32.29	24.83
ntsz–21b	New Zealand–Tonga	183.9829	-27.2518	197.1	23.37	5
ntsz–22a	New Zealand–Tonga	183.6608	-26.4975	180	29.56	18.63
ntsz–22b	New Zealand–Tonga	184.0974	-26.4975	180	15.82	5
ntsz–23a	New Zealand–Tonga	183.7599	-25.5371	185.8	32.42	20.56
ntsz–23b	New Zealand–Tonga	184.1781	-25.5752	185.8	18.13	5
ntsz–24a	New Zealand–Tonga	183.9139	-24.6201	188.2	33.31	23.73
ntsz–24b	New Zealand–Tonga	184.3228	-24.6734	188.2	22	5
ntsz–25a	New Zealand–Tonga	184.1266	-23.5922	198.5	29.34	19.64
ntsz–25b	New Zealand–Tonga	184.5322	-23.7163	198.5	17.03	5
ntsz–26a	New Zealand–Tonga	184.6613	-22.6460	211.7	30.26	19.43
ntsz–26b	New Zealand–Tonga	185.0196	-22.8497	211.7	16.78	5
ntsz–27a	New Zealand–Tonga	185.0879	-21.9139	207.9	31.73	20.67
ntsz–27b	New Zealand–Tonga	185.4522	-22.0928	207.9	18.27	5
ntsz–28a	New Zealand–Tonga	185.4037	-21.1758	200.5	32.44	21.76
ntsz–28b	New Zealand–Tonga	185.7849	-21.3084	200.5	19.58	5
ntsz–29a	New Zealand–Tonga	185.8087	-20.2629	206.4	32.47	20.4
ntsz–29b	New Zealand–Tonga	186.1710	-20.4312	206.4	17.94	5
ntsz–30a	New Zealand–Tonga	186.1499	-19.5087	200.9	32.98	22.46
ntsz–30b	New Zealand–Tonga	186.5236	-19.6432	200.9	20.44	5
ntsz–31a	New Zealand–Tonga	186.3538	-18.7332	193.9	34.41	21.19

Continued on next page

Table C.7 – continued from previous page

Segment	Description	Longitude(°E)	Latitude(°N)	Strike(°)	Dip(°)	Depth (km)
ntsz–31b	New Zealand–Tonga	186.7339	-18.8221	193.9	18.89	5
ntsz–32a	New Zealand–Tonga	186.5949	-17.8587	194.1	30	19.12
ntsz–32b	New Zealand–Tonga	186.9914	-17.9536	194.1	16.4	5
ntsz–33a	New Zealand–Tonga	186.8172	-17.0581	190	33.15	23.34
ntsz–33b	New Zealand–Tonga	187.2047	-17.1237	190	21.52	5
ntsz–34a	New Zealand–Tonga	186.7814	-16.2598	182.1	15	13.41
ntsz–34b	New Zealand–Tonga	187.2330	-16.2759	182.1	9.68	5
ntsz–35a	New Zealand–Tonga	186.8000	-15.8563	149.8	15	12.17
ntsz–35b	New Zealand–Tonga	187.1896	-15.6384	149.8	8.24	5
ntsz–36a	New Zealand–Tonga	186.5406	-15.3862	123.9	40.44	36.72
ntsz–36b	New Zealand–Tonga	186.7381	-15.1025	123.9	39.38	5
ntsz–37a	New Zealand–Tonga	185.9883	-14.9861	102	68.94	30.99
ntsz–37b	New Zealand–Tonga	186.0229	-14.8282	102	31.32	5
ntsz–38a	New Zealand–Tonga	185.2067	-14.8259	88.4	80	26.13
ntsz–38b	New Zealand–Tonga	185.2044	-14.7479	88.4	25	5
ntsz–39a	New Zealand–Tonga	184.3412	-14.9409	82.55	80	26.13
ntsz–39b	New Zealand–Tonga	184.3307	-14.8636	82.55	25	5

Table C.7: Earthquake parameters for New Zealand–Tonga Subduction Zone unit sources.

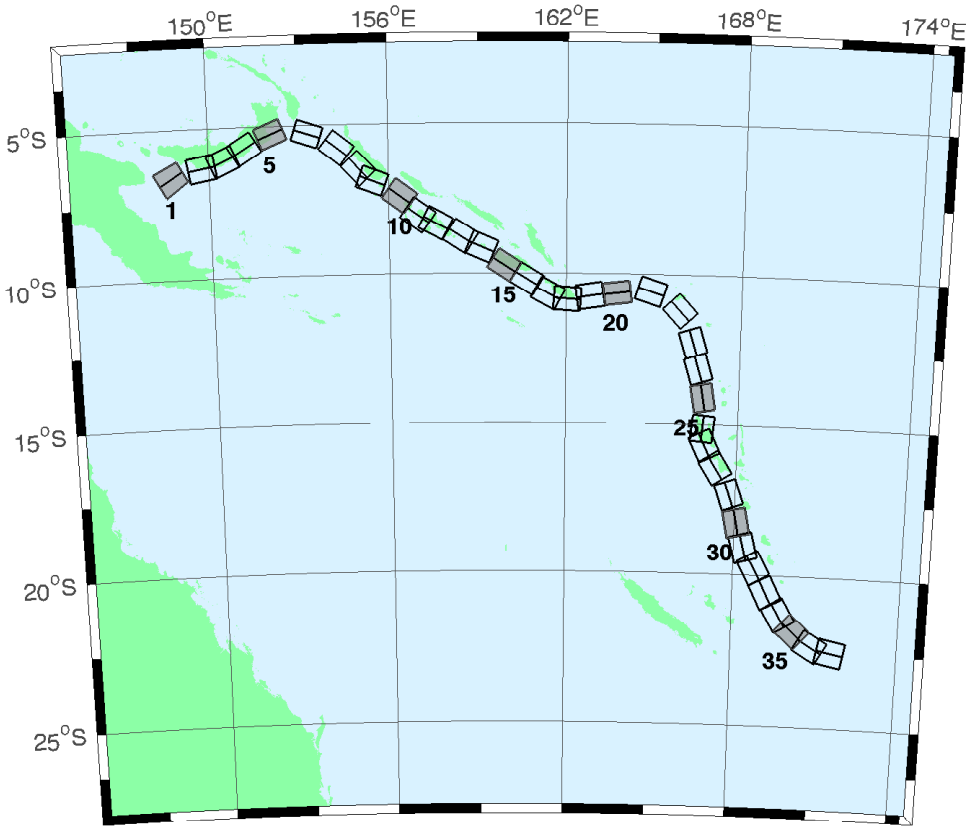

Figure C.8: New Britain–Vanuatu Zone unit sources.

Segment	Description	Longitude(°E)	Latitude(°N)	Strike(°)	Dip(°)	Depth (km)
nvsz–1a	New Britain–Vanuatu	148.6217	-6.4616	243.2	32.34	15.69
nvsz–1b	New Britain–Vanuatu	148.7943	-6.8002	234.2	12.34	5
nvsz–2a	New Britain–Vanuatu	149.7218	-6.1459	260.1	35.1	16.36
nvsz–2b	New Britain–Vanuatu	149.7856	-6.5079	260.1	13.13	5
nvsz–3a	New Britain–Vanuatu	150.4075	-5.9659	245.7	42.35	18.59
nvsz–3b	New Britain–Vanuatu	150.5450	-6.2684	245.7	15.77	5
nvsz–4a	New Britain–Vanuatu	151.1095	-5.5820	238.2	42.41	23.63
nvsz–4b	New Britain–Vanuatu	151.2851	-5.8639	238.2	21.88	5
nvsz–5a	New Britain–Vanuatu	152.0205	-5.1305	247.7	49.22	32.39
nvsz–5b	New Britain–Vanuatu	152.1322	-5.4020	247.7	33.22	5
nvsz–6a	New Britain–Vanuatu	153.3450	-5.1558	288.6	53.53	33.59
nvsz–6b	New Britain–Vanuatu	153.2595	-5.4089	288.6	34.87	5
nvsz–7a	New Britain–Vanuatu	154.3814	-5.6308	308.3	39.72	19.18
nvsz–7b	New Britain–Vanuatu	154.1658	-5.9017	308.3	16.48	5
nvsz–8a	New Britain–Vanuatu	155.1097	-6.3511	317.2	45.33	22.92
nvsz–8b	New Britain–Vanuatu	154.8764	-6.5656	317.2	21	5
nvsz–9a	New Britain–Vanuatu	155.5027	-6.7430	290.5	48.75	22.92
nvsz–9b	New Britain–Vanuatu	155.3981	-7.0204	290.5	21	5

Continued on next page

Table C.8 – continued from previous page

Segment	Description	Longitude(°E)	Latitude(°N)	Strike(°)	Dip(°)	Depth (km)
nvsz–10a	New Britain–Vanuatu	156.4742	-7.2515	305.9	36.88	27.62
nvsz–10b	New Britain–Vanuatu	156.2619	-7.5427	305.9	26.9	5
nvsz–11a	New Britain–Vanuatu	157.0830	-7.8830	305.4	32.97	29.72
nvsz–11b	New Britain–Vanuatu	156.8627	-8.1903	305.4	29.63	5
nvsz–12a	New Britain–Vanuatu	157.6537	-8.1483	297.9	37.53	28.57
nvsz–12b	New Britain–Vanuatu	157.4850	-8.4630	297.9	28.13	5
nvsz–13a	New Britain–Vanuatu	158.5089	-8.5953	302.7	33.62	23.02
nvsz–13b	New Britain–Vanuatu	158.3042	-8.9099	302.7	21.12	5
nvsz–14a	New Britain–Vanuatu	159.1872	-8.9516	293.3	38.44	34.06
nvsz–14b	New Britain–Vanuatu	159.0461	-9.2747	293.3	35.54	5
nvsz–15a	New Britain–Vanuatu	159.9736	-9.5993	302.8	46.69	41.38
nvsz–15b	New Britain–Vanuatu	159.8044	-9.8584	302.8	46.69	5
nvsz–16a	New Britain–Vanuatu	160.7343	-10.0574	301	46.05	41
nvsz–16b	New Britain–Vanuatu	160.5712	-10.3246	301	46.05	5
nvsz–17a	New Britain–Vanuatu	161.4562	-10.5241	298.4	40.12	37.22
nvsz–17b	New Britain–Vanuatu	161.2900	-10.8263	298.4	40.12	5
nvsz–18a	New Britain–Vanuatu	162.0467	-10.6823	274.1	40.33	29.03
nvsz–18b	New Britain–Vanuatu	162.0219	-11.0238	274.1	28.72	5
nvsz–19a	New Britain–Vanuatu	162.7818	-10.5645	261.3	34.25	24.14
nvsz–19b	New Britain–Vanuatu	162.8392	-10.9315	261.3	22.51	5
nvsz–20a	New Britain–Vanuatu	163.7222	-10.5014	262.9	50.35	26.3
nvsz–20b	New Britain–Vanuatu	163.7581	-10.7858	262.9	25.22	5
nvsz–21a	New Britain–Vanuatu	164.9445	-10.4183	287.9	40.31	23.3
nvsz–21b	New Britain–Vanuatu	164.8374	-10.7442	287.9	21.47	5
nvsz–22a	New Britain–Vanuatu	166.0261	-11.1069	317.1	42.39	20.78
nvsz–22b	New Britain–Vanuatu	165.7783	-11.3328	317.1	18.4	5
nvsz–23a	New Britain–Vanuatu	166.5179	-12.2260	342.4	47.95	22.43
nvsz–23b	New Britain–Vanuatu	166.2244	-12.3171	342.4	20.4	5
nvsz–24a	New Britain–Vanuatu	166.7236	-13.1065	342.6	47.13	28.52
nvsz–24b	New Britain–Vanuatu	166.4241	-13.1979	342.6	28.06	5
nvsz–25a	New Britain–Vanuatu	166.8914	-14.0785	350.3	54.1	31.16
nvsz–25b	New Britain–Vanuatu	166.6237	-14.1230	350.3	31.55	5
nvsz–26a	New Britain–Vanuatu	166.9200	-15.1450	365.6	50.46	29.05
nvsz–26b	New Britain–Vanuatu	166.6252	-15.1170	365.6	28.75	5
nvsz–27a	New Britain–Vanuatu	167.0053	-15.6308	334.2	44.74	25.46
nvsz–27b	New Britain–Vanuatu	166.7068	-15.7695	334.2	24.15	5
nvsz–28a	New Britain–Vanuatu	167.4074	-16.3455	327.5	41.53	22.44
nvsz–28b	New Britain–Vanuatu	167.1117	-16.5264	327.5	20.42	5
nvsz–29a	New Britain–Vanuatu	167.9145	-17.2807	341.2	49.1	24.12
nvsz–29b	New Britain–Vanuatu	167.6229	-17.3757	341.2	22.48	5
nvsz–30a	New Britain–Vanuatu	168.2220	-18.2353	348.6	44.19	23.99
nvsz–30b	New Britain–Vanuatu	167.8895	-18.2991	348.6	22.32	5
nvsz–31a	New Britain–Vanuatu	168.5022	-19.0510	345.6	42.2	22.26
nvsz–31b	New Britain–Vanuatu	168.1611	-19.1338	345.6	20.2	5
nvsz–32a	New Britain–Vanuatu	168.8775	-19.6724	331.1	42.03	21.68
nvsz–32b	New Britain–Vanuatu	168.5671	-19.8338	331.1	19.49	5
nvsz–33a	New Britain–Vanuatu	169.3422	-20.4892	332.9	40.25	22.4
nvsz–33b	New Britain–Vanuatu	169.0161	-20.6453	332.9	20.37	5
nvsz–34a	New Britain–Vanuatu	169.8304	-21.2121	329.1	39	22.73
nvsz–34b	New Britain–Vanuatu	169.5086	-21.3911	329.1	20.77	5
nvsz–35a	New Britain–Vanuatu	170.3119	-21.6945	311.9	39	22.13
nvsz–35b	New Britain–Vanuatu	170.0606	-21.9543	311.9	20.03	5
nvsz–36a	New Britain–Vanuatu	170.9487	-22.1585	300.4	39.42	23.5
nvsz–36b	New Britain–Vanuatu	170.7585	-22.4577	300.4	21.71	5
nvsz–37a	New Britain–Vanuatu	171.6335	-22.3087	281.3	30	22.1
nvsz–37b	New Britain–Vanuatu	171.5512	-22.6902	281.3	20	5

Table C.8: Earthquake parameters for New Britain–Vanuatu Subduction Zone unit sources.

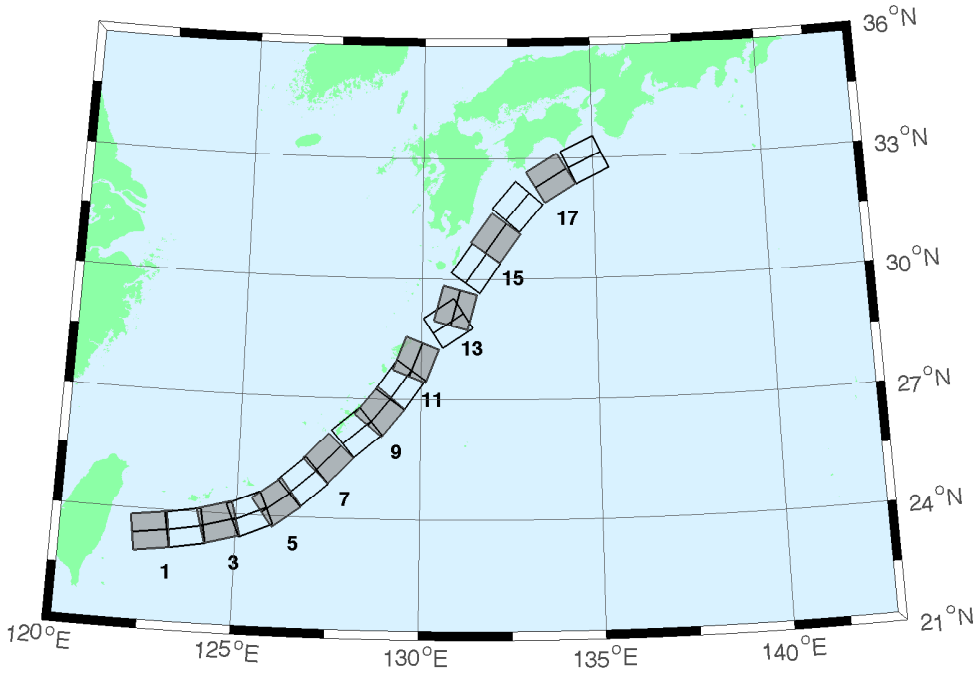

Figure C.9: Ryukyu–Nankai Zone unit sources.

Segment	Description	Longitude(°E)	Latitude(°N)	Strike(°)	Dip(°)	Depth (km)
rnsz–1a	Ryukyu–Nankai	122.6672	23.6696	262	14	11.88
rnsz–1b	Ryukyu–Nankai	122.7332	23.2380	262	10	3.2
rnsz–2a	Ryukyu–Nankai	123.5939	23.7929	259.9	18.11	12.28
rnsz–2b	Ryukyu–Nankai	123.6751	23.3725	259.9	10	3.6
rnsz–3a	Ryukyu–Nankai	124.4604	23.9777	254.6	19.27	14.65
rnsz–3b	Ryukyu–Nankai	124.5830	23.5689	254.6	12.18	4.1
rnsz–4a	Ryukyu–Nankai	125.2720	24.2102	246.8	18	20.38
rnsz–4b	Ryukyu–Nankai	125.4563	23.8177	246.8	16	6.6
rnsz–5a	Ryukyu–Nankai	125.9465	24.5085	233.6	18	20.21
rnsz–5b	Ryukyu–Nankai	126.2241	24.1645	233.6	16	6.43
rnsz–6a	Ryukyu–Nankai	126.6349	25.0402	228.7	17.16	19.55
rnsz–6b	Ryukyu–Nankai	126.9465	24.7176	228.7	15.16	6.47
rnsz–7a	Ryukyu–Nankai	127.2867	25.6343	224	15.85	17.98
rnsz–7b	Ryukyu–Nankai	127.6303	25.3339	224	13.56	6.26
rnsz–8a	Ryukyu–Nankai	128.0725	26.3146	229.7	14.55	14.31
rnsz–8b	Ryukyu–Nankai	128.3854	25.9831	229.7	9.64	5.94
rnsz–9a	Ryukyu–Nankai	128.6642	26.8177	219.2	15.4	12.62
rnsz–9b	Ryukyu–Nankai	129.0391	26.5438	219.2	8	5.66
rnsz–10a	Ryukyu–Nankai	129.2286	27.4879	215.2	17	12.55
rnsz–10b	Ryukyu–Nankai	129.6233	27.2402	215.2	8.16	5.45
rnsz–11a	Ryukyu–Nankai	129.6169	28.0741	201.3	17	12.91
rnsz–11b	Ryukyu–Nankai	130.0698	27.9181	201.3	8.8	5.26
rnsz–12a	Ryukyu–Nankai	130.6175	29.0900	236.7	16.42	13.05
rnsz–12b	Ryukyu–Nankai	130.8873	28.7299	236.7	9.57	4.74
rnsz–13a	Ryukyu–Nankai	130.7223	29.3465	195.2	20.25	15.89
rnsz–13b	Ryukyu–Nankai	131.1884	29.2362	195.2	12.98	4.66

Continued on next page

Table C.9 – continued from previous page

Segment	Description	Longitude(°E)	Latitude(°N)	Strike(°)	Dip(°)	Depth (km)
rnsz–14a	Ryukyu–Nankai	131.3467	30.3899	215.1	22.16	19.73
rnsz–14b	Ryukyu–Nankai	131.7402	30.1507	215.1	17.48	4.71
rnsz–15a	Ryukyu–Nankai	131.9149	31.1450	216	15.11	16.12
rnsz–15b	Ryukyu–Nankai	132.3235	30.8899	216	13.46	4.48
rnsz–16a	Ryukyu–Nankai	132.5628	31.9468	220.9	10.81	10.88
rnsz–16b	Ryukyu–Nankai	132.9546	31.6579	220.9	7.19	4.62
rnsz–17a	Ryukyu–Nankai	133.6125	32.6956	239	10.14	12.01
rnsz–17b	Ryukyu–Nankai	133.8823	32.3168	239	8.41	4.7
rnsz–18a	Ryukyu–Nankai	134.6416	33.1488	244.7	10.99	14.21
rnsz–18b	Ryukyu–Nankai	134.8656	32.7502	244.5	10.97	4.7

Table C.9: Earthquake parameters for Ryukyu–Nankai Subduction Zone unit sources.